

혈관 및 중재적방사선과학 연구회지



〈특집 : Vascular Disease: Imaging and Intervention〉

제 9 호 · 2002년

혈관 및 중재적방사선과학연구회
대한방사선의학회

목 차

특 집 : Vascular Disease: Imaging and Intervention

줄기세포를 이용한 신생혈관 조성	〈서울의대〉 김 호 수	1
타카야수 동맥염의 진단 및 치료	〈성균관대의대〉 최연현·도영수	4
베체트 증후군에 의한 혈관계 질환	〈연세의대〉 원종윤·이도연	17
슬와동맥 포획 증후군	〈순천향의대〉 조 준 희	22
혈관성 흉곽 출구 증후군	〈경북의대〉 성 창 규	28
기타 동맥 질환	〈울산의대〉 윤 현 기	35

1. Vascular Imaging

Case 1. 전류손상에 의한 동정맥 누공	39
Case 2. 응모막암종의 간전이: 혈관조영술 소견	41
Case 3. 슬와동맥에 발생한 Cystic Adventitial Disease	44

2. Embolotherapy

Case 4. 하지 동정맥류의 미세코일 색전술	46
Case 5. 거대동맥류를 동반한 혈관근지방종: 초선택적 동맥색전술을 이용한 치료	48
Case 6. 혈관이형성증으로 인한 급성 소장출혈: 혈관조영술을 이용한 진단과 치료	50
Case 7. 공장 위장관 자율신경증: 위장관출혈과 색전술을 이용한 치료	52
Case 8. 비장 동맥에 생긴 다발성 가성 동맥류의 미세코일 색전술	56
Case 9. 자궁동맥에 발생한 가성동맥류의 코일 색전술	60
Case 10. 분만 후 자궁출혈 환자에서의 난소동맥 색전술	62

3. Vascular Stent Placement

Case 11. 타카야수 동맥염에 의한 양측 신동맥 협착의 일차성 스텐트 삽입술	64
Case 12. 만성 장간막허혈에서의 풍선 혈관성형술과 스텐트 설치	67
Case 13. 간 이식 후 발생한 간문맥 협착의 스텐트 삽입	70

4. Vascular Stent-Graft Placement

<i>Case 14.</i> 베체트병 환자의 복부대동맥재건술 후 근위문합부에 발생한 가성동맥류에 대한 스텐트-그라프트 설치술	72
<i>Case 15.</i> 스텐트-그라프트를 이용한 염증성 복부 대동맥류의 치료	75
<i>Case 16.</i> 심부전의 증상을 보인 총장골 동정맥류의 스텐트-그라프트를 이용한 치료	78
<i>Case 17.</i> 코일과 스텐트-그라프트를 이용한 장골동맥류의 치료	81

5. Intervention for Hemodialysis

<i>Case 18.</i> 혈액 투석용 동정맥루 환자에서 발생한 동맥협착의 풍선혈관성형술	84
--	----

6. Thrombolysis

<i>Case 19.</i> 급성 하지동맥 허혈증에 대한 혈전용해술 도중 발생한 출혈 합병증	86
<i>Case 20.</i> 장골정맥 압박 증후군(May-Thurner syndrome)에서 카테터를 이용한 혈전용해술과 정맥 스텐트 설치술 후 합병된 뇌출혈	89

7. Central Venous Catheterization

<i>Case 21.</i> 상대정맥협착 환자에서 중심정맥도관의 재위치	94
---	----

8. Biliary Intervention

<i>Case 22.</i> 폐쇄풍선을 이용한 담도 결석의 경피적경유두제거술	96
<i>Case 23.</i> 간이식환자에서 경피경간담관배액술 후 합병된 늑골 골수염	99

9. Gastrointestinal and Genitourinary Intervention

<i>Case 24.</i> 피복 금속 스텐트를 이용한 위-십이지장 문합부의 양성 협착 및 장관루 치료	101
<i>Case 25.</i> NBCA를 이용한 신낭종 소작술	104

가 0.2%
 가
 (mobilization)
 [2]
 가 ?
 3%
 [3] (umbilical cord blood) 가
 가 가
 가
 가
 가
 [1]
 가 , [2]
 가 가 , [3]
 가
 [4]
 telomere가
 가
 2%
 (1).

(4) - (endothelial progenitor cell : EPC) ? (6) 가 ()

1997 Tufts St. Elizabeth Medical Center
 CD34

(EPC)가 (2). :
 Hematopoietic stem cell(HSC) 가 , Flk -
 1(KDR), tie - 2, CD34, Sca1, c - kit EPC HSC
 가 가
 VeCadherin , 가 VeCadherin
 . HSC가
 CD34, Flk - 1
 가 , [1] Dil - acetyl LDL
 , [2] VEGF nitric oxide
 DAF - 2DA , [3] PECAM - 1(CD31) 가
 , [4] vWF , [5] vascular endothelial cadherin
 , [6] KDR

(5) - 가 ; X - gal 가
 (6).

(3).
 [1] (7). 가

(8).

[3] :
CD34
-
(9).

(7)

가

(preclinical study)

(10).

(8) 가?

가

- [1]
[2] (mobilization)
[3] (homing)
1. Asahara T, Kalka C, Isner JM. Stem cell therapy and gene transfer for regeneration. *Gene Therapy* 2000;7:451-457
 2. Asahara T, Murohara T, Sullivan A, et al. Isolation of putative progenitor endothelial cells for angiogenesis. *Science* 1997;275:964-967
 3. Murohara T. Therapeutic vasculogenesis using human cord blood-derived endothelial progenitors. *TCM* 2001;11:303-307
 4. Kalka C, Isner JM, Asahara T, et al. Transplantation of ex vivo expanded endothelial progenitor cells for therapeutic neovascularization. *PNAS* 2000;97:3422-3427
 5. Kawamoto A, Gwon HC, Iwaguro H, et al. Therapeutic potential of ex vivo expanded endothelial progenitor cells for myocardial ischemia. *Circulation* 2001;103:634-637
 6. Asahara T, Masuda H, Takahashi T, et al. Bone marrow origin of endothelial progenitor cells responsible for postnatal vasculogenesis in physiological and pathological neovascularization. *Circ Res* 1999;85:221-228
 7. Shintani S, Murohara T, Ikeda H, et al. Augmentation of postnatal neovascularization with autologous bone marrow transplantation. *Circulation* 2001;103:897-903
 8. Kamihata H, Matsubara H, Nishiue T, et al. Implantation of bone marrow mononuclear cells into ischemic myocardium enhances collateral perfusion and regional function via side supply of angioblasts, angiogenic ligands, and cytokines. *Circulation* 2001;104:1046-1052
 9. Murohara T, Ikeda H, Duan J, et al. Transplanted cord blood derived endothelial precursor cells augment postnatal neovascularization. *J Clin Invest* 2000;105:1527-1536
 10. Tateishi E, Masaki H, Matsubara H, et al. Clinically feasible therapeutic angiogenesis using autologous implantation of bone marrow-derived mononuclear cells to ischemic limbs. *Jpn Circ J* 2001;65(Suppl 1-A);181



TA
가 TA가
가 (1).
(Takayasu arteritis, TA) TA 가
,
TA ,
(1). 가 , 가 (1).
(superantigen) T -
가 HSP - 65, HLA, ICAM - 1
TA (1).
20 5
가
2.
(1).
가 (phase) 1) pre - pulseless phase,
2) vessel inflammation phase, 3) fibrotic phase
1 , ,
, 2
, 3
(2)
(3)가
(1).
HLA
가 , Bw52, DR7, DQw52가 , 가
(2). HLA - TA
(1). 가
(1).
가 (4).
(3)
TA 34 32 (94.1%) 가

50

3.

가

가 (skipped lesion)
(mucopolysaccharide)가

(1).
(plasma cell)

(internal elastic lamina)

50 - 80%

(1), 6 - TA (5).

16%

(1). 7 - 55% 40 TA

74% (1). 33 - 76% (6, 7). 40 TA

Table 1. Comparison of Proposed Criteria for Takayasu 's Arteritis

Authors Criteria	Ishikawa	Sharma et al.	American College of Rheumatology 1990
Obligatory	Age at disease onset < 40 yr		
Major Criteria	1. Left mid subclavian artery lesion 2. Right mid subclavian artery lesion	1. Left mid subclavian artery lesion 2. Right mid subclavian artery lesion 3. Characteristic signs and symptoms of at least one month duration ¹	1. Age at disease onset < 40 yr 2. Claudication of extremities 3. Decreased brachial artery pulse 4. BP difference > 10 mm Hg 5. Bruit over subclavian artery or aorta 6. Arteriogram abnormality
Minor Criteria	1. High ESR 2. Carotid artery tenderness 3. Hypertension 4. Aortic regurgitation or annuloaortic ectasia 5. Pulmonary artery lesion 6. Left mid common carotid artery lesion 7. Distal brachiocephalic trunk lesion 8. Descending thoracic aorta lesion 9. Abdominal aortic lesion	1. High ESR 2. Carotid artery tenderness 3. Hypertension 4. Aortic regurgitation or annuloaortic ectasia 5. Pulmonary artery lesion 6. Left mid common carotid artery lesion 7. Distal brachiocephalic trunk lesion 8. Descending thoracic aorta lesion 9. Abdominal aortic lesion 10. Coronary artery lesion	
Necessary Criteria for High Probability of TA	2 major or 1 major and 2 minor or 4 minor criteria	2 major or 1 major and 2 minor or 4 minor criteria	At least 3 of these 6 criteria

¹Limb claudication, pulselessness or pulse difference in limbs, an unobtainable or significant blood pressure difference (> 10 mm Hg systolic BP difference), fever, neck pain, transient amaurosis, blurred vision, syncope, dyspnea or palpitations.

(giant cell arteritis) MRI

(1). 가

가

TA 가

Sharma (8) Ishikawa(6)

(major criteria)

(minor criteria)

(Table 1). 가

(Fig. 1, 2),

, CT, MRI

(vasa vasorum)

10 20

(erythrocyte sedimentation rate, ESR), C- (C - reactive protein)

(

ESR

56%

44%

(9).

(

), ESR

(9).

가 . TA

1/5

(1),

가

CT,

가

TA

(10 - 12).

(12)

33 79%(26/33)가

, 61%(20/33)

, 94%(31/33)가

CT MRI

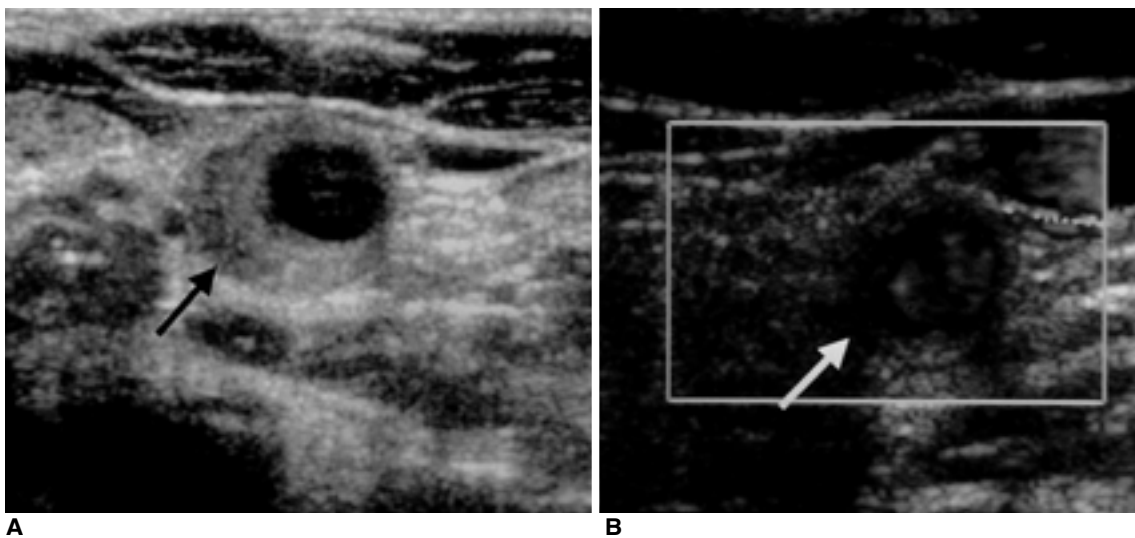


Fig. 1. 15-year-old female with fever and neck tenderness due to acute TA.
A. Carotid sonography shows wall thickening of the left common carotid artery (arrow).
B. After nine months of medical treatment, the wall thickness (arrow) was improved.

(Figs 3, 4). MRI (13) ESR (Fig. 7).
 (10%, 1/10) MRI가 MRI (FOV) 14 cm × 14 cm 16 cm ×
 , ESR 20 mm/hr 4 mm
 100%(15/15) MRI가 16 cm
 . ESR, CRP T2
 92.3% 84.6%
 ESR CRP 0.78,
 0.63 가
 CT , 가
 (14)(Fig. 5, 가
 6). 가
 (Fig. 6). CT 가

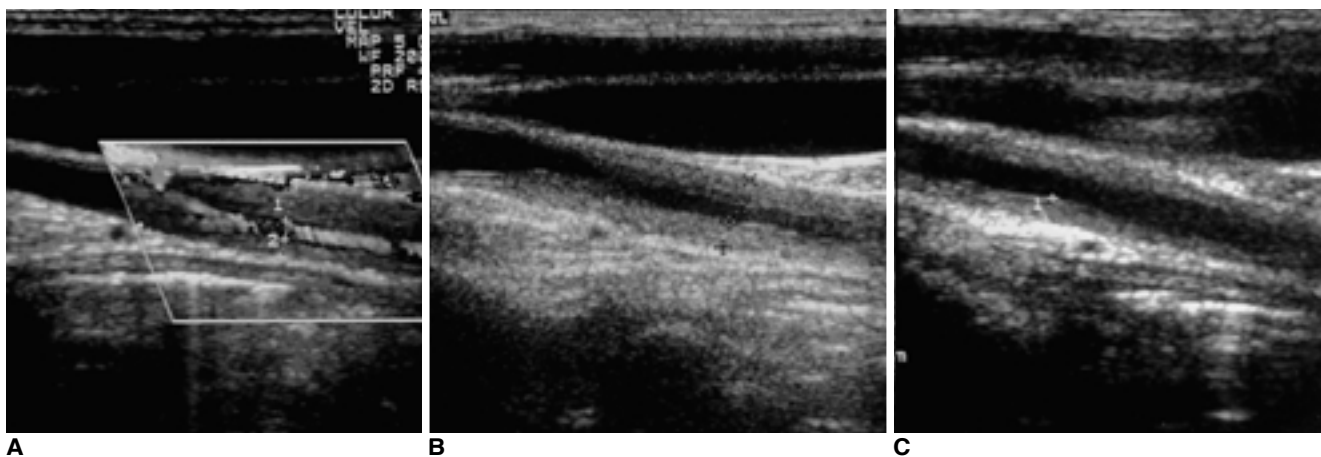


Fig. 2. Chronic and persistently active TA (40-year-old female).
A. Initial longitudinal sonogram reveals concentric wall thickening in the left common carotid artery.
B. A 2-year follow-up study shows still thick wall in the carotid artery.
C. After 4-years medical treatment, wall thickness was improved, but with residual thickening in the arterial wall. The patient also had recently aggravated bone and joint lesions.



Fig. 3. Acute TA with fever, general weakness, and anemia (25-year-old female).
A. Precontrast T1-weighted spin echo MR image shows mild wall thickening of the descending thoracic aorta (arrow) and pericardial effusion (asterisk).
B. Postcontrast spin echo MR image shows strong enhancement of the aortic wall and periaortic tissue (arrow).
C. Postcontrast spin echo MR image after medical treatment for 9 months shows improved wall thickness and minimal enhancement of the lesion.

ROI
가
가

가
, 40
가
가
5 - 7 mm

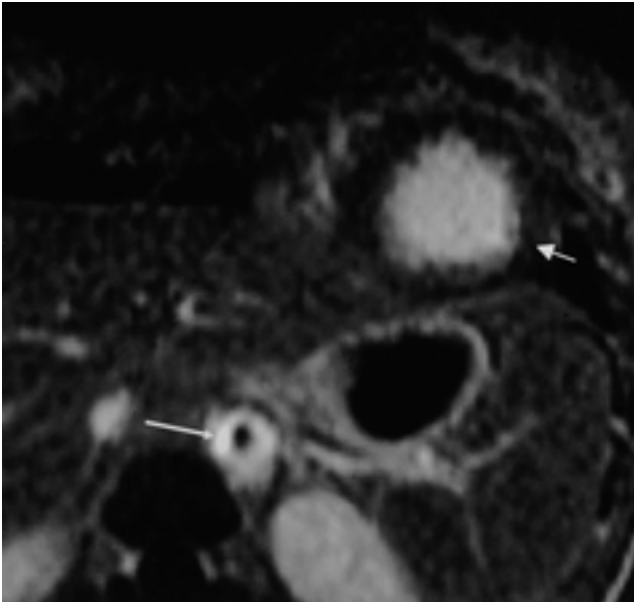


Fig. 4. Chronic active TA (16-year-old female). Postcontrast breath-hold MR imaging shows contrast accumulation in the wall of proximal abdominal aorta (long arrow). This special, fast SPGR-EPI hybrid sequence was originally designed for myocardial infarction imaging. The signal intensity of the normal myocardium (short arrow) is much lower than that of the aortic wall. Also note luminal stenosis of the aorta.

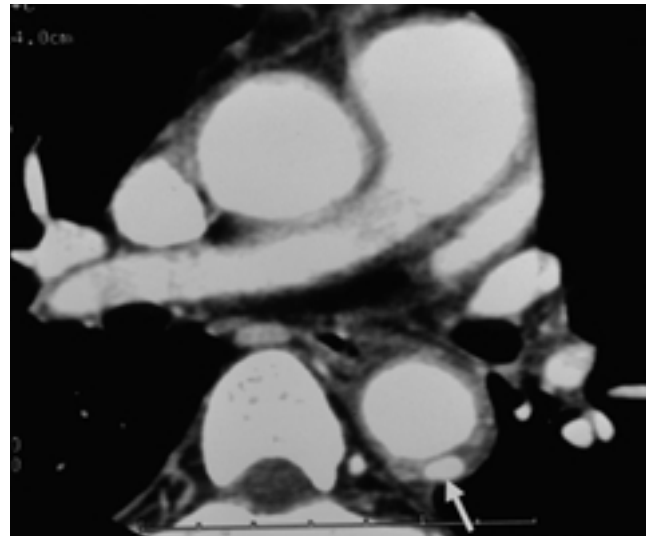
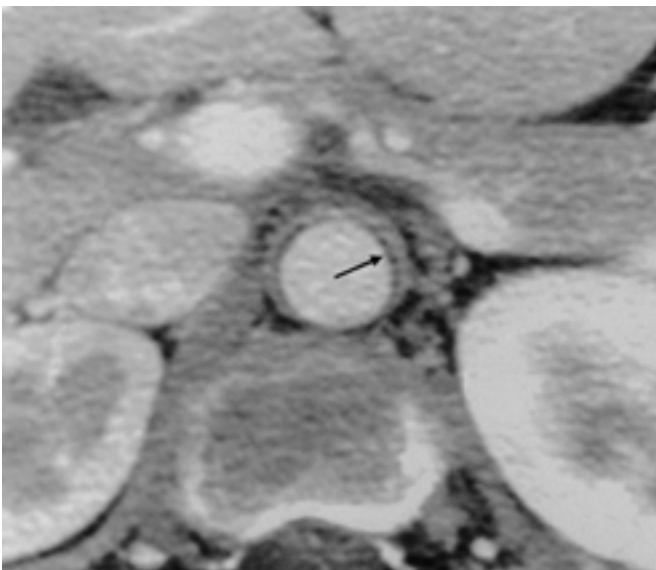
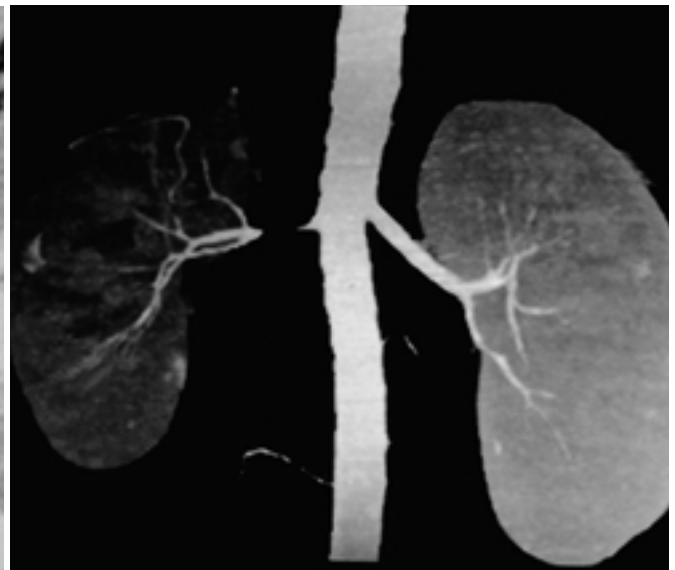


Fig. 5. Active TA in early vasculitis phase (25-year-old female). CT shows wall thickening with ulceration (arrow) in the descending thoracic aorta.



A Late Phase CT



B

Fig. 6. Chronic active TA with hypertension (15-year-old female).

A. Late phase postcontrast CT image shows concentric wall thickening of the abdominal aorta with mural enhancement. A low-attenuation ring (arrow) is seen in the inner wall.

B. Maximum intensity projection image of CT angiography shows severe stenosis of right renal artery in this patient.

mm 가 .
 가 .
 Glucocorticoid cyclophosphamide, methotrexate .
 MRI
 가 .
 (Fig. 2). (15) TA 9
 12 ESR, CRP 85
 mm/hr 28 mm/hr, 5.9 mg/dl 1.0 mg/dl (Figs 8, 9). 가
 가 2.8 mm 1.7 mm ,
 가 3.0 mm 1.9 mm CT MRI , CT angiography
 4.3 mm (CTA), MR angiography(MRA)가 TA
 3.7 mm , 2.7 mm 2.9 (16, 17) (Figs. 6, 10 - 14).

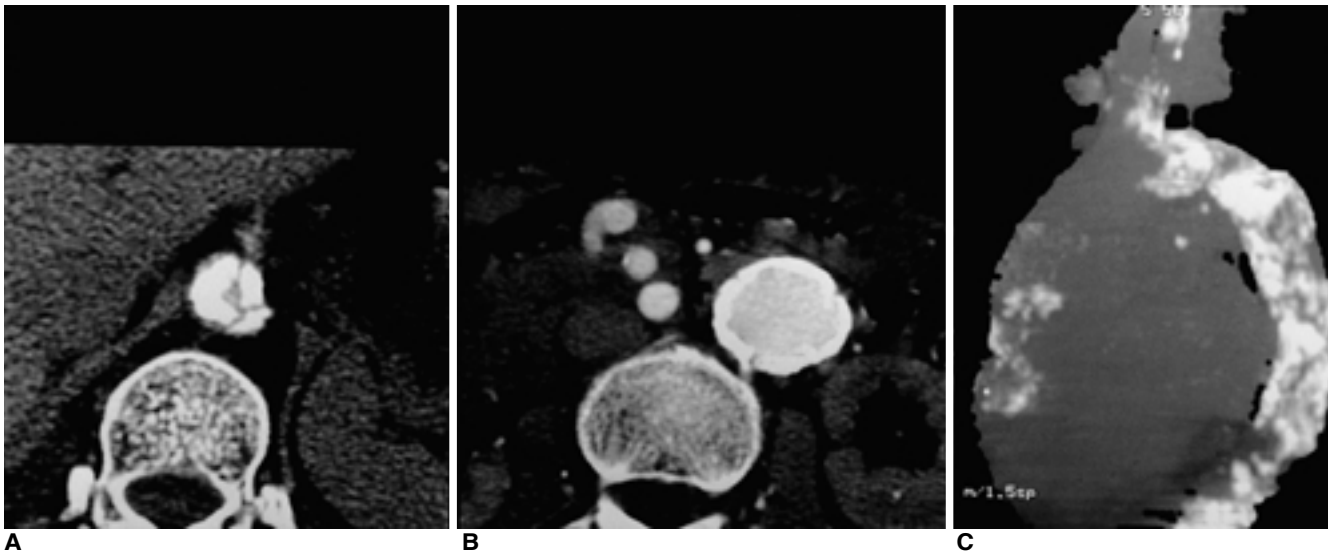


Fig. 7. Chronic sequelae of TA (54-year-old female).
A. CT shows dense calcifications with severe luminal stenosis of the descending thoracic aorta.
B. Aneurysmal change is also seen in the abdominal aorta.
C. Maximum intensity projection image of CT angiography shows diffuse calcifications in the thoracic aorta.

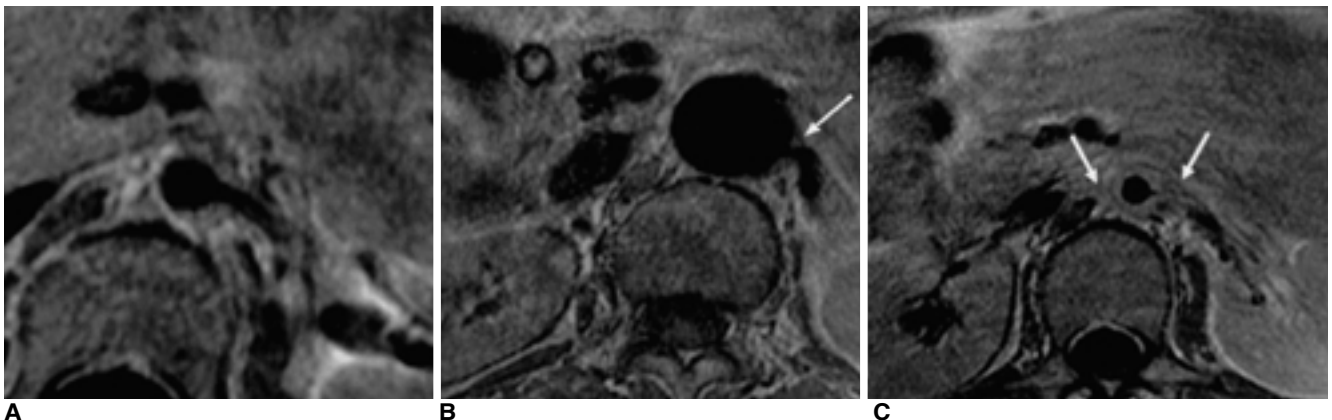


Fig. 8. Varying degrees of renal arterial involvement are shown by contrast-enhanced spin echo T1-weighted images.
A. Aortic mural thickening is visible in the renal artery ostium without stenosis in a patient in chronic active stage.
B. Mild stenosis of renal artery ostium (arrow) in chronic inactive stage.
C. Severe stenosis of both proximal renal arteries (arrows) due to aortic and renal artery wall thickening in chronic active

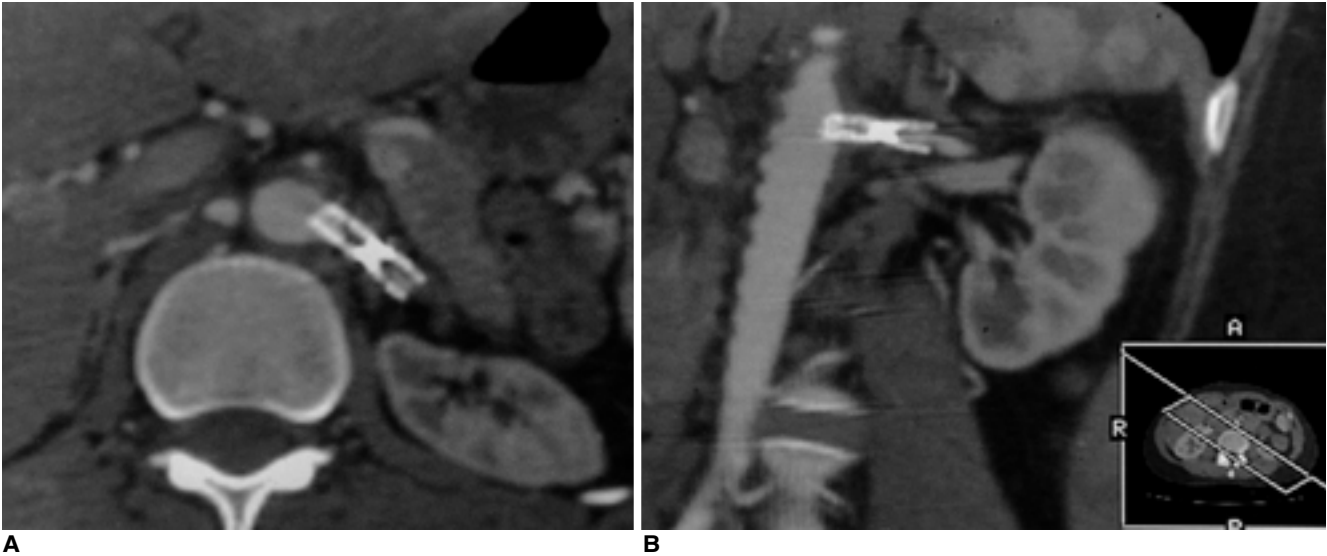


Fig. 9. Multislice CT angiography was performed to evaluate the patency of a renal artery stent in a 21-year-old female. Reformatted images along the long axis of the Palmaz stent (**A**, oblique axial; **B**, coronal views) shows stenosis in the mid portion of the stent due to insufficient expansion.



Fig. 10. Contrast-enhanced MR angiography demonstrates multiple arterial involvement in a 40-year-old male in fibrotic stage of TA. Note occlusion of both subclavian arteries and left distal superficial femoral and popliteal arteries, stenosis of left renal artery, and aneurysm of right popliteal artery.

, MRA, CTA
 가 가 .
 CTA가 MRA
 . MRA
 가
 가 MRA sequence
 moving -
 table technique
 spin echo
 MRA
 (Fig. 10).
 MRA
 MRI
 가
 cine MRI true FISP
 MRI
 (perfusion test),
 (Fig. 15). MR

가 . Multislice CT CTA

6. TA 가 , MRI, CT , MRI CT 가 , MRA, CTA가 (TA) TA , , , , 가 TA가 32 - 93% TA immunosuppressive therapy . NIH 60 20% TA



Fig. 11. Contrast-enhanced MR angiography was performed to evaluate the status of arch vessels in a 30-year-old female with chronic active TA. MIP image shows occlusion of right subclavian artery (arrow), diffusely narrowed right common carotid artery (short arrows), ectatic change of left common carotid artery (arrowheads), and focal stenosis of mid left subclavian artery (open arrow).

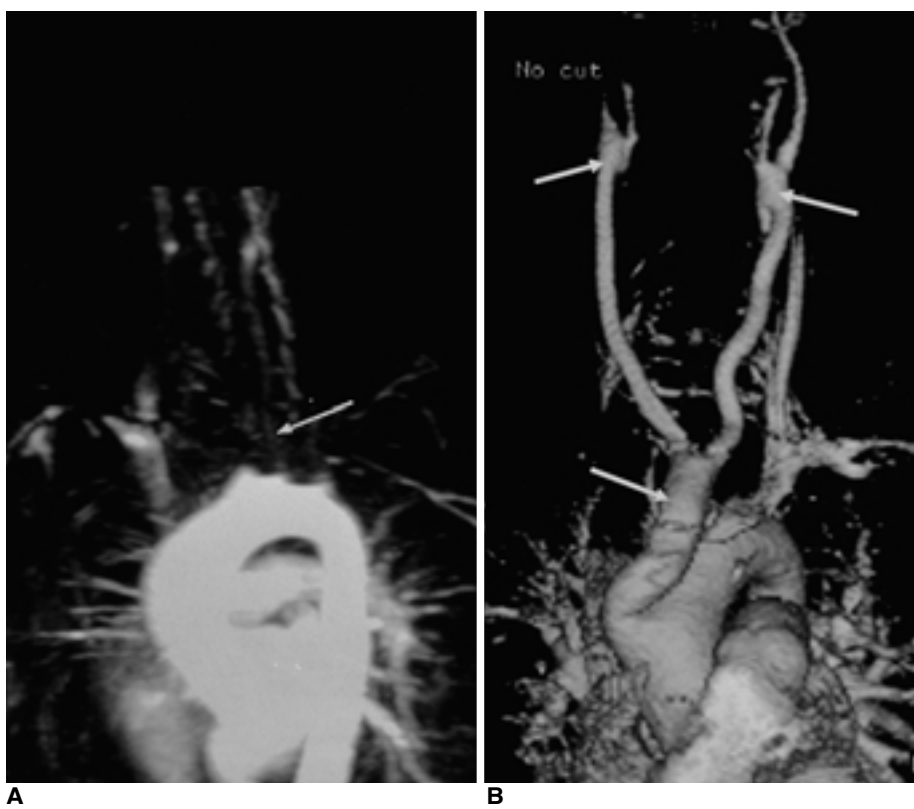


Fig. 12. Severe arch vessel involvement in a 38-year-old female.
A. Contrast-enhanced MR angiography (MIP image) shows occlusion of right innominate artery and right proximal-to-mid common carotid artery and severe stenosis of left common carotid artery (arrows) and left subclavian artery.
B. A follow-up MR angiography was performed after surgery. A Y-graft (arrows) from the ascending aorta to the both distal common carotid arteries is patent on a volume-rendered image.

immunosuppressive therapy가
 80% corticosteroid
 40% cytotoxic drug
 가 , 45% , 23% drug-free
 remission (18). immuno-suppressive therapy가

(19). , ,
 (extremity claudication)

(Table 2). , , ,
 가

. TA
 (lack of symptom,
 ESR, CRP)

TA aorta, renal artery, subclavian artery, carotid
 artery

1. (Fig. 16)

. suprarenal aorta renal

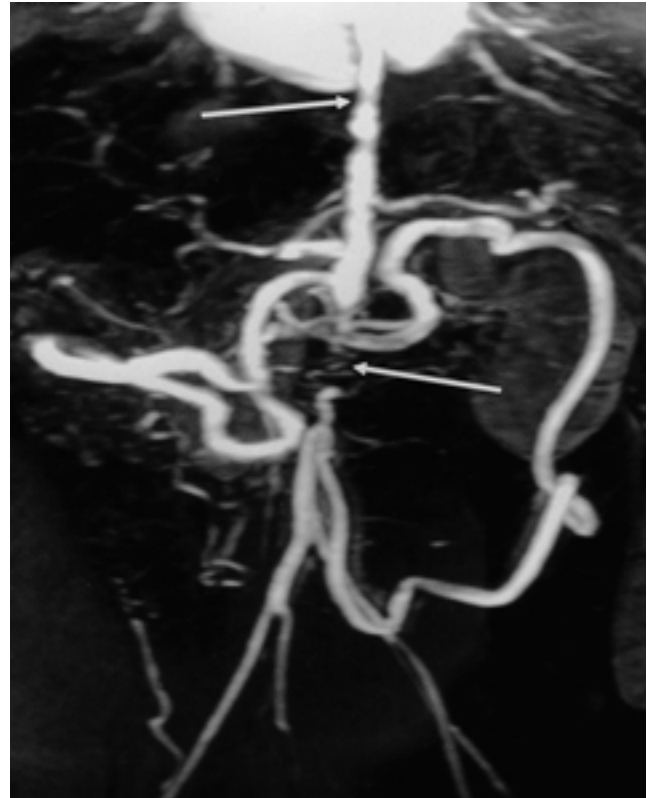
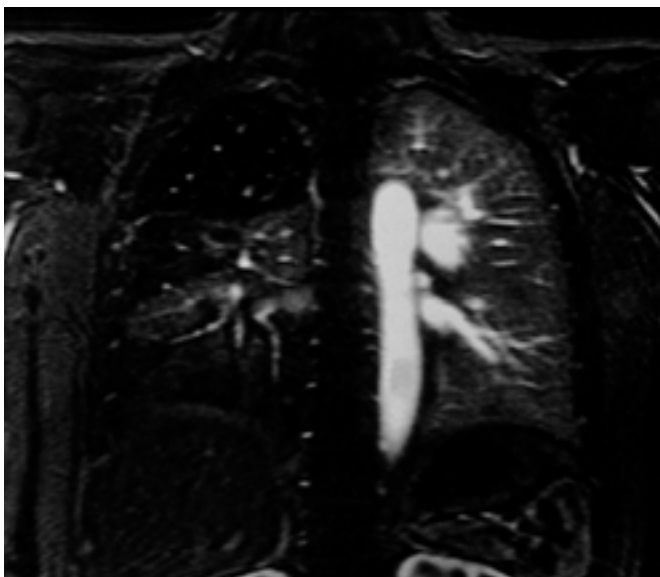
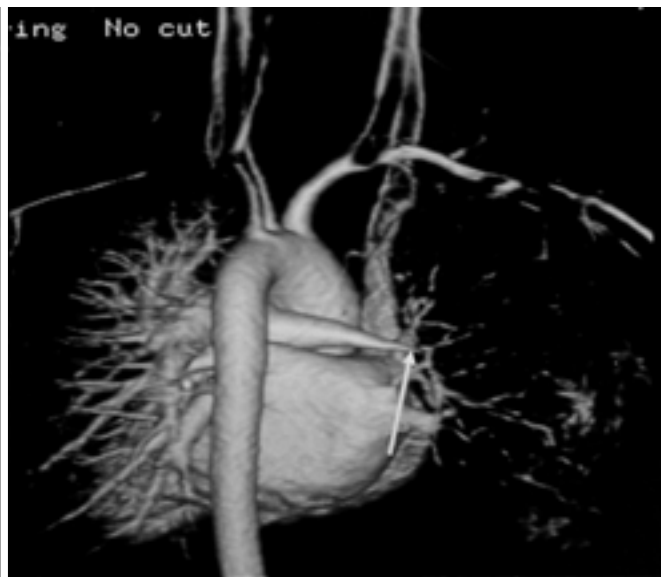


Fig. 13. Severe stenosis of abdominal aorta and distal thoracic aorta in a 49-year-old female in firotic stage. MIP image of contrast-enhanced MR angiography shows severe segmental stenosis of aorta (arrows) and well-developed collaterals between superior and inferior mesenteric arteries.



A



B

Fig. 14. Pulmonary artery involvement in a 35-year-old female with chronic active TA.

A. A source image of contrast-enhanced MR angiography shows large perfusion defects in the right lung.

B. A volume-rendered image (posterior view) of contrast-enhanced MR angiography shows pencil-sharp narrowing of the distal right pulmonary artery (arrow). Also note stenosis of right subclavian and both common carotid arteries and occlusion of left subclavian artery.

ischemia가 , myocarditis/
cardiomyopathy, valvular regurgitation
가
60 -
100%
가 15 - 30
2 - 4 . 90%
90%
60%
가

Table 2. Indications for angioplasty or revascularization

Hypertension in the setting of renal artery stenosis
Extremity ischemia limiting routine activities of daily living
Clinical features of cerebral ischemia and/or
critical stenosis of at least three cerebral vessels
Moderate aortic regurgitation
Coronary artery stenosis leading to ischemia

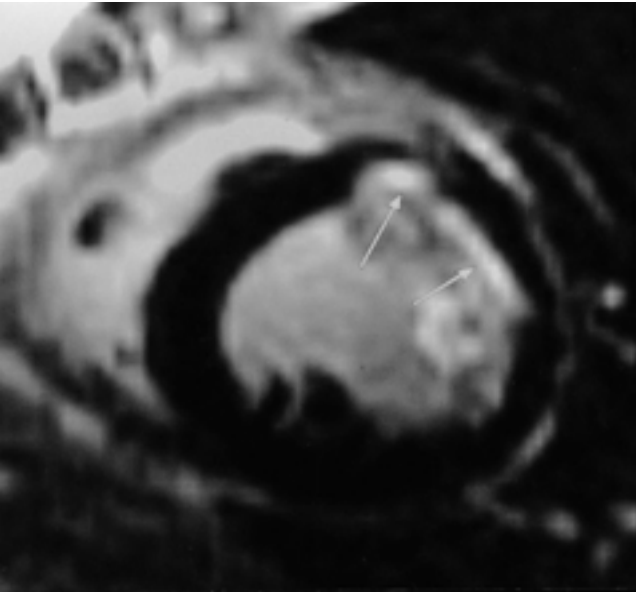
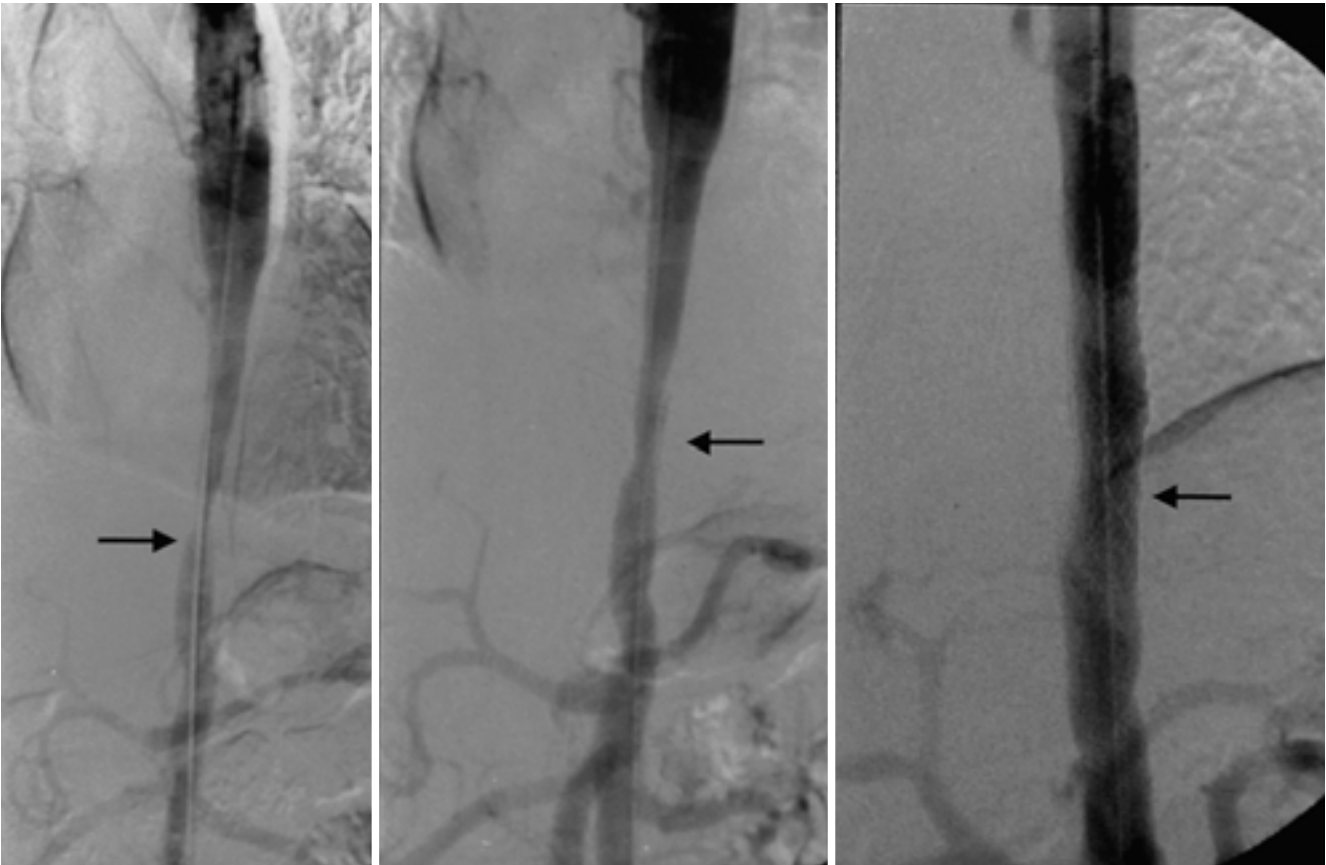


Fig. 15. Myocardial infarction demonstrated in a 34-year-old male with TA in fibrotic phase. A delayed myocardial image (short-axis view) obtained 5 minutes after contrast material injection shows hyperenhancement (arrows) in the superior wall suggestive of previous subendocardial infarction.



A
Fig. 16. A. Thoracic aortogram of a 33-years-old female with lower limb claudication and hypertension shows focal severe stenosis (arrow) of the descending thoracic aorta.
B. Aortogram after balloon angioplasty shows dissection (arrow) localized to the dilated segment with inadequate reduction of the stenosis.
C. Aortogram after Palmaz stent (arrow) shows marked improvement of the aortic lumen. Symptoms were resolved.

. (< 3 cm) 가
 20% 가
 6
 dissection
 obstructive dissection
 (20, 21). 36 - 60
 Fava 5
 가
 2/3
 (22,
 23). Tyagi obstructive
 dissec - tion, ineffective angioplasty, recurrent restenosis
 12 가
 91.6% 6 - 30
 2/5
 (24).
 dissection, ineffective angioplasty 가
 obstructive
 (27).
 100%
 2. (Fig. 17)
 TA
 3. (Fig. 18)
 TA 75%

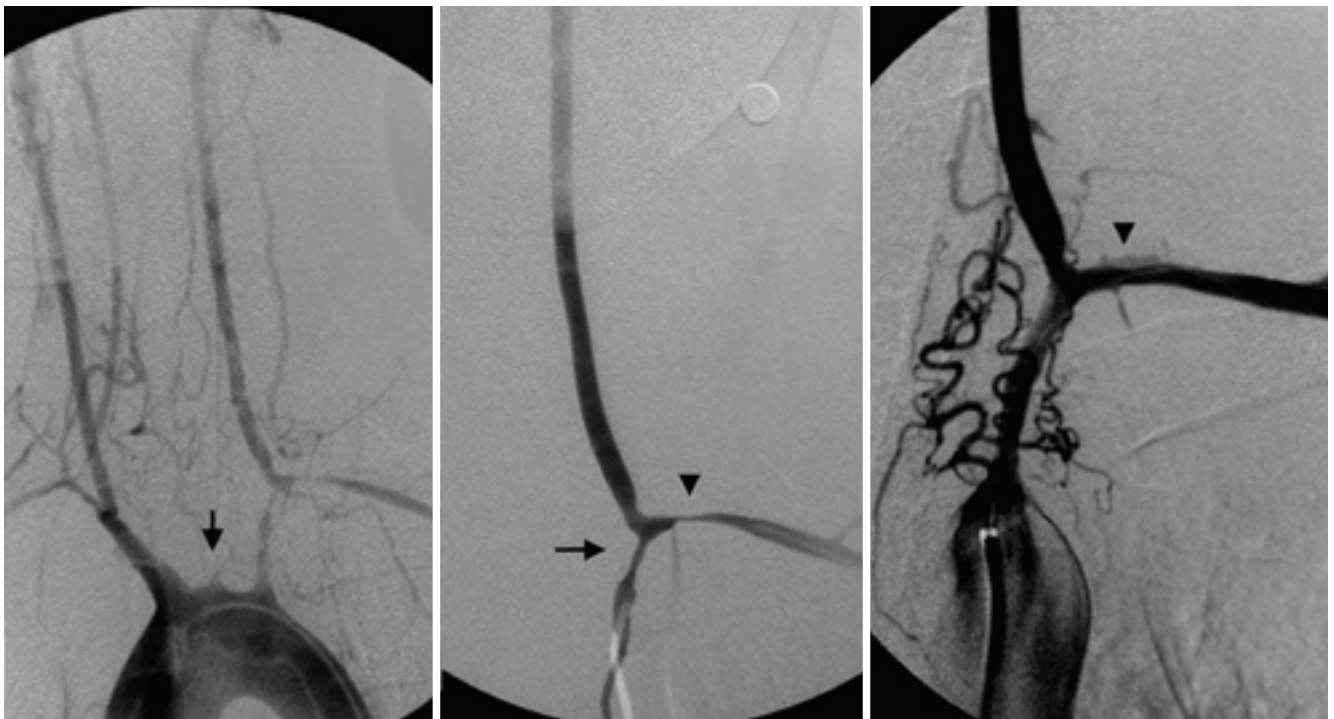


Fig. 17. A, B. Arch aortogram and left subclavian angiogram of a 22-years-old female with dizziness show total occlusion of left common carotid artery and severe stenosis of left subclavian artery.
C. Left subclavian angiogram after balloon angioplasty shows marked improvement of the lumen. There is focal dissection (arrow head) which does not disturb blood flow. Symptom was recurred due to restenosis 4 months later.

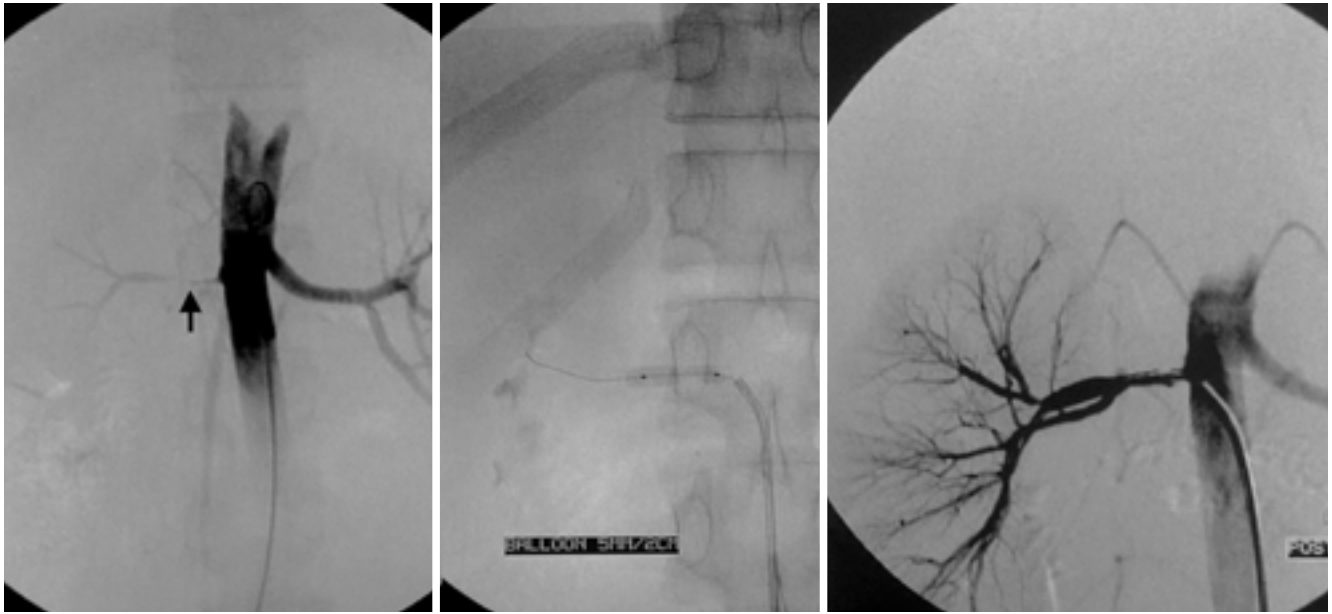


Fig. 18. **A.** Abdominal aortogram of a 16-year-old female with hypertension shows severe segmental luminal narrowing of right renal artery.
B. During balloon dilatation of right renal artery.
C. Abdominal aortogram after angioplasty shows improvement of the lumen.

TA
81 - 86% 1 - 18
21% (28, 29),
5 75%
가
(29).
가
(30).
dissection obstructive
dissection
4.
TA
obstructive dissection, ineffective angioplasty
가 , MR, CT, Doppler

1. Kerr GS. Takayasu's arteritis. *Rheum Dis Clin North Am* 1995; 21:1041-1058
2. Park Y-B, Hong SK, Choi KJ, et al. Takayasu arteritis in Korea: clinical and angiographic features. *Heart Vessels* 1992;7:55-59
3. 1984;27:431-437
4. Sueyoshi E, Sakamoto I, Hayashi K. Aortic aneurysm in patients with Takayasu's arteritis: CT evaluation. *AJR* 2000;175:1727-1733
5. Lie JT, members and consultants of the American College of Rheumatology Subcommittee on classification of vasculitis. *Arthritis Rheum* 1990;33:1074-1087
6. Ishikawa K. Diagnostic approach and proposed criteria for the clinical diagnosis of Takayasu's arteriopathy. *J Am Coll Cardiol* 1988;12:964-972
7. Arend WP, Michel BA, Bloch DA, et al. The American College of Rheumatology 1990 criteria for the classification of Takayasu arteritis. *Arthritis Rheum* 1990;33:1129-1134
8. Sharma BK, Jain S, Suri S, Numano F. Diagnostic criteria for Takayasu arteritis. *Int J Cardiol* 1996(Suppl);54:127-133
9. Kerr GS, Hallahan CW, Giordano J, et al. Takayasu arteritis. *Ann Intern Med* 1994;120:919-929
10. Raninen RO, Kupari MM, Pamillo MS et al. Ultrasonography in the quantification of arterial involvement in Takayasu's arteritis. *Scand J Rheumatol* 2000;29:56-61
11. Park SH, Chung JW, Lee JW, Han MH, Park JH. Carotid involvement in Takayasu's arteritis: evaluation of the activity by ultrasonography. *J Ultrasound Med* 2001;20:371-378
12. Carotid and subclavian sonography in

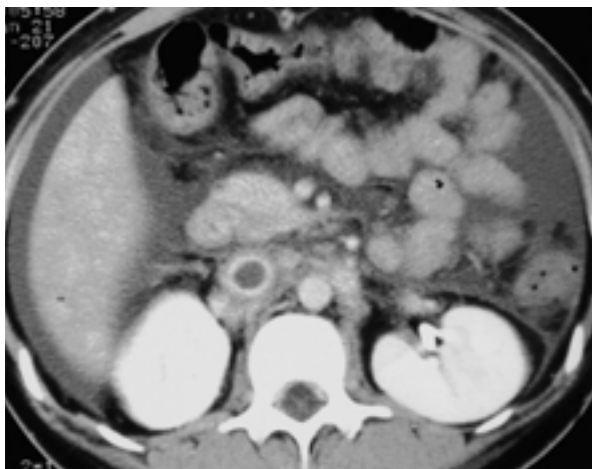
- the diagnosis of Takayasu 's arteritis. 2000; 19:361
13. Choe YH, Han B-K, Koh E-M, Kim D-K, Do YS, Lee WR. Takayasu 's arteritis: assessment of disease activity with contrast-enhanced MR imaging. *AJR* 2000;175:505-511
 14. Park JH, Chung JW, Im J-G, Kim SK, Park YB, Han MC. Takayasu arteritis: evaluation of mural changes in the aorta and pulmonary artery with CT angiography. *Radiology* 1995;196:89-93
 15. 2001; 31:II-250
 16. Yamada I, Nakagawa T, Himeno Y, Numano F, Shibuya H. Takayasu arteritis: evaluation of the thoracic aorta with CT angiography. *Radiology* 1998;209:103-109
 17. Choe YH, Kim D-K, Koh E-M, Do YS, Lee WR. Takayasu 's arteritis: diagnosis with MR imaging and MR angiography in acute and chronic active stages. *J Magn Reson Imaging* 1999; 10:751-757
 18. Kerr GS, Hallahan CW, Giordano J, et al. Takayasu arteritis. *Ann Intern Med* 1994;120:919-929
 19. Hoffman G. Treatment of resistant Takayasu 's arteritis. *Rheum Dis Clin North Ame* 1995;21:73-80
 20. Tyagi S, Khan AA, Kaul UA, Arora R. Percutaneous transluminal angioplasty for stenosis of the aorta due to aortic arteritis in children. *Pediatr Cardiol* 1999;20:404-410
 21. Tyagi S, Kaul UA, Nair M, Sethi KK, Arora R, Khalilullah M. Balloon angioplasty of the oarta in Takayasu 's arteritis: initial a long-term results. *Am Heart J* 19992;124:876-882
 22. Tyagi S, Kaul UA, Nair M, et al. Balloon angioplasty of the aorta in Takayasu 's arteritis: initial and long-term results. *Am Heart J* 1992;124:876-882
 23. Fava MP, Foradori GB, Garcia CB, et al. Percutaneous transluminal angioplasty in patients with Takayasu arteritis: five-year experience. *J Vasc Interv Radiol* 1993;4:649-652
 24. Tyagi S, Kaul UA, Arora R. Endovascular stenting for unsuccessful angioplasty of the aorta in aortoarteritis. *Cardiovasc Dis* 1999;22:452-456
 25. Joseph S, Mandalam KR, Rao VR, et al. Percutaneous transluminal angioplasty of the subclavian artery in nonspecific aortoarteritis: results of long-term follow-up. *J Vasc Interv Radiol* 1994;5:573-580
 26. Tyagi S, Verma PK, Gambhir DS, Kaul UA, Saha R, Arora R. Early and long-term results of subclavian angioplasty in aortoarteritis (Takayasu disease): comparison with atherosclerosis. *Cardiovasc Intervent Radiol* 1998;21:219-224
 27. Bali HK, Jain S, Jain A, Sharma BK. Stent supported angioplasty in Takayasu arteritis. *Int J Cardiol* 1998;66(Suppl 1):S205-211
 28. Sharma S, Saxena A, Talwar KK, Mehta SN, Rajani M. Renal artery stenosis caused by nonspecific arteritis (Takayasu disease): results of treatment with percutaneous transluminal angioplasty. *AJR* 1992;158:417-422
 29. Deyu Z, Lisheng L, Ruping D, Haiying W, Guozhang L. Percutaneous transluminal renal angioplasty in aortoarteritis. *Int J Cardiol* 1998;66(Suppl 1):S205-211
 30. Arora P, Kher V, Singhal MK, et al. Renal artery stenosis in aortoarteritis: spectrum of disease in children and adults. *Kidney Blood Press Res* 1997;20:285-289

Vascular Involvement of Behcet 's Syndrome

(Behcet 's syndrome)

가

(1). 가 3.4 - 26%
97%가 (superficial thrombophlebitis) 가
(erythema nodosum) , (acne) 25%
(papular) (Fig. 1) (2). 114
10.5%
가 (3). 3.6%
(underlying disease) 1731 41
20 40



A



B

Fig. 1. 23-year-old female with Behcet 's disease was admitted due to lower extremity swelling.
A. Contrast enhanced CT scan taken at venous phase shows complete obstruction and thrombus filling of IVC.
B. IVC venogram shows complete occlusion of infrarenal IVC and multiple retroperitoneal and paravertebral collateral venous drainage.

(4). 가 가

3.6 - 25

(4, 5). Hasan 2179

24

(6).

12 1

(neutrophil), (lymphocyte),

(plasma cell) (media)

(adventitia) (vasa

vasorum) (muscle

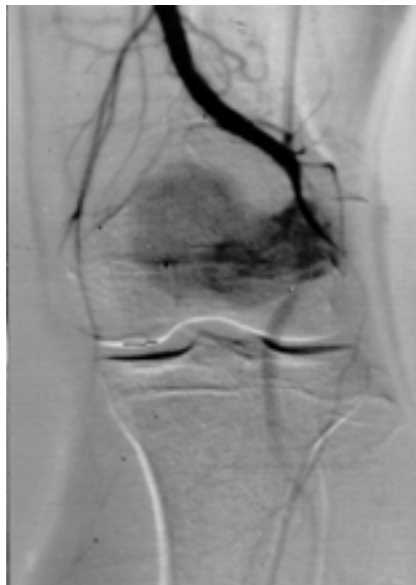
cell)

가

1.5 - 2.2 % (7). (transmural



A



B

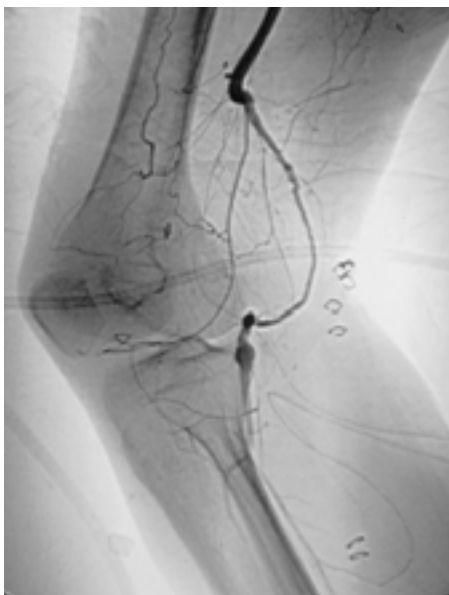
Fig. 2. 31-year-old man had been admitted due to the calf pain and claudication.

A. Sagittal T-1 weighted MR image shows large pseudoaneurysm in popliteal fossa.

B. Digital subtracted angiography shows contrast filling into the pseudoaneurysm sac that arises from the popliteal artery.

C. He underwent the autologous saphenous venograft.

D. 27-months after the operation, his symptoms were recurred. Popliteal arteriogram shows recurrent pseudoaneurysm in distal anastomosis site of graft, which was not resolved by the compression treatment.



C



D

necrosis) 가 , 10
가 가 , 1
- (aortoenteric fistula) 1 55 15.7 ± 16.2
(9). 12 5 가 2 25
가 (13.6) (16).
azathioprine, chlorambucil,
가 cyclophosphamide 가
(17, 18). Huong
가 60% (10). 2 67%
(interposition) 가 가 가 20% , 가
가 (Fig. 2), 가 100% (17).
(extra - anastomotic) 가 가 가
(endothelium) 가 가 가
(11 - 13). 가
(ligation) 가
(1, 14).
. Okada 8
4
(14), Sasaki 4
2
(15). , 12
coil histoacryl
가 (Fig. 3). 가 (stent -

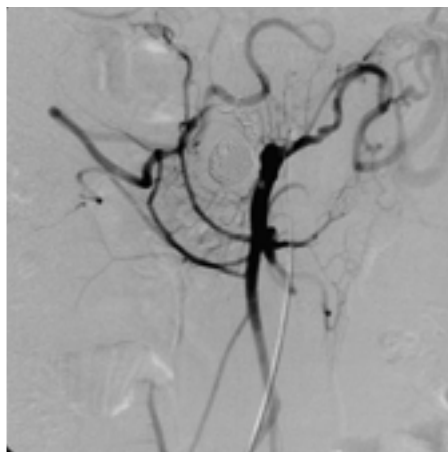
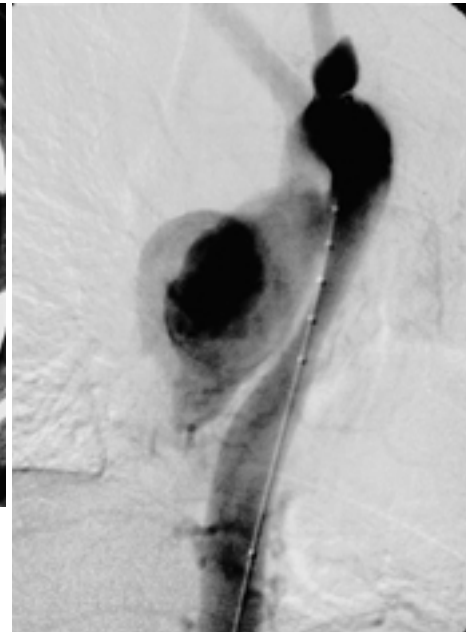


Fig. 3. A pseudoaneurysm at the proximal common hepatic artery (CHA) in 32-year-old male patient.
A. CHA is originated from the superior mesenteric artery. A pseudoaneurysm is arising at the proximal CHA.
B. Aneurysm sac was embolized with multiple Guglielmi detachable coils and platinum coils.

graft) (bifurcated) 가 6
mm 가 가 (19), Bonnotte
90% 가 (Fig. 4). 가 coil 6
, (20). 가
3 가
. Vasseur



A



B



C



D

Fig. 4. A, B. A 37-year-old man with Behcet 's disease. Contrast enhanced CT scan (**A**) and aortogram (**B**) shows 10×8×6 cm sized large saccular aneurysm in the proximal descending thoracic aorta, which is suggested to be a pseudoaneurysm from Behcet 's vasculitis. Aortic lumen is compressed and displaced to left antero-lateral aspect by the aneurysm. **C.** 30 mm diameter, 9 cm length stent-graft was deployed upon the aneurysm inlet and aneurysm sac is completely excluded on aortogram. **D.** On 6 months follow-up CT scan, the thrombosed aneurysm is resolved remaining the minimal periaortic soft tissue densities.

, 6-59 (: 28)

가

1

3

(21).

가 9

azathioprine prednisolone

13-24

11 9

2 가 가

가

(22).

가

가

가

1. International Study group For Behcet's Disease. Criteria for diagnosis of Behcet disease. *Lancet* 1990;335:1078-1080
2. Wechsler B, Thi HDL, Gennes C, et al. Arterial manifestations of Behcet's disease. 12 cases. *Rev Med Interne* 1989;10:303-311
3. Eun HC, Chung H, Choi SJ. Clinical analysis of 114 patient with Behcet's disease. *J Korean Med Assoc* 1984;27:933-937
4. Koc Y, Gullu I, Akpek G, et al. Vascular involvement in Behcet's disease. *J Rheumatol* 1992;19:402-410
5. Hamza M. Large artery involvement in Behcet's disease. *J Rheumatol* 1987;14:554-559
6. Tuzun H, Besirli K, Sayin A, et al. Management of aneurysms in Behcet's syndrome: An analysis of 24 patients. *Surgery* 1997; 121:150-156
7. Matsumoto T, Uekusa T, Fukuda Y. Vasculo-Behcet's disease: a pathologic study of eight cases. *Hum Pathol* 1991;22:45-51
8. Koike S, Matsumoto K, Kokubo M. A case of aorto-enteric fistula after reconstruction of abdominal aortic aneurysm

associated with Behcet's disease and reference to reported 95 cases in Japan. *Jpn J Surg* 1988;89:945-951

9. Dhobb M, Ammar F, Bensaid Y, Benjelloun A, Benabderrazik T, Benyahia B. Arterial manifestations in Behcet's disease: four new cases. *Ann Vasc Surg* 1986;1:249-252
10. Bruce PR, Michael LM, Victoria JT, Harold AM. Endoluminal repair of an internal carotid artery pseudoaneurysm. *JVIR* 1998;9:245-248
11. 가 Stent-Graft 1. *Korean Circulation J* 1998;28:1404-1408
12. Freyrie A, Paragona O, Cenacchi G, Pasquinelli G, Guiducci G, Faggioli GL. True and false aneurysms in Behcet's disease: case report with ultrastructural observations. *J Vasc Surg* 1993;17:762-767
13. Jenkins AMcL, Macpherson AIS, Nolan B, Housley E. Peripheral aneurysms in Behcet's disease. *Br J Surg* 1976;63: 199-202
14. Okada K, Eishi K, Takamoto S, et al. Surgical management of Behcet's aortitis: a report of eight patients. *Ann Thorac Surg* 1997;64:116-119
15. Sasaki S, Takigami KY, Shiiya N, Matsui Y, Sakuma M. Surgical experiences with peripheral arterial aneurysms due to vasculo-Behcet's disease. *J Cardiovasc Surg* 1998;39:147-150
16. 2002; 35:36-42
17. Huong DLT, Wechsler B, Papo T, et al. Arterial lesions in Behcet's disease. A study in 25 patients. *J Rheumatol* 1995;22: 2103-2113
18. Hamuryudan V, Yurdakul S, Moral E, et al. Pulmonary arterial aneurysms in Behcet's syndrome: A report of 24 cases. *Br J Rheumatol* 1994;33:48-51
19. Vasseur MA, Haulon S, Beregi JP, Le Tourneau T, Prat A, Warembourgh H. Endovascular treatment of abdominal aneurismal aortitis in Behcet's disease. *J Vasc Surg* 1998;27: 974-976
20. Bonnotte B, Krause D, Ranton AL, et al. False aneurysm of the internal carotid artery in Behcet's disease: successful combined endovascular treatment with stent and coils. *Rheumatology (Oxford)* 1999;38:576-577
21. Park JH, Chung JW, Joh JH, et al. Aortic and arterial aneurysms in Behcet's disease: management with stent-grafts; initial experience. *Radiology* 2001;220:745-750
22. Koo BK, Shim WH, Yoon YS, et al. Endovascular therapy combined with immunosuppressive treatment for pseudoaneurysms in patients with Behcet's disease. *J Endovasc Ther* 2002;(under revision)

슬와동맥 포획 증후군

Popliteal Artery Entrapment Syndrome

조 준 희

순천향대학교 의과대학

1. Introduction

슬와동맥은 다이아몬드 모양의 popliteal fossa에서 피하지방층의 아래에 위치하는 동맥으로 슬와정맥과는 평행하게 주행하고 있다. 이들 중, 정맥은 비복근(gastrocnemius muscle) medial head의 외측에 위치하며, 이들 사이의 구조적인 결함으로 혈류장애에 의한 환자의 증상을 유발하는 질환을 슬와동맥 포획 증후군(popliteal artery entrapment syndrome: PAES)이라 한다. 슬와동맥 포획(Popliteal artery entrapment: PAE)은 해부학적으로 알려지기는 오래되었으나, 임상에서 진단되고 치료되기는 비교적 오래지 않은 일이다. 초기에는 단지 이들 근육과 혈관의 주행관계의 이상만 파악되었으나, 점점 증례가 증가하면서 여러 가지 구조물들의 복합적인 변이로 설명되고 있으며, 동맥 주행방향의 이상, 근육의 abnormal insertion, 정맥의 이상 소견 및 신경 분지와와의 관계 등을 기준으로 현재까지 다섯 가지 category로 분류되어 사용되고 있다.

PAE는 초기에는 주로 일측성이 많이 보고 되었으나, 점차 양측성인 증례가 증가하고 있으며, 많게는 양측성이 50%에 육박할 것으로 판단된다. 환자는 주로 동맥허혈증상을 보이며, 평소에 건강하던 사람이 갑자기 파행을 보이며 병원을 찾게 된다. 치료는 해부학적인 이상을 교정해 주는 목적으로 시행되어야 하며, 동맥폐색, 동맥류형성 등의 합병증이 발생하기 이전에 하는 것이 좋다. 과거에는 혈관조영술이 diagnosis of choice 였지만, 도플러, CT, MR등을 이용한 근육과 동맥, 정맥의 이상에 대한 보고가 점점 많아지고 있다.

2. Historical Background

Scotland의 Edinburgh에서 1879년 당시 의학도였던 T. P. Anderson Stuart가 60대 남자의 절단된 다리를 해부하던 중 슬와동맥의 주행이 이상하다는 것을 발견했고, 그는 이를 "... The popliteal artery, after passing through the

opening in the adductor magnus, instead of, as it usually dose, coursing downwards and outwards towards the middle of the popliteal space, so as to lie between the two heads of the gastrocnemius muscle, passes almost vertically downward internally to the inner head of the gastrocnemius. It reaches the bottom of the space by turning that head, and then passes downwards and outwards beneath it ..."으로 기록했다고 알려지며, 이 기록이 현재까지 알려진 PAE에 대한 최초의 기록이라고 알려져 있다. 그 뒤 약 80년이 흐른 뒤에 PAE에 의한 합병증을 치료한 것이 발표되었는데, 1959년 Netherlands의 Hamming JJ의 보고였다. 슬와동맥 포획 증후군이라는 용어는 1965년 Love JW와 Whelan TJ에 의해 처음으로 사용되었으며, 1967년 Rich NM 등은 슬와정맥의 포획에 대해 기술하면서 비복근의 medial head의 이상소견에 대해서도 함께 기술하였다. 이후 여러 병원에서 새로운 증례들에 대한 보고들이 나왔으며, 특히 미국의 군병원에서 많은 환자들이 보고되었다.

3. Pathophysiology and Classification

이 질환의 원인은 선천성 기형으로 설명되며, 초기에 발표된 논문들에서는 비복근에 의해 슬와동맥 또는 정맥이 눌려 증상을 일으키는 것으로 설명되었으나, 이후 fibrotic band, 신경, 근육의 accessory head 등에 의한 혈관의 압박 등으로도 발생되며, 때로 bypass graft 수술 이후에도 발생되고 있다. 또한, 해부학적 이상이 없는 경우에서도 비슷한 증상을 일으키는 경우가 보고되고 있으며, functional PAE라는 용어로 분류된다. PAE를 일으켰던 혈관의 조직학적 검사의 소견은 혈관의 혈전, 협착, longitudinal muscle of tunica media의 proliferation, 내막비후, 협착후 확장, 동맥류형성 등을 보이며, 이는 혈관벽의 외부 압박에 의한 반복적인 외상이 그 기전일 것으로 설명된다. 이러한 변화는 동맥경화에 의한 혈관벽의 변화와는 구분되어지며, 이러한 사실은 동맥경화의 가능성이 상대적으로 낮은 젊은 운동선수 등 근육질의

체격을 가진 사람에서 비교적 많이 증상을 일으키는 것을 설명하기도 한다.

초기 이 질환에 대한 분류는 1970년 Insua JA 등에 의해 시작되었으며, 이후 1979년 Rich NM 등에 분류가 추가되어 현재까지 가장 많이 인용되어 오고 있다. 이들에 의한 분류를 보면 다음과 같다.

Type I. 비복근의 medial head는 정상적인 위치에서 기시하는 것으로 관찰되며, 슬와동맥이 이 근육의 내측으로 감아 돌면서 아래로 주행하는 모양을 보인다.

Type II. 비복근의 medial head가 정상보다 약간 외측에서 기시하는 경우로 슬와동맥은 비교적 정상적인 주행을 하는 듯이 보이나, 근육 때문에 약간 내측으로 전위되어 있다.

Type III. 비복근의 original medial head는 정상적인 위치에 있으며, 슬와동맥도 정상적인 주행을 하고 있으나, 비복근 medial head의 accessory slip이 있어 이에 의해 슬와동맥이 눌러지는 경우이다.

Type IV. 슬와동맥이 비복근의 구조물이 아닌 deep popliteus muscle, 또는 다른 fibrous band에 의해 눌러지는 경우로, 이 경우에는 슬와동맥이 비복근의 medial head를 내측으로 감아 도는 이상 소견(Type I)이 동반되거나, 정상적인 경우도 같이 포함되어 분류되며, 두 경우 모두에서 동맥이 눌러지는 곳은 비복근이 아닌 popliteus muscle, 또는 fibrotic band가 있는 level이다.

Type V. 상기 기술한 어떤 분류에 상관 없이, 슬와동맥과 정맥이 동반되어 압박을 받는 경우에 type V로 분류된다.

4. Clinical Presentation

이 질환은 환자의 대부분이 calf 이하의 파행을 주소로 병원을 찾게 되며, 특히 동맥경화의 위험인자가 적은 젊은 사람이 이 증상을 호소하는 경우에 반드시 감별 대상에 포함되어

야 할 질환이다. 이외에 cramping, coldness, blanching, paresthesis, numbness, rest pain, leg ulcer등의 증상을 보이기도 한다. 이러한 증상은 동맥협착의 정도, 측부순환의 발달 유무 등에 연관되어지며, 대부분이 만성 진행성 증상을 나타낸다. 그러나, 동맥의 만성변화 (협착후확장, 동맥류 형성) 이후에 급성 혈전, 원위부 색전 등에 의한 급성 증상을 나타내기도 한다.

이 질환의 기본 개념이 비복근 등 근육의 기형에 근거한 것이기 때문에 근육을 과다하게 사용하는 운동 이후에 증상이 발병되는 경우가 많으며, 활동적인 사람에게서 상대적으로 증상의 발현 가능성이 높다.

발병률은 정확하게 알려져 있지 않으며, 보고자에 따라 0.16%에서 많게는 3.5%까지 변이가 심하며, 남자에서 여자보다 흔하게 나타난다. 양측성 PAES는 초기에는 많이 보고되지 않았으나 점점 진단되는 환자가 많아짐에 따라 양쪽을 침범한 경우가 많이 보고되는데, 저자에 따라 20% 내외에서 67% 까지 보고하고 있다. 그러나, 양측성인 경우라도 한쪽만의 증상을 호소하는 경우가 대부분이므로, PAES를 의심하는 환자에서 증상을 나타내지 않은 반대편의 다리를 검사하는 것은 필수적이라 하겠다.

이학적 검사로 슬와동맥 및 dorsalis pedis등의 동맥 혈류를 직접 만져 보는 것, treadmill test, 발을 active dorsiflexion 시키면서 stress test를 하는 동안에 동맥 혈류를 직접 만져 보는 것 등이 도움이 된다.

5. Diagnostic Imaging

1) Doppler examination

초음파를 이용한 검사는 color wave Doppler 및 duplex scan이 가능하며, bed-side study로 가능하고, 비침습적 검사의 대표적인 검사방법으로 슬와동맥의 주행을 직접 볼 수

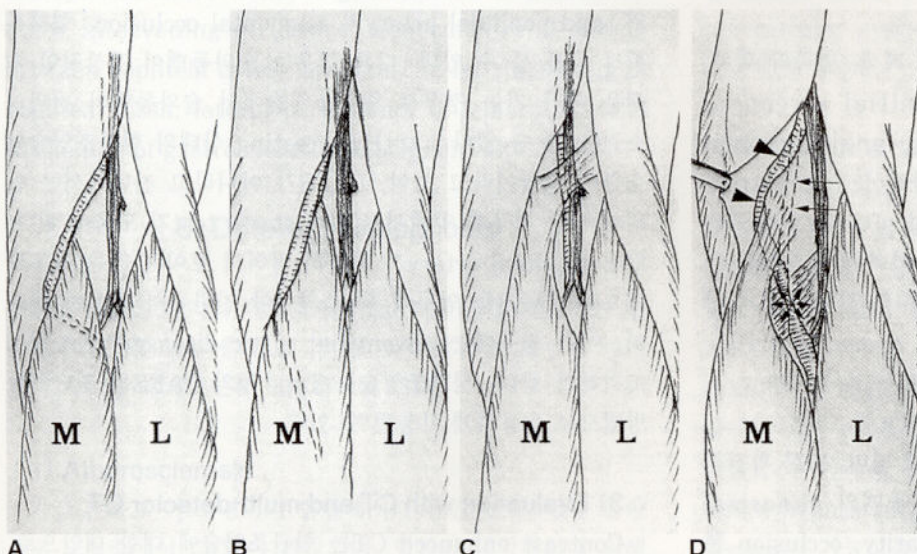


Fig. 1. Types of PAES. A: type I, B: type II, C: type III, D: type IV. Especially with type IV, popliteal artery can go down along each lateral (arrowheads) and medial (arrows) side of gastrocnemius muscle, but popliteal artery is compressed (asterisk) at the level of abnormally thickened popliteus muscle or fibrotic band, not at the level of gastrocnemius muscle. Legends: popliteal artery (A), popliteal vein (V), medial (M) and lateral (L) head of gastrocnemius muscle. (Adapted from Insua JA, et al. Popliteal artery entrapment syndrome, Arch Surg 1970, 101:771)

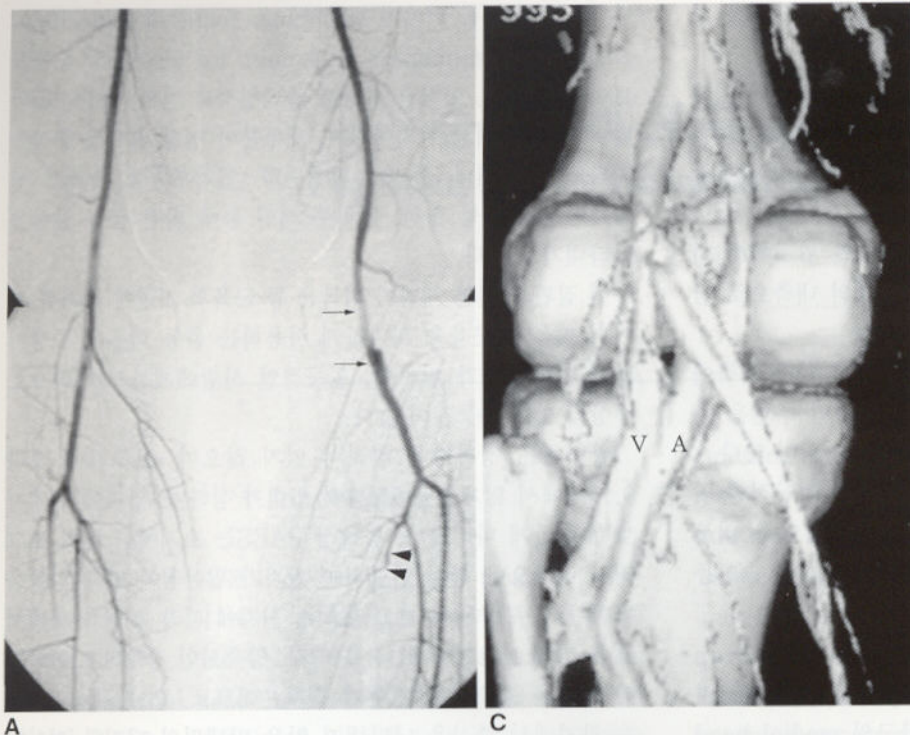
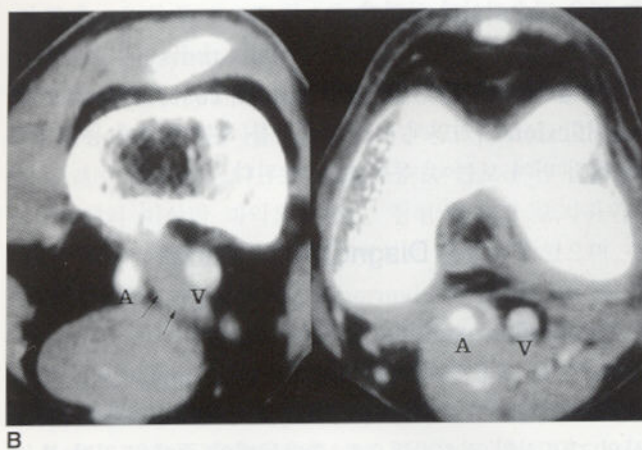


Fig. 2. Type II PAES.

A. Conventional angiography of a 38-year-old man shows slight medial displacement of left popliteal artery with luminal stenosis and post-stenotic dilatation (arrow). Also notes abrupt cut-off of posterior tibial artery (arrowheads), suggestive of distal embolism.

B. Axial scan of CT shows more lateral attachment of the medial head (arrows) of the gastrocnemius muscle intervening between popliteal artery (A) and vein (V), and in inferior aspect, popliteal artery is somewhat enlarged and partially thrombosed.

C. CT-angiography shows a wide spread between popliteal artery and vein, but it does not show distal embolism.



도 있으며, 슬와동맥의 혈류를 봄으로써 폐색, 협착의 위치, 협착후동맥류 등을 관찰할 수 있어 initial screening method로서의 진가를 발휘한다. 또한, ankle/brachial index를 얻을 수 있으며, scanning을 하면서 동시에 stress test가 가능해 많은 정보를 얻을 수 있다. 그러나, 비복근을 비롯한 근육의 주행을 모두 평가하기가 어려워 추가적인 검사가 필요하게 되며, 시술자의 숙련도에 따라 진단이 되지 않을 가능성 등이 있다.

2) Angiographic demonstration

가장 고전적인 방법이지만, 가장 기본이 되며, 또한 확진적인 검사법이라 할 수 있다. 이는 슬와동맥의 abnormal appearance, course, luminal irregularity, occlusion 뿐

만 아니라, 상하의 다른 혈관의 상태 및 distal run-off, occlusion, degree of development of collateral flow, level of reconstituted artery below knee, thrombosis, level and extent of diseased segment 등을 확인할 수 있고, 협착후동맥류의 정도 및 범위 등을 비교적 쉽게 할 수 있다. 혈관조영술은 시술 도중에 rest 상태의 image 뿐 아니라, 환자의 발을 active plantar flexion, passive dorsiflexion 하는 등으로 stress test를 시행할 수 있다. 혈관조영술만을 기준으로 할 때, PAES를 크게 두 가지의 부류로 나눌 수가 있는데, 첫째는 슬와동맥이 내측전위 되어 있는 경우로 resting 상태의 혈관조영술에서 슬와동맥의 내측전위, mid-popliteal artery의 segmental occlusion, 협착후 확장 등을 볼 수 있다. 다른 경우는 슬와동맥이 정상적인 주행을 따라 가는 경우로 혈관조영술에서 슬와동맥의 전위의 소견을 볼 수 없다. 그러므로, resting 상태의 혈관조영술의 소견이 정상이라고 하여, PAES가 아니라고 진단해서는 안 되며 이런 경우에 앞에서 설명한 stress test가 도움이 된다. Mid-popliteal artery가 완전히 막혀서 보이지 않는 경우도 있으며 PAES를 염두에 두고 있어야 진단에서 놓치지 않으며, 이런 경우에는 adventitial cystic disease의 가능성도 고려해야 한다. 정맥조영술은 Type V의 PAES를 진단하는 방법으로 유용하게 사용될 수 있다.

3) Evaluation with CT and multi-detector CT

Contrast enhanced CT는 혈관조영술에 대한 대안으로,

심하지 않은 증상을 호소하는 모든 환자들을 대상으로 비교적 쉽게 검사할 수 있으므로 초기 검사로 이용될 수 있다. 또한 CT는 기본적으로 cross sectional image를 보여주며, 슬와동맥 자체뿐 아니라, 주위의 근육 등 연부조직 병변도 같이 보여주고 이들 사이의 관계도 보여줌으로써 진단에 도움을 준다. 슬와동맥이 완전 폐색되어 있는 경우에 혈관조영술에서는 보이지 않는 thrombosed arterial structure를 보여주며, bony protrusion, intervening muscle 등이 있는 경우에도 이를 보여주며, 증상을 나타내지 않는 반대쪽을 동시에 검사할 수 있는 것도 하나의 큰 장점이다. 최근 널리 이용되고 있는 multidetector-CT는 이러한 기존 CT의 장점을 가질 뿐 아니라 reconstruction image등을 이용하여 실제 혈관조영술을 하는 것과 같은 좋은 화질의 영상을 보여줌으로써 혈관조영술을 대체 할 수 있을 것으로 본다.

4) Imaging with MR

MR은 CT처럼 patent or stenotic popliteal artery 뿐 아니라 완전 폐색되어 있는 경우에도 thrombosed arterial structure를 보여주며, 주위의 근육, bony protrusion, intervening lesion 등이 있는 경우 등에서 연부조직 병변도 같이 보여주고 이들 사이의 관계도 보여줌으로써 진단에 도움을 준다. 또한 CT처럼 비침습적이며, 심한 증상을 나타내지 않는 환자나 증상이 전혀 없는 반대쪽을 동시에 검사할 수 있는 것도 하나의 장점이며, 조영제를 사용하지 않고도 imaging이 가능하고 soft tissue delineation이 더 좋다는 것이 CT보다 더 유용한 검사라 할 수 있다. MR-angiography를 응용하면 혈관조영술에 못지않은 혈관의 영상소견도 가능하기 때문에 많은 저자들이 시도하고 있는 진단법이기도 하다. MR imaging이나 MR-angiography에서 볼 수 있는 소견은 displaced, stenotic or occluded popliteal artery, post-stenotic dilatation of popliteal artery, abnormal head of gastrocnemius muscle or other intervening structure, abnormal relationship between popliteal artery and muscle, fat thickening in popliteal fossa, lateral prominency of femoral cortical thickening of gastrocnemius attachment site 등이다.

6. Differential diagnosis

비교적 젊은 나이의 환자에서 calf의 허혈을 호소하는 경우에 PAES를 염두에 두고 검사를 해야겠지만, 다음의 여러 가지 가능성을 배제하도록 노력하여야 한다.

1) Atherosclerosis

가장 흔하고 어느 영역의 혈관에서나 유발될 수 있는 질환으로 노령층에서 더 많이 관찰되며, 혈관의 내막변화에 의해

서 죽종(atheroma)이 형성되고 이에 의해 협착을 일으키며, 혈전, 폐색을 일으키므로 허혈을 유발한다. 이 질환은 국소 침범은 드물며, 주로 신동맥 이하의 복부 대동맥과 ilio-femoral and lower portion의 동맥을 광범위하게 침범하므로 비교적 쉽게 구분될 수 있다. 영상소견에서도 diffuse narrowing, luminal irregularity, wall calcification, aneurysmal dilation 등의 다양한 소견으로 나타난다. 그러나, 이들 환자에 있어서는 combined PAES의 가능성이 있으므로 항상 염두에 두고 있어야 한다.

2) Fibromuscular Dysplasia (FMD)

신동맥 협착의 원인으로는 잘 알려져 있지만 사지 동맥을 침범하는 경우는 전체 FMD의 5% 정도로 드물며, 슬와동맥에만 국한되어 있는 경우는 이중에서도 찾아보기 힘들다. 동맥경화 등의 소견이 없으며, 다른 혈관, 특히 신혈관에서 특징 소견을 보이는 환자가 사지 혈관에서도 비슷한 소견을 보이면 진단할 수 있다. 혈관조영술에서 특징적인 "string-of-beads" 양상의 국소 동맥 협착이 관찰되며, 도플러에서는 동맥 협착을 유발하는 다른 질환과 비슷한 소견을 보이며, CT-또는 MR-angiography에서 혈관조영술과 동일한 소견을 볼 수 있다.

3) Cystic Adventitial Disease

흔하지 않은 질환으로 PAES와 같은 위치인 슬와동맥을 주로 침범하고 동맥벽에 낭종이 생기며 이에 의해서 슬와동맥의 협착을 유발하며, 특히 혈관조영술에서 슬와동맥의 segmental occlusion을 보이는 경우에 감별대상에 포함되어야 하며 arterial focal lesion으로 나타날 수 있다. 동맥 혈전이 형성되기 이전에는 smooth curvilinear filling defect with luminal narrowing의 소견으로 관찰된다. 그러나 동맥의 내측 전위, 협착후확장 등의 소견은 보이지 않는다. 도플러, CT, MR등에서는 슬와동맥을 encroachment 시키는 perivascular cystic lesion을 직접 볼 수 있으므로 비교적 진단에 용이하다.

4) Buerger's disease

PAES처럼 비교적 젊은 나이의 환자에서 호발하며 하지를 침범하므로 감별해야 할 질환이지만 PAES와는 달리 resting pain이 심한 것이 임상증상의 특징이며, 흡연력과 상지 혈관을 같이 침범하는 것이 감별점이다. 영상 소견은 ASO 등과 비슷한 소견을 보이나, aorto-iliac artery가 spared되어 있는 것이 다른 점이다. 실제로 보고되는 증례 중에는 슬와동맥을 침범한 혈전을 Buerger's disease로 생각하고 두 차례에 걸친 thrombectomy 이후에 PAES로 진단되어 bypass surgery를 받은 증례도 있으므로 combined disease의 가능성을 꼭 염두에 두어야 할 것이다.

5) Functional PAES

엄밀히 말하자면 PAES에는 포함 될 수 없는 범주의 소견으로 봐야 한다. 하지만 PAES와 마찬가지로 calf claudication을 일으킬 수 있으므로 감별 질환에서 잠깐 언급하고자 한다. 이것은 해부학적으로 정상인 비복근, 건(tendon)과 슬와동맥이 전제 조건이며, rest 상태의 imaging diagnosis도 정상 소견을 보인다. 이는 단지 근육이 아주 발달된 운동 선수에게서 hypertrophy된 비복근에 의해 이들 사이에 위치한 슬와동맥이 압박을 받기 때문에 증상을 일으키는 것이며, 도플러 등을 이용한 stress test에서 비복근, plantaris muscle등에 의해서 동맥 압박, 외측 전위 등의 소견을 보인다.

7. Treatment

PAES는 기본적인 해부학적 구조의 이상에서 기원하는 질환이므로 다른 어떤 치료보다도 이를 교정해주는 surgical bypass가 treatment of choice이다. 수술은 환자의 다리를 약 10도 정도로 구부린 상태에서 동맥의 주행을 따라 무릎의 후내측에서 외측으로 S-모양의 피부절개를 통해 접근하여 포획된 슬와동맥을 release 시키기 위하여, abnormal muscle, fibrous band의 제거, saphenous venous patchy or bypass graft를 한다. 이러한 수술적 치료를 하기에 앞서 혈전을 치료하기 위하여 transcatheter thrombolysis, angioplasty를 시행하기도 하지만 혈전용해술이 성공적으로 되더라도 근본적인 해부학적인 구조적 결함을 해결하기 위한 수술적 치료가 꼭 동반되어야 한다. 또한, 환자가 당장은 동맥협착, 폐색을 보이지 않는 경한 증상을 가졌다 하더라도 만성 경과로 진행되어 동맥협착, 혈전, 협착후동맥류 형성 등의 합병증이 생기면 수술과정이 어려워질 뿐 아니라, 궁극적으로 하지 절단으로 진행될 가능성이 있으므로 PAES로 진단된 환자에 있어 미리 수술적으로 교정해주는 것은 꼭 필요하다고 하겠다.

8. Conclusion

이상의 내용에서 PAES의 전반적인 내용에 대해 알아보았다. 다시 한 번 요약하면, PAES는 발생 단계에서부터 잘못 구성되어 있는 popliteal fossa의 구조물에 의해서 일어나며, 운동량이 많아지고, 근육이 발달하는 시기인 비교적 젊은 나이의 사람들에서 증상이 나타나는 것으로 알 수 있다. 그러므로 상대적으로 운동량이 적은 사람이라면 나이가 많은 사람에게서도 동반되어서 나타날 수 있다는 것을 꼭 감안해야 할 것이며, 여자에게서는 남자보다는 드물게 증상을 나타낸다. 서울대학교 병원에서의 10명의 PAES 환자에 대한 경험에서 보면, 연령분포는 17세에서 63세까지, 평균 37세로 다른 저

자들의 보고 평균 25.7세(분포: 15-56세)에 비하여 나이가 많으며, 모든 환자들이 남자이라는 사실은 특이할 만하다. 이들 중 bilateral PAES로 진단된 환자의 빈도는 10명 중 4명이며, 이들이 호소하는 증상은 chronic and/or acute claudication으로 다른 저자들의 경우와 비슷하다.

방사선학적 진단 방법은 초음파, CT, MR 및 혈관조영술이 모두 각각의 특성을 가지고 도움이 되며, 초음파는 혈관자체의 구조적 결함, 협착 정도, 합병증의 유무를 비교적 쉽게 평가할 수 있으나, 주위 구조물들과의 관계를 파악하기 어려우며, 궁극적으로 추가적인 검사가 필요하게 되므로 initial screening method로 적합한 방법이다. CT는 axial image를 이용하여 혈관자체의 모양 및 혈전, 동맥류의 유무, 주위 구조물들과의 관계를 비교적 쉽게 평가할 수 있으며, CT-angiography를 응용하여, 측부순환의 정도, 협착의 위치 등을 비교적 쉽게 평가할 수 있으나, 원위부의 작은 혈관들에 대한 색전 등을 평가하기가 어려우며 조영제를 사용해야 하는 점은 여전히 단점으로 남는다. 최근 도입되어 임상에서 많이 활용되고 있는 multidetector-CT, 3-D reconstruction soft ware등을 이용하면 이러한 평가에 대한 결과치가 나아질 것으로 생각되며, 앞으로 더 연구가 진행되어야 할 부분이다. MR은 조영제를 사용하지 않고도 imaging이 가능하며, CT에서 얻을 수 있는 정보 외에도 연조직 대조도가 뛰어나 근육과 혈관 사이의 보다 정확한 관계를 볼 수 있고, fibrotic band, surrounding nerve에 의한 포획의 구분이 가능해 질 것으로 기대된다. 그러나, 상기 이들의 imaging modality들이 아직까지는 원위부 색전을 충분히 평가하기에는 부족하므로 색전이 의심되는 환자에게서 혈관조영술은 제외할 수 없는 방법이다. 혈관조영술에서는 슬와동맥의 classical finding을 볼 수 있으면 쉽게 PAES로 진단하나, 모든 PAES의 환자에서 이런 소견을 보이는 것이 아니어서 이들 환자들이 간과될 수 있으므로 rest study에서 슬와동맥이 정상 주행을 보이는 환자에서 stress image를 시행하는 것은 꼭 필요하다고 하겠다.

이들 환자에 대한 치료는 궁극적으로 수술적인 방법이며, interventional radiologist가 transcatheter thrombolysis를 시행하여 환자 및 수술자에게 도움을 줄 수 있으나, 성공적인 혈전용해술이 되었다 하여 수술을 연기하는 것은 합병증을 야기하여 환자나 수술자 모두를 힘들게 하므로 조기 수술이 바람직한 방법이라 하겠다. 또한, PAES는 다른 혈관 질환과 비슷한 증상을 유발하기 때문에 임상에서 다른 질환으로 오진할 가능성이 높으며 치료방침이 다른 허혈성 질환과는 다르기 때문에 방사선과 의사는 환자와 임상 사이에서 정확한 진단을 내려주어 환자가 다리를 잃는 불행한 사태가 일어나지 않도록 꼭 염두에 두어야 할 질환이다.

참 고 문 헌

1. Collins PS, McDonald PT, Lim RC. Popliteal artery entrapment: An evolving syndrome. *J Vasc Surg* 1989;10:484-490
2. Greenwood LH, Yrizarry JM, Hallett JW. Popliteal artery entrapment: Importance of the stress runoff for diagnosis. *Cardiovasc Intervent Radiol* 1986;9:93-99
3. Chernoff DM, Walker AT, Khorasani R, et al. Asymptomatic functional popliteal artery entrapment: Demonstration at MR imaging. *Radiology* 1995;195:176-180
4. McGulness G, Durham JD, Rutherford RB, Thickman D,

- Kumpe DA. Popliteal artery entrapment: Findings at MR imaging. *J Vasc Interv Radiol* 1991;2:241-245
5. Atilla S, Ilgnt ET, Akpek SA, et al. MR imaging and MR angiography in popliteal artery entrapment syndrome. *Eur Radiol* 1998;8:1025-1029
6. Ikeda M, Iwase T, Ashida K, Tankawa H. Popliteal artery entrapment syndrome- Report of a case and study of 18 cases in Japan. *Am J Surg* 1981;141:726-730
7. Gibson MHL, Mills JG, Johnson GE, Downs AR. Popliteal entrapment syndrome. *Ann Surg* 1977;185:341-348
8. Abrams HL. *Abrams angiography- Vascular and interventional radiology*, 3rd ed. Little, Brown and Company Boston

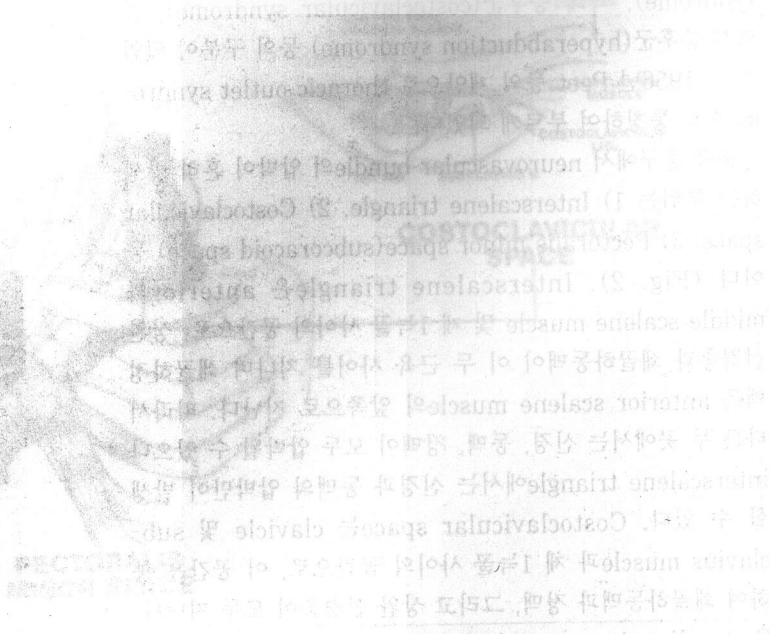


Fig. 2. Anatomy of the thoracic outlet (left) to (right).

Vascular Thoracic Outlet Syndromes

(brachial plexus) 1 thoracic wall

(upper border) 3

(Fig. 1).

(thoracic outlet) ,

osseous structure fibromuscular element 가 95%

1) cervical rib, anomalous first rib, exostosis, anomalous coracoclavicular joint, clavicle malunion pseudoarthrosis osseous abnormalities 2) scalene muscle abnormal insertion hypertrophy, congenital ligaments fibrous band fibro-muscular abnormalities neurovascular structures

provocative maneuver , (cervical rib syndrome), 1 (first rib syndrome), (scalenus anticus syndrome), (costoclavicular syndrome), (hyperabduction syndrome) , 1956 Peet thoracic outlet syndrome

(paresthesia) 가 , (lower trunk) C8 T1 가 (C5, C6, C7) 가 가 5%

neurovascular bundle

1) Interscalene triangle, 2) Costoclavicular space, 3) Pectoralis minor space(subcoracoid space) (Fig. 2). Interscalene triangle anterior middle scalene muscle 1 , anterior scalene muscle interscalene triangle Costoclavicular space clavicle sub-clavius muscle 1 , Pectoralis minor space(subcoracoid space) pectoralis minor lateral

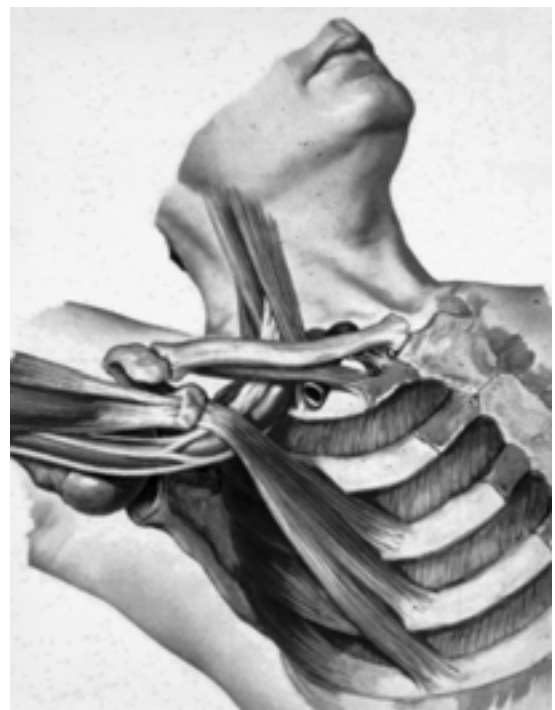


Fig. 1. Anatomy of the thoracic outlet.

3% 4% 1% 2% 20 50 ,

가 가 .

가

10 .

Raynaud , , 가 가 .

costoclavicular space interscalene triangle

, pectoralis minor space

가 가 .

가

Etiology

가 50% 80%

가 가

interscalene triangle

cervical rib

. Cervical rib 가

50% 1

7

(Arterial Thoracic Outlet Syndromes, Fig. 3)

. Congenital fibromuscular band anterior scalene muscle

12% .

가

가

가

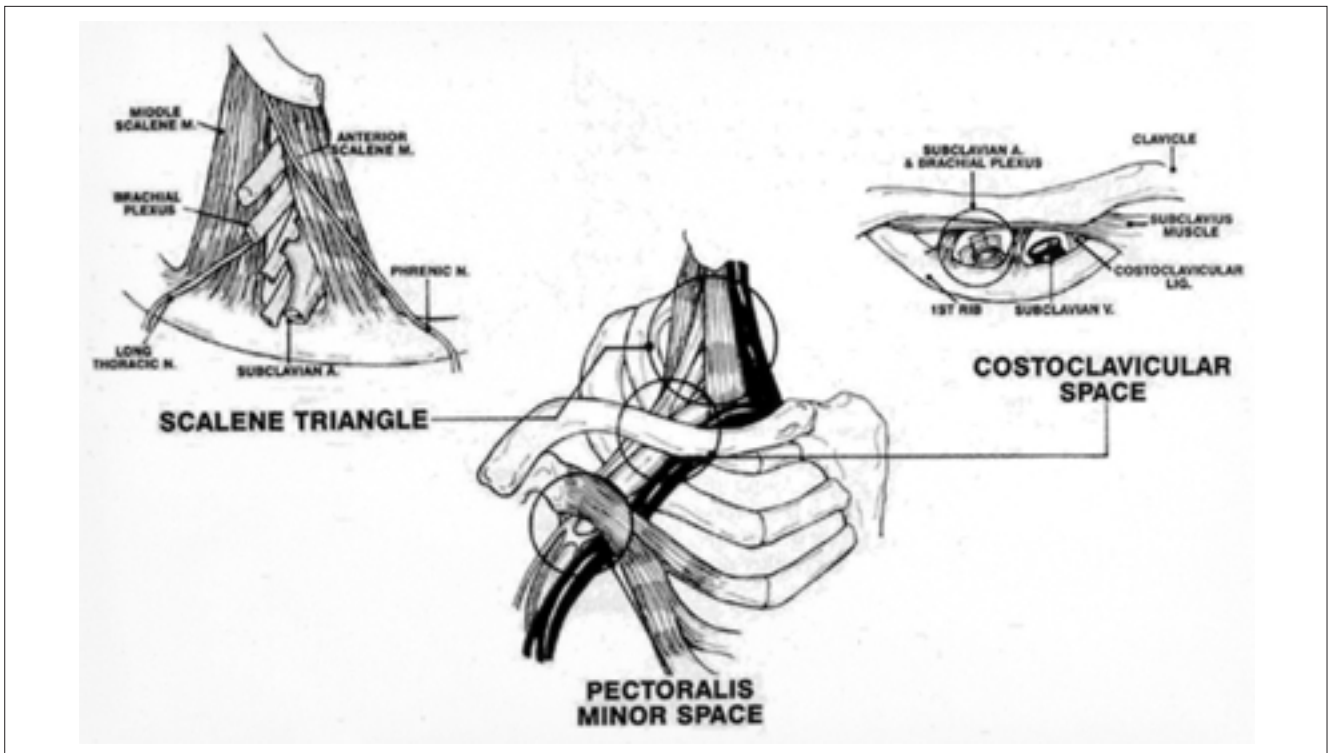
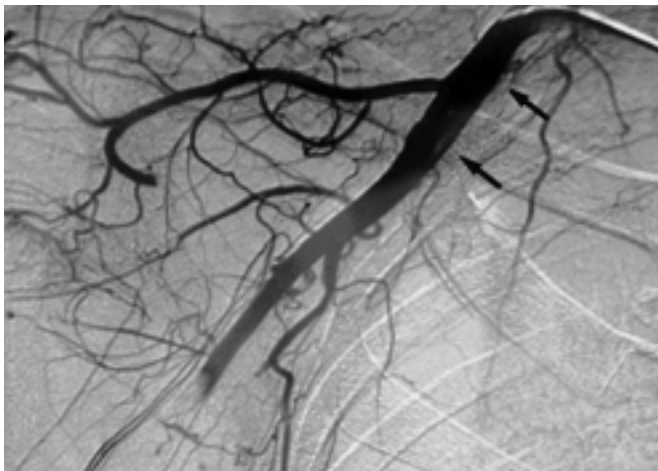


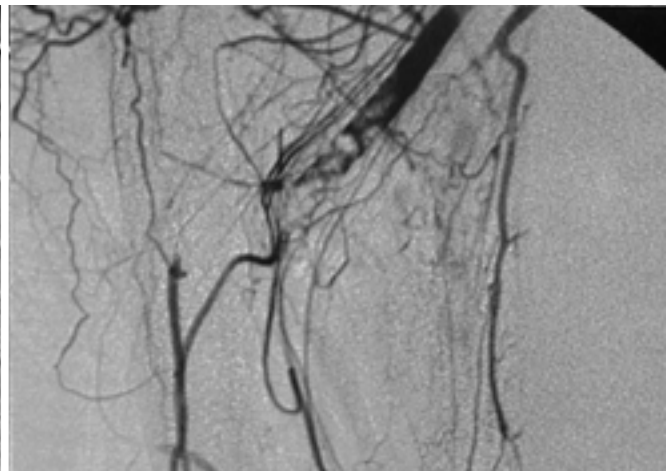
Fig. 2. Anatomy of the thoracic outlet area demonstrating the three main spaces.

가
malunion 가 , 1
exostosis
Clinical Manifestations and Diagnosis
(poststenotic dilatation) 가
가 (microembolization)

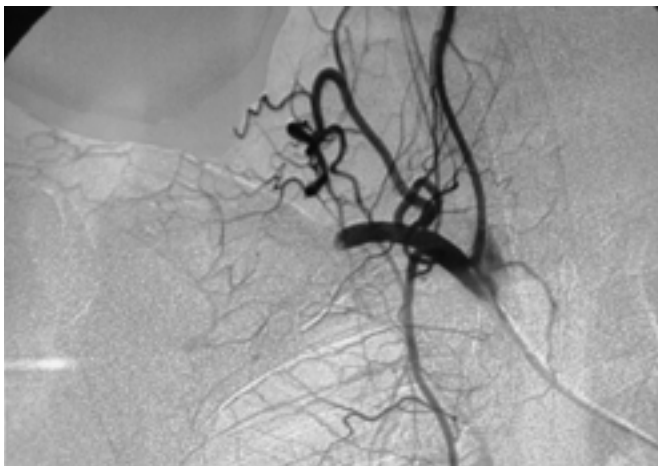
가
vertebral artery right common carotid artery
retrograde propagation 가
가
Raynaud
가



A



B



C

Fig. 3. Preoperative arteriogram of a 29-year-old man with acute embolic ischemia of the arm caused by extrinsic compression of the subclavian artery.
A, B. Right subclavian arteriogram shows complete occlusion of the axillary-brachial artery. Mild post-stenotic dilatation of the subclavian artery is seen (arrows).
C. When the arm is abducted, right subclavian artery is occluded due to extrinsic compression as it crosses the first rib.

가 . 가 . , .

가 . , , (hyperabduction test) .

가 , cervical rib, 가 가 .

1 neutral position

가 stress position

25 - 50% 가 , .

Treatment

가 .

(bruit) , 1)

2)

가 endarter -

ectomy intimectomy ,

3) thromboembolectomy bypass surgery

MR MR angiography

CT CT angiography,

mural thrombus, 가

3 가 가 .

가 가

angulation poststenotic

dilatation aneurysm .

가

Neutral position stress position

(Venous Thoracic Outlet Syndromes, Fig. 4)

가

teres major (lower margin)

(basilic vein)

1 .

가 .

, scalene muscle tone 가

interscalene space

(Adson test) .

1875 1884

Schroetter 's syndrome Paget von Schroetter가

(primary axillosubclavian vein thrombosis) Paget -

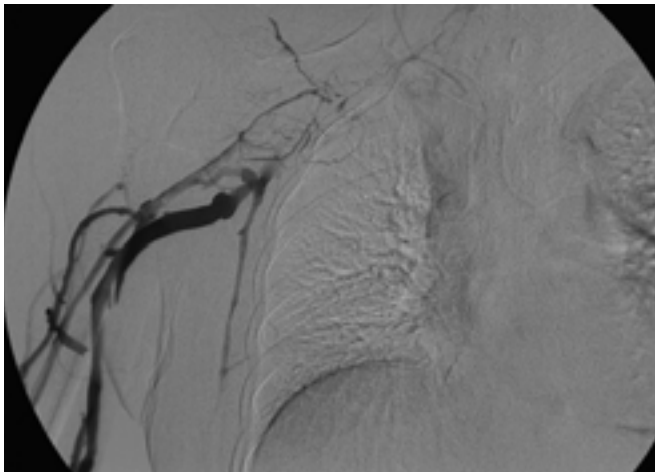
(effort thrombosis)

50% .

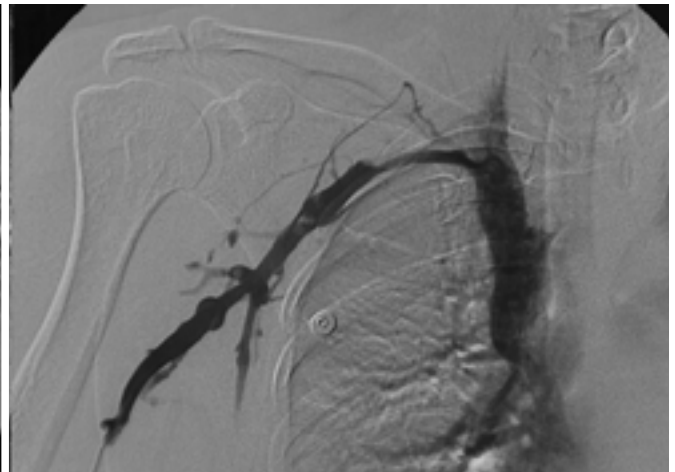
costoclavicular space

(costoclavicular maneuver or Wright test)

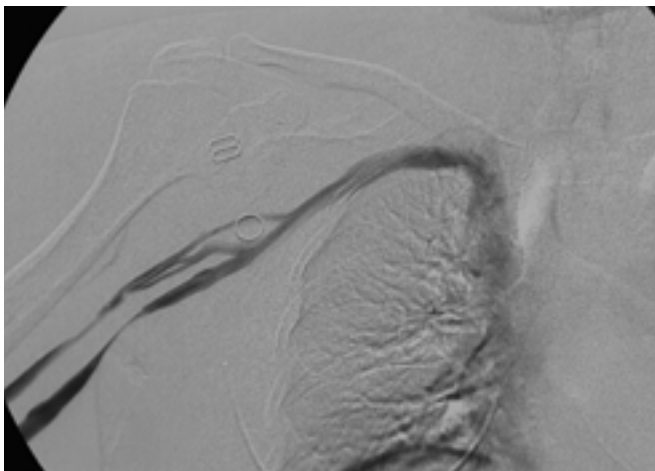
, 가	, 가, ,	가 .
Paget Schroetter	Etiology	
31	75%	costoclavicular space가
가	2	
4%	1%	large costoclavicular ligament or
25%, 40%		subclavius muscle, more anterior insertion of anterior scalene muscle, congenital fibromuscular band, pectoralis minor muscle tendon . cervical rib exostosis



A



B



C

Fig. 4. Venogram of a 50-year-old woman with acute primary axillosubclavian vein thrombosis.

A. Initial venogram prior to therapy shows obstruction with extensive intraluminal thrombosis in right axillosubclavian vein. The patient had a history of strenuous exercise at health club before onset of symptoms.

B. Venogram following successful catheter-directed thrombolysis shows a residual intrinsic stenosis at the subclavian vein.

C. Venogram following percutaneous transluminal balloon angioplasty of the subclavian vein demonstrates restoration of normal venous flow.

Clinical Manifestations and Diagnosis

가 .

가 .

0% 36%

가 .

가 .

가 , 가 ,

가 .

가 .

가 20 가 ,

position neutral stress position urokinase

. Neutral position pectoralis major muscle

가 , 12 - 24

30 costoclavicular space 가

costoclavicular space가 Stress positional venography 가 57%

position 가

position stress ,

positional venography ,

가 .

가 MR

Treatment 가

가 .

가 가 가 .

, positional venography

transaxillary first rib resection 가

1

가 ,

가 venolysis vein
reconstruction 가 pectoralis minor
space 1 pectoralis minor tendon

가

2 - 3

가

가

Summary

neutral

stress position

Positional venography

1. Angle N, Gelabert HA, Farooq MM, et al. Safety and efficacy of early surgical decompression of the thoracic outlet for Paget-Schroetter syndrome. *Ann Vasc Surg* 2001;15:37-42
2. Bjarnason H, Hunter DW, Crain MR, Ferral H, Miltz-Miller SE, Wegryn SA. Collapse of a Palmaz stent in the subclavian vein. *Am J Roentgenol* 1993;160:1123-1124
3. Coletta JM, Murray JD, Reeves TR, et al. Vascular thoracic outlet syndrome: successful outcomes with multimodal therapy. *Cardiovasc Surg* 2001;9:11-15
4. Gelabert HA, Machleder HI. Diagnosis and management of arterial compression at the thoracic outlet. *Ann Vasc Surg* 1997; 11:359-366
5. Gomes MR, Tomaso H, Nazarian GK, et al. Upper-extremity deep vein thrombosis and chronic pulmonary embolism resulting in pulmonary artery hypertension. *Am J Roentgenol* 1998;170:1532-1534
6. Hall LD, Murray JD, Boswell GE. Venous stent placement as an adjunct to the staged, multimodal treatment of Paget-Schroetter syndrome. *J Vasc Interv Radiol* 1995;6:565-569
7. Hurlbert SN, Rutherford RB. Subclavian-axillary vein thrombosis. In Rutherford RB. *Vascular surgery*. 5th ed. Philadelphia: Saunders, 2000:1208-1221
8. Kieffer E, Ruotolo C. Arterial complications of thoracic outlet compression. In Rutherford RB. *Vascular surgery*. 5th ed. Philadelphia: Saunders, 2000:1200-1207
9. Machleder HI. Evaluation of a new treatment strategy for Paget-Schroetter syndrome: spontaneous thrombosis of the axillary-subclavian vein. *J Vasc Surg* 1993;17:305-315
10. Rayan GM, Jensen C. Thoracic Outlet Syndrome: provocative examination maneuvers in a typical population. *J Shoulder Elbow Surg* 1995;4:113-117
11. Remy-Jardin M, Doyen J, Remy J, et al. Functional anatomy of the thoracic outlet: evaluation with spiral CT. *Radiology* 1997; 205:843-851
12. Sanders RJ, Cooper MA, Hammond SL, Weinstein ES. Neurogenic thoracic outlet syndrome. In Rutherford RB. *Vascular surgery*. 5th ed. Philadelphia: Saunders, 2000:1184-1200
13. Thompson RW, Petrinc D. Surgical treatment of thoracic outlet compression syndromes: diagnostic considerations and transaxillary first rib resection. *Ann Vasc Surg* 1997;11:315-323
14. Urschel HC Jr, Razzuk MA. Neurovascular compression in the thoracic outlet: changing management over 50 years. *Ann Surg* 1998;228:609-617
15. Urschel HC Jr, Razzuk MA. Paget-Schroetter syndrome: what is the best management? *Ann Thorac Surg* 2000;69:1663-1668

Miscellaneous Arterial Disorders

2.5:1 . , ,
malaise . PAN 20 - 50%
hepatitis B C hepatitis
virus humoral immune response
immune complex
70%, (, ,)
(, ,) 45% 65%,
PAN acute, reparative, chronic phase
가 가 . Acute
phase polymorphonuclear
leukocyte elastic lamina , media
fibrinoid necrosis가 ,
amorphous eosinophilic mass가 . Late acute
phase microaneurysm
(Fig. 1). small arteries
. Reparative chronic phase intima

Polyarteritis nodosa(PAN) medium and small arteries

- Large-Vessel Arteritides
 - Takayasu 's arteritis
 - Temporal arteritis (“giant cell arteritis”)
 - Behcet 's disease
 - Arteritis associated with collagen-vascular disease
 - Infection-related arteritis
- Small- and Medium-Vessel Arteritides
 - Polyarteritis nodosa
 - Buerger 's disease (“thromboangitis obliterans”)
 - Kawasaki 's disease
 - Substance-abuse vasculitis
 - Arteritis associated with collagen-vascular disease
 - Infection-related arteritis

- Idiopathic arteritides
 - Polyarteritis nodosa
 - Giant cell arteritides
 - Takayasu 's arteritis
 - Temporal arteritis (" giant cell arteritis ")
 - Buerger 's disease
 - Behcet 's disease
- Secondary arteritides
 - Infection-related arteritis
 - Vasculitis in collagen-vascular disease
 - systemic lupus erythematosus, rheumatoid arthritis
 - Scleroderma, ankylosing spondylitis
 - Reiter 's syndrome, relapsing polychondritis
 - Sjogren 's syndrome, dermatomyositis/polymyositis
 - Substance-abuse vasculitis
 - Kawasaki 's disease
 - Renal transplant vasculitis

media fibroblast가
 fibro - obliterative occlusion late
 ischemia
 가
 hepatic(60%), renal(47%), mesenteric(38%) artery
 small arteries microaneurysm,
 . Microaneurysm
 diagnostic 1 - 5 mm
 saccular shape bifurcation area
 . PAN
 microaneurysm
 neurofibromatosis, Wegener 's granulomatosis, Kawasaki 's disease, fibromuscular dysplasia, septic embolism
 Corticosteroid, cytotoxic drug
 5 80%
 (, , ,) transcatheter
 embolization 가

Takayasu 's disease

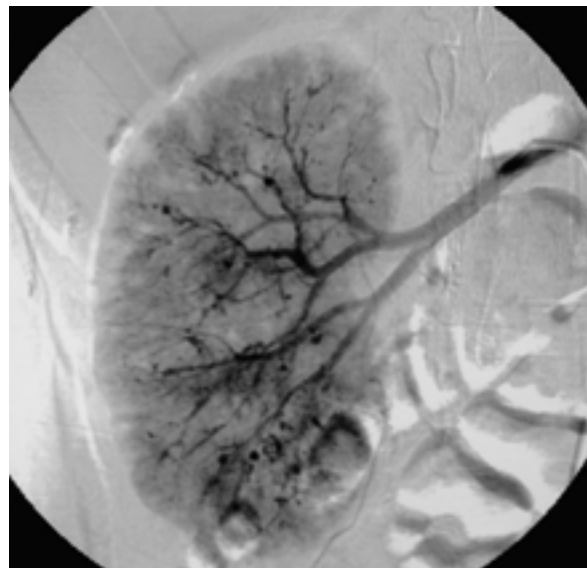


Fig. 1. Right renal angiogram in a 39-year-old man with polyarteritis nodosa shows multiple tiny saccular aneurysms in right renal arteries.

2. Giant Cell Arteritides

Takayasu 's arteritis temporal arteritis가
 media granulomatous inflam - matory
 infiltrate giant cell 가
 media adventitia
 media internal elastic lamina
 medial fibrosis
 intima adventitia fibrosclerosis permanent
 stenosis, occlusion elastic fiber
 가
 (malaise, , , ,
 , normocytic anemia)

Takayasu 's arteritis
 temporal arteritis . Temporal
 arteritis Takayasu 's arteritis
 phase flu - like
 syndrome

temporal headache, tender and reddened
 temporal arteries, jaw claudication
 symptomatic artery temporal artery



Fig. 2. Hand angiogram in a 34-year-old man with scleroderma shows irregular narrowing and occlusion of multiple digital arteries.

1. 50
2. head, neck, upper extremity arteries
Takayasu's arteritis
3. Polymyalgia rheumatica(acting stiffness in the proximal joints) Raynaud's phenomenon
Takayasu's arteritis
4. Aortic aneurysm aortic stenosis
- 5.

3. Infection - related Arteritis

Arteritis bacteria, fungi, spirochetes, viruses, Mycobacteria, Rickettsia
" mycotic aneurysm "

emboli, vasa vasorum hematogeneous seeding, osteomyelitis contiguous invasion, direct injury with contamination perforation, aneurysm pseudoaneurysm, occlusion, thrombosis

가 Staphylococcus, Streptococcus, Salmonella, Syphilis, Tuberculosis

stent stent - graft

4. Arteritis Due to Collagen - Vascular Disease

Systemic lupus erythematosus(SLE) hypersensitivity vasculitis intimal fibrosis

PAN arteritis, microaneurysm digital artery, mesenteric artery branch, PAN - like microaneurysm SLE

hypercoagulable condition arterial thrombosis가

Rheumatoid arthritis arteritis가 digital artery, nerve sheath arteriole, mesenteric arterial branches digital



Fig.3. Ascending aortogram in an 11-year-old boy with Kawasaki's disease shows saccular aneurysm of left coronary artery.



Fig.4. Hand angiogram in a 43-year-old woman with Raynaud's disease after contrast injection immediately following the intraarterial injection of PGE1 shows the markedly relieved vascular spasm, but occlusive disease of the digital arteries remains evident.

ischemia, peripheral neuropathy, bowel infarction

scleroderma 가 , , 가 , , (Fig. 2). 80% Raynaud 's phenomenon . Ankylosing spondylitis aortic valve aortic root inflammatory infiltration valve insufficiency . Relapsing chondritis aortitis aortic aneurysm . Reiter ' s syndrome(nongonococcal urethritis, conjunctivitis, arthritis) 50% ankylosing spondylitis . Sjogren 's syndrome (dry mouth, dry eyes) micros-copic cutaneous artery vasculitis가 , necrotizing vasculitis가 . Polymyositis/dermatomyositis 25%

5. Substance - abuse Vasculitis

(met)amphetamine, heroin, cocaine, phenylpropano - lamine, ephedrine, methylphenidate . segmental artery “ beaded ” “ sausage ” nonspecific angiographic finding PAN .

6. Kawasaki 's Disease

“ Mucocutaneous lymph node syndrome ” . coronary arteritis가 . axillary, iliac, renal, internal mammary, mesenter - ic, bronchial arteries 가 . saccular aneurysm 가 가 (Fig. 3).

7. Renal Transplant Vasculitis

Table 3. Causes of Raynaud 's phenomenon

Idiopathic
Systemic rheumatic disorders
scleroderma, SLE, rheumatoid arthritis, etc.
Vasculitis
Buerger 's disease, temporal arteritis
Occupational
rock drillers, grinders, pneumatic hammer operators, etc.
Drugs
beta-blockers, ergot, bleomycin, cyclosporin A, etc.
Arterial occlusive disease
embolic/thrombotic occlusions, carpal tunnel syndrome, thoracic outlet syndrome

가 . cortical filling arterial washout . arterio - venous shunting .

8. Raynaud 's phenomenon

arteriole episodic vasospasm triad (1. episodic, self - limited attacks of reversible, white color changes of the fingers, 2. precipitation of the attacks by cold, 3. symptoms of numbness, tingling, pain) 가 (Table 3), primary Raynaud 's phenomenon or Raynaud 's disease , secondary Raynaud 's phenomenon . vasodilator vasculitis (Fig. 4).

1. Miller DL, Cole PE, Sproat IA, Williams DM. Systemic vasculitides. In: Haskal ZJ, Kerlan RK, Trerotola SO. SCVIR syllabus-thoracic and visceral vascular interventions. 1996;323-352

2. Calabrese LH, Hoffman GS, Clough JD. Systemic vasculitis. In: Young JR, Olin JW, Bartholomew JR. Peripheral vascular diseases. 2nd ed. 1996;380-403

3. Hellmann DB, Flynn JA. Clinical presentation and natural history of Takayasu 's arteritis and other inflammatory arteritis. In: Perler BA, Becker GJ. Vascular intervention-a clinical approach. 1998;249-256

Case 1

AV Fistula caused by Electric Burn

: Fistula, arteriovenous

Electric burn

: 53 /

: 6 22,000V

(both arms below elbow & both legs below knee)

53 가

CT

가

:

CT

(Fig. 1).

Terumo guide wire (Terumo,

Tokyo, Japan)

. 5 F cobra

catheter(Cook, Bloomington, IN, U.S.A.)

가

(Fig. 2).

가

가

가 0.2 - 1.3%,

3 - 4%

80%

20%

elastin collagen

thermal denaturation

coagulation cascade

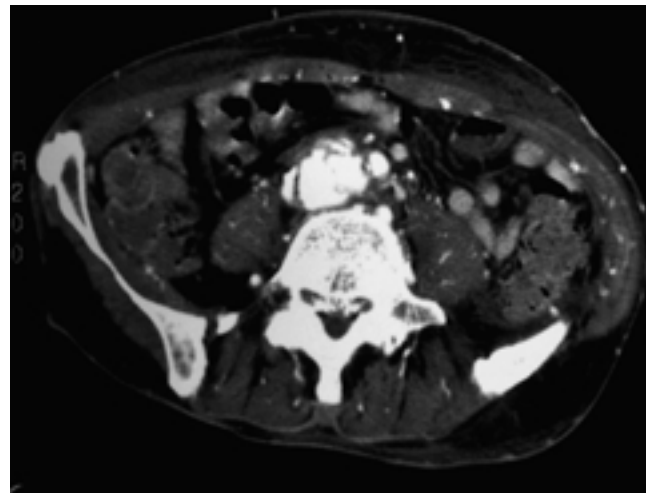


Fig. 1. Arterial phase CT scan shows simultaneous contrast enhancement of aorta and dilated inferior vena cava.

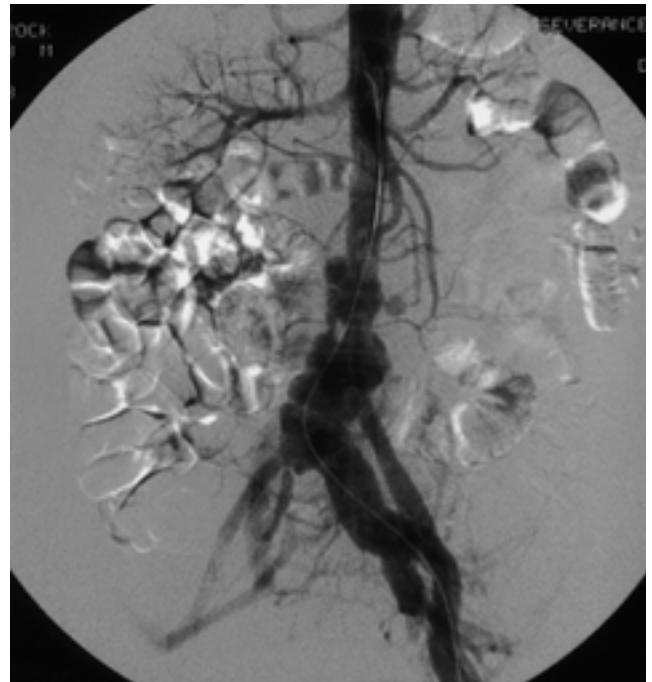


Fig. 2. Abdominal aortogram shows simultaneous contrast media filling of the aorta and IVC and iliac veins, suggesting arteriovenous fistula. Aneurysmal dilatation of distal infrarenal aorta and left iliac vein is also noted.

가

, 1990

(50%), (64%), (35%), 가 (21%), , Lau aortocaval fistula (7%) (100%), 2 . 30%

(57%), (28%), (21%), , (28%) 가 .

Mayo clinic 1970 - 1997
18 aortocaval fistula
90 6%, 39%

Case 2

Hepatic Metastasis from Choriocarcinoma: Angiographic Findings and Coil Embolization

Key words :Choriocarcinoma

Liver neoplasm, metastases

Liver neoplasm, angiography

Case : 33-year-old woman

Clinical history : The patient presented with upper abdominal pain, and distension and weight loss (4kg for one month). Her past medical history was unremarkable. An intrauterine device was inserted after the last pregnancy 4 years ago.

Diagnosis : Hepatic metastasis from choriocarcinoma

Imaging Findings and Interventional Procedures

Abdominal CT showed multiple, irregularly shaped, heterogeneously enhanced mass lesions in the liver and spleen, suggesting hepatic metastasis from splenic angiosarcoma or a multifocal hepatocellular

carcinoma (Fig. 1).

Diagnostic celiac angiogram demonstrated multiple hypervascular masses with abnormal tumor vessels, saccular aneurysmal dilatations of the peripheral end

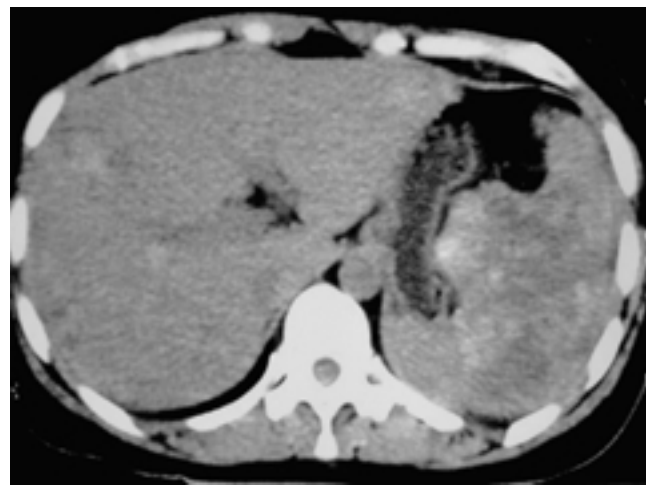


Fig. 1. The contrast-enhanced CT shows multifocal ill-defined, heterogeneously enhanced masses in both lobes of the liver and the spleen.

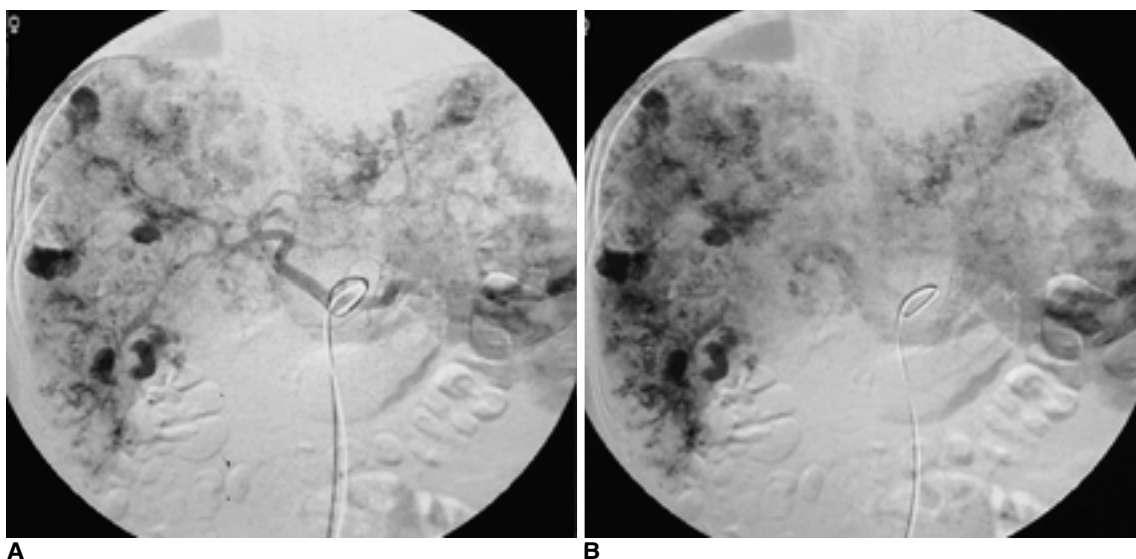


Fig. 2. A. Celiac angiogram on arterial phase shows multiple hypervascular masses with abnormal tumor vessels and saccular aneurysmal dilatations of the peripheral end of hepatic arteries in the liver and spleen.
B. Celiac angiogram on venous phase shows persistent visualization of aneurysmal vascular lakes in the liver and spleen, but active bleeding is not identified.

of hepatic arteries on arterial phase and persistent visualization of vascular lakes on venous phase in the liver and spleen. But active bleeding was not identified (Fig. 2A, B). SMA angiogram showed normal portal venous flow.

Diagnostic laparoscopic biopsy of the hepatic masses was done, and the histopathologic examination revealed metastatic choriocarcinoma in the liver. The serum beta hCG concentration was greatly elevated to 2,000,000 mIU/mL.

Five days after the admission, sudden alteration of laboratory data suggestive of active bleeding was noted, and the patient underwent exploratory laparotomy, which revealed massive hemoperitoneum and active bleeding from the liver and spleen. Despite the surgical procedure, bleeding control was unsuccessful.

Emergency celiac angiogram demonstrated massive extravasation of contrast media from the segmental branches of the both hepatic arteries as well as the branch of the splenic artery. After the superselection of the segmental arteries of both hepatic lobes and the spleen, immediate embolization was successfully performed using 16 Tornado microcoils (two 4 mm × 2 mm-sized coils, four 3 mm × 2 mm-sized coils, five 5 mm × 2 mm-sized coils, and five 6 mm × 2 mm-sized coils; Cook, Bloomington, IN, U.S.A.) and Gelfoam particles. Post-embolization celiac angiogram demonstrated no further extravasation of contrast

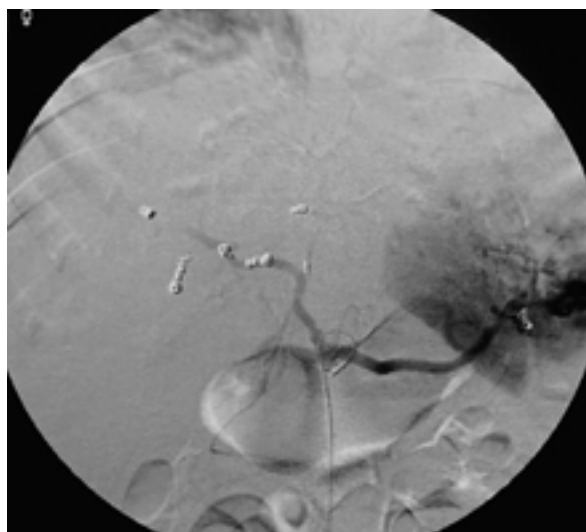


Fig. 3. After embolization using 16 microcoils and Gelfoam particles, celiac angiogram demonstrates no further extravasation of contrast media.

media and intact portal flow (Fig. 3). However, levels of AST and ALT had continuously and rapidly increased, suggesting progression to hepatic failure and acidosis. The follow-up CT scan performed 13 days after embolization also showed an extensive, low attenuated area in the enlarged liver and spleen, representing massive hepatic infarction and necrosis. Although the exact cause of this hepatic infarction was unknown, it was assumed that the embolization was the probable cause. The patient's condition continued to deteriorate, and she died on the 22th post-embolization day.

Discussion

Choriocarcinoma metastasizes hematogenously, producing a dramatic rise in beta hCG. The majority of metastases go to the lung (75%), vagina (50%), ovaries, brain, ureter, and bowel. Hepatic involvement is not common (10%), and occurs late in the disease course. Regression of the primary tumor after it has metastasized is not uncommon, and one third of cases are manifested by the complications of metastatic disease. Because of highly vascular nature of metastatic lesion similar to the primary tumor, hemorrhage from the tumor either spontaneously or after biopsy can be of a great concern. In our case, multiple hypervascular hepatic masses was presented with hemoperitoneum and severe anemia in a woman of childbearing age without an antecedent history of pregnancy or uterine abnormalities. Our initial diagnosis was either hepatic metastasis from splenic angiosarcoma or a multifocal hepatocellular carcinoma.

In our case, the characteristic angiographic findings for metastatic choriocarcinoma in the liver were hypervascular masses with aneurysmal dilatations of the peripheral end of hepatic arteries (grapelike appearance) on arterial phase and persistent vascular lakes on venous phase, as compared with other hypervascular hepatic masses. These angiographic findings are similar to those of hemangioma, but hemangioma has unique CT findings that peripheral enhancement with centripetal flow unlike metastatic choriocarcinoma. Also metastatic choriocarcinoma can be differentiated from hepatocellular carcinoma because vascular lakes in the hepatocellular carcinoma

do not retain the contrast media as long as those of choriocarcinoma.

In this case, because we did not rule out a possibility of metastatic choriocarcinoma, diagnostic laparoscopic biopsy was performed, resulting in massive hemoperitoneum. In conclusion, the possibility of choriocarcinoma should be emphasized in women of childbearing age who present with hepatic masses. Because of the risk of hemorrhage, liver biopsy should be deferred until the blood serum level of beta hCG is measured, especially if typical angiographic findings

of choriocarcinoma are demonstrated.

References

1. Hillard AE, Allen RW, Beale G. Metastatic choriocarcinoma: correlation of MRI, CT, and angiography. *South Med J* 1993;86: 1299-1302
2. Green CL, Angtuaco TL, Shab HR, Parmley TH. Gestational trophoblastic disease: a spectrum of radiologic diagnosis. *Radiographics* 1996;16:1371-1384
3. Alvey CG, Loehry CA. Hepatic metastases due to choriocarcinoma. *Postgrad Med J* 1988; 64: 941-942

Case 3

Cystic Adventitial Disease Cystic Adventitial Disease of the Popliteal Artery

: Cystic adventitial disease, arteries
Popliteal arteries, angiography, CT

0.5 × 4 cm

: 56 /

(cystostomy)

(cystic decompression)

: 6 가 1 km

ABI 0.92

500 m

ankle brachial index (ABI) 0.69

: Cystic adventitial disease of the popliteal artery

2 cm

가

(Fig. 1).

(gastrocnemius)

(Fig. 2).

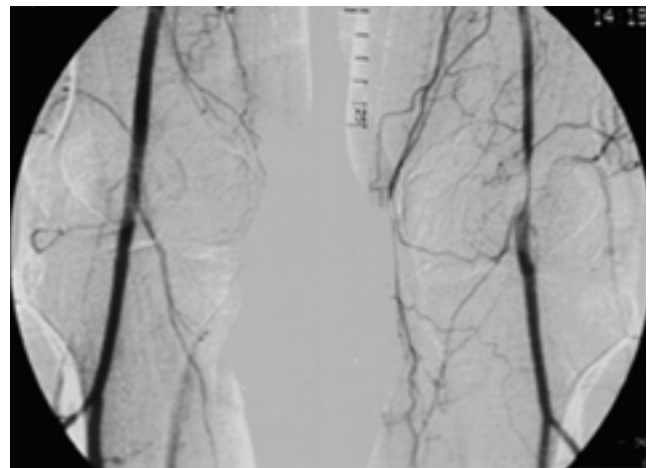


Fig. 1. Femoral angiogram shows smoothly tapered stenosis of left popliteal artery with adequate distal run off. No evidence of atherosclerotic change is noted.

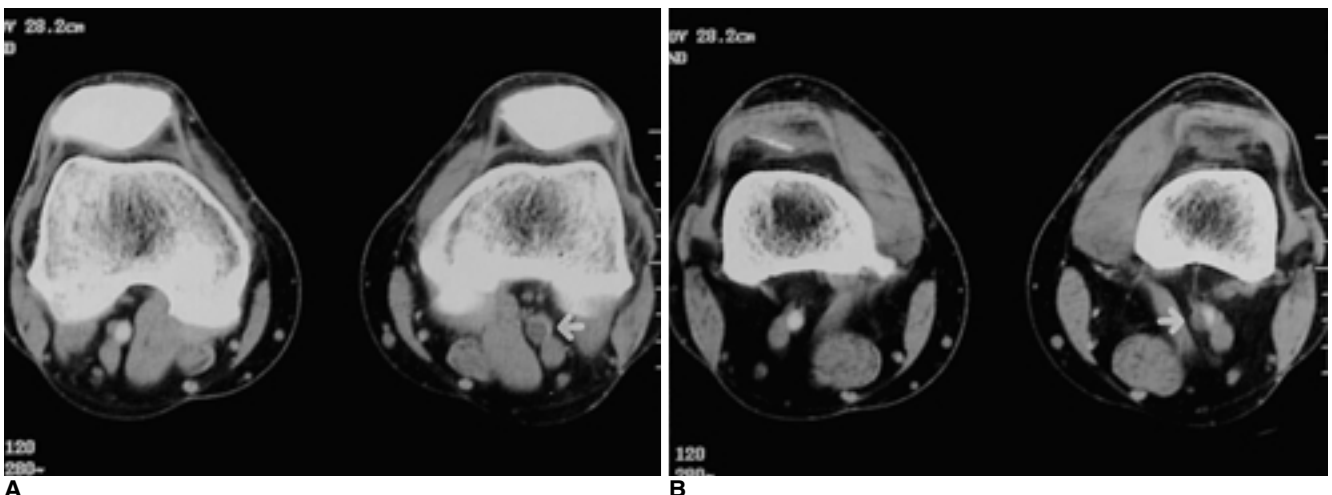


Fig. 2. A. Contrast-enhanced axial CT scan through the upper popliteal fossa shows cystic mass abutting on the left popliteal artery (arrow).
B. Contrast-enhanced axial CT scan at the level of mid popliteal fossa reveals a slitlike compression of the left popliteal arterial lumen (arrow) and appropriate location of gastrocnemius muscle.

Cystic adventitial disease

1000 1

5 80% 50

85%

(tendon sheath) (joint capsule) (ganglion)

가

(concentric compression)

(eccentric compression)

(scimitar deformity)

(poststenotic dilatation)

30%

(complete occlusion)

가

가

Burger's disease, (popliteal artery entrapment syndrome)

1. Flanigan DP, Burham SJ, Goodreau JJ, Summury of cases of adventitial cystic disease of the popliteal artery. Ann Surg 1979;189:165-175
2. Fitzjohn TP, White FE, Loose HW, Proud G. Computed tomography and sonography of cystic adventitial disease. Br J Radiol 1986;59:933-935
3. Kim JS, Chung JW, Park JH, Kim SJ, Han MC. Cystic adventitial disease of the popliteal artery demonstrated by CT & MR imaging : a case report. J Korean Radiol Soc 1997;37:835-837
4. Bunker SR, Lauten GJ, Hutton Jr SR. Cystic adventitial disease of the popliteal artery. AJR 1981;136:1209-1212

Case 4

Microcoil Embolization for the Treatment of Arterio-Venous Fistula in Lower Extremity

: Arterio - venous fistula
Embolization

: 74 /

:

: Arterio-venous fistula in lower extremity

tibioperoneal trunk

(Fig. 1).

puncture , 5 Fr sheath

, 5 Fr Torcon NB Advantage angiographic catheter (Cook, Bloomington, IN, U.S.A.) 0.032 Terumo guide wire (Terumo, Tokyo, Japan)

neuromicroferret catheter (Cook, Bloomington, IN, U.S.A.)

feeding artery

2.4 mm

가

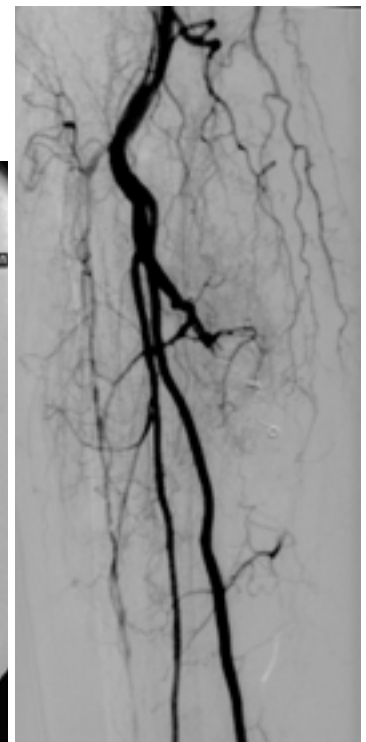
가



1



2



3

Fig. 1. Selective arteriogram of lower extremity while 5 Fr angiographic catheter tip is located in popliteal artery. It shows arteriovenous fistula (arrow) and early draining veins.

Fig. 2. Angiogram obtained via microcatheter using hand-injection technique after coil embolization with three successive 4 mm × 2 mm sized microcoils shows complete occlusion of the feeding artery for the arteriovenous fistula, and no more evidence of arteriovenous fistula or early draining veins.

Fig. 3. Selective arteriogram of lower extremity after coil embolization shows no evidence of delayed retrograde filling of the arteriovenous fistula.

, MWCE - 18S - 4/2 Tornado microcoil(Cook, Bloomington, U.S.A.)

microcoil
manual compression
neuromicroferret catheter hand injection
technique , coil
manual compression release
, manual compression release
microcoil
(Fig. 2). neuromicroferret
catheter 5 Fr angiographic catheter tip
(Fig. 3).

(AVF)
가 . AVF
가
가 , vascular steal phenomenon cardiac
output 가
AVF
endovas - cular
therapy access route
spring coil, detachable balloon, PVA tissue
adhesives(IBCA) 가
detachable balloon PVA fistula
recanalization recurrence가 . IBCA
distal migration
AVF coil embolization 가
가 access 가 coil
fistula
venous valve heart chamber

가
가
access
proximal artery manual
compression
manual compression
arterial sheath contralateral side
balloon proximal artery
balloon 가 microcatheter
(shaft 2.7 Fr)
balloon catheter 가
, ballooning procedure mother vessel
intimal injury 가 stenosis 가
access , 가
migration
migration venous valve heart chamber
coil
AVF manual
compression coil migration

1. Anderson JH, Wallace S, and Gianturco C. Transcatheter intravascular coil occlusion of experimental arteriovenous fistulas. AJR 1977;129:795-799
2. Yakes WF, Rossi P, Odink H. How do I it: Arteriovenous malformation management. CVIR 1996;19:65-71
3. Yakes WF, Luethke JM, Merland JJ, et al. Ethanol embolization of arteriovenous fistulas: a primary mode of therapy. JVIR 1990;1:89-96

Case 5

Giant Aneurysm associated with Angiomyolipoma:
Superselective Transarterial Embolization

: Angiomyolipoma, kidney
Selective arterial embolization
:36 /
: 가 1 .
(Fig. 4).

CT CT
(mixed attenuated)
6cm intraluminal thrombus
가 (Fig. 1, 2).
가 4 cm
(Fig. 3).

5F Cobra catheter
(Cook, Bloomington, IN, U.S.A.) micro - catheter
, superior segmental artery ,

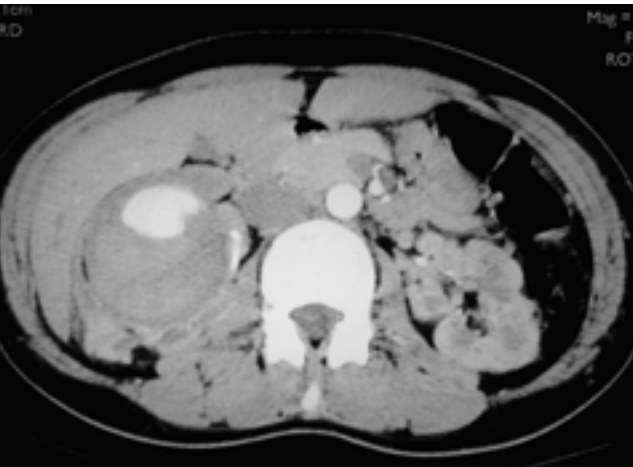


Fig 1. Contrast-enhanced axial CT scan shows a 6 cm-sized, high density lesion with partial contrast media filling in the upper pole of the right kidney.



Fig. 2. An MIP image of CT angiogram shows a partially thrombosed aneurysm, which is supplied by superior segmental artery (arrowhead) of the right renal artery in the upper pole. And also is seen a hypervascular mass (small arrowheads) in the lower pole of the right kidney.

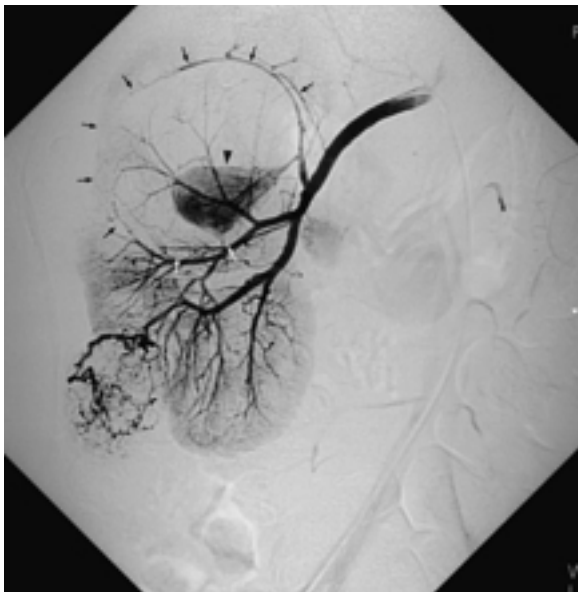


Fig 3. Right renal angiogram shows a large pseudoaneurysm (arrowhead) supplied by superior segmental arterial branch within the large space-occupying lesion (arrows) in the upper pole of the right kidney. A hypervascular lesion with abnormal vessels in the lower pole is also shown.



Fig 4. After the embolization of a pseudoaneurysm and a hypervascular lesion with microcoils (arrows) and PVA particles respectively, angiogram shows no more evidence of the previous pseudoaneurysm in the upper pole and the hypervascular lesion in the lower pole of the right kidney.

가
가
가
가
coil, polyvinyl alcohol
particle gelfoam alcohol

1. Han YM, Kim JK, Roh BS, et al. Renal angiomyolipoma: selective arterial embolization - Effectiveness and changes in long-term follow up. Radiology 1997;204:65-70
2. Donal RS. General Urology. Los Attos, California: LANGE medical publications, 1984;307-310
3. Smith D.C. Treatment of renal angiomyolipoma. N Engl J Med 1983;33:1400

Case 6

Acute Small Bowel Hemorrhage Caused by Angiodysplasia: Angiographic Diagnosis and Management

: Interventional procedure
Angiodysplasia
Microcatheter
Bowel infarction
:87 /

: 가 (Hgb :6.6 mg/dL).
:

5F Yashiro catheter (Cook, Bloomington, IN, U.S.A.)
microcatheter
(vascular tuft) (early draining vein)
(Fig. 1, 2).

ileal branch distal arcade

microcatheter 0.7mm
straight - type coil(Cook, Bloomington, IN, U.S.A.) 2
vascular tuft early draining vein (Fig.
3, 4).
. 3

가
,
가
(80%), S
(20%). 25%
, 90% , 85%

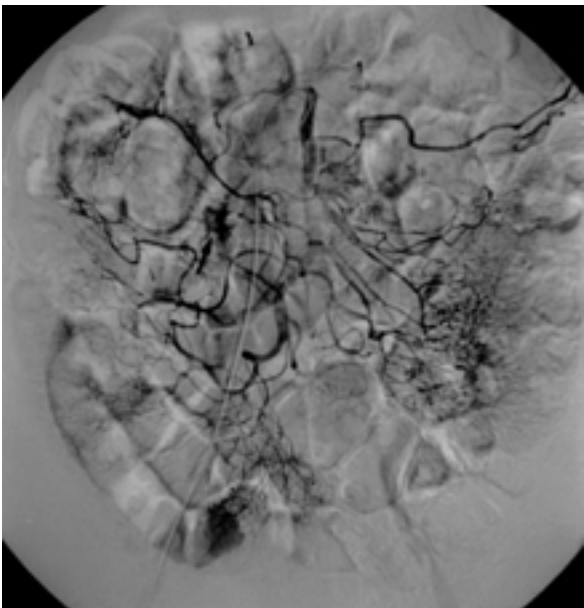


Fig. 1. Superior mesenteric angiogram shows a hypervascular lesion (arrow) in the terminal ileum.

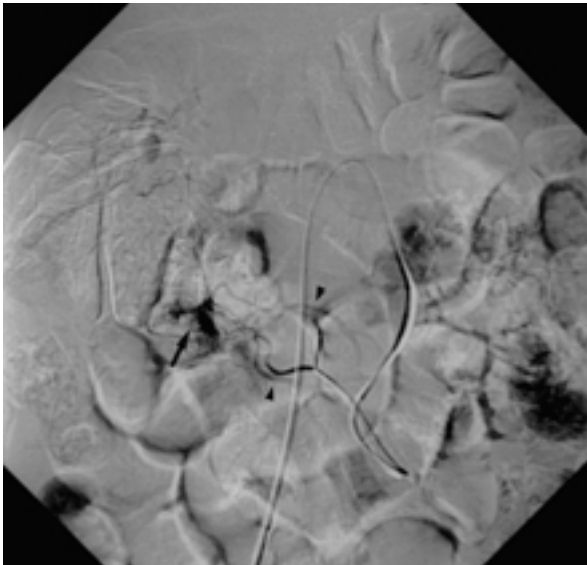


Fig. 2. Mid-arterial phase of a superselective angiogram shows a vascular tuft (arrow) and paired draining veins (arrowheads), suggesting a possibility of angiodysplasia.

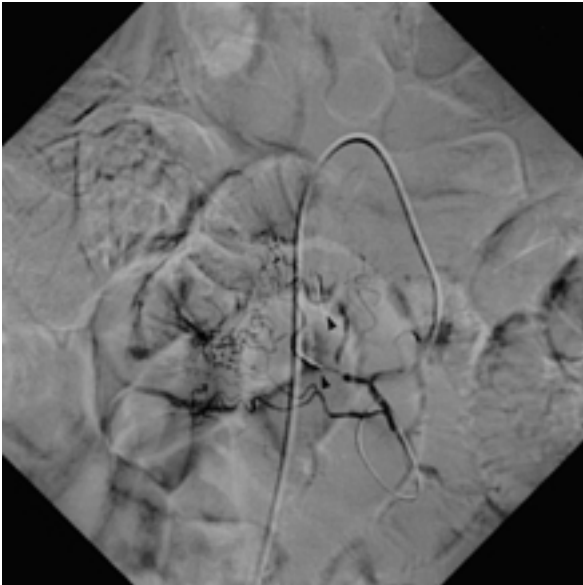


Fig. 3. Superselective angiogram obtained after embolization of arterial feeders using two microcoils (arrowheads) demonstrates no more evidence of the previous vascular tuft and the early draining veins.

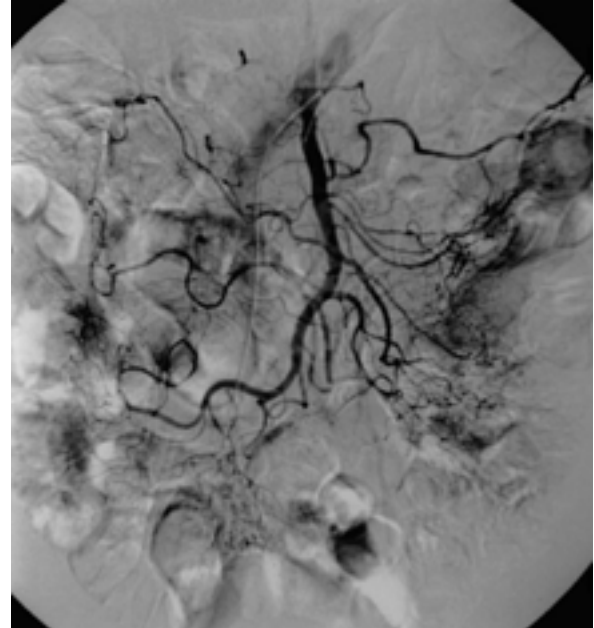


Fig. 4. Final superior mesenteric angiogram shows no more evidence of the previous hypervascular lesion in the terminal ileum.

(vascular tuft)

가 . Microcatheter

coil

. Gelfoam pledgets polyvinyl alcohol particle

가 , polyvinyl alcohol 가

coil

(perfusion pressure)

proximal arcade level

, vasa recta level

가

colonic arcade level

vasa recta

1. Funaki B, Kostelic JK, Lorenz J, et al. Superselective microcoil embolization of colonic hemorrhage. *AJR* 2001;177: 829-836
2. Gore RM, Levine MS. Textbook of gastrointestinal radiology. 2nd ed. Philadelphia: Saunders, 2000;108-109:1054-1055
3. Boley SJ, Sprayegen S, Sammartano RJ, et al. The pathophysiologic basis for the angiographic signs of vascular ectasia of the colon. *Radiology* 1977;125:615-621

Case 7

:

Transcatheter Coil Embolization of Lower Gastrointestinal Bleeding: Jejunal Gastrointestinal Autonomic Nerve (GAN) Tumors Manifesting Melena

Key Words: Gastrointestinal autonomic nerve tumors
Jejunum - Gastrointestinal tract,
Hemorrhage
Embolization, Interventional therapy

Case : 75-year-old man

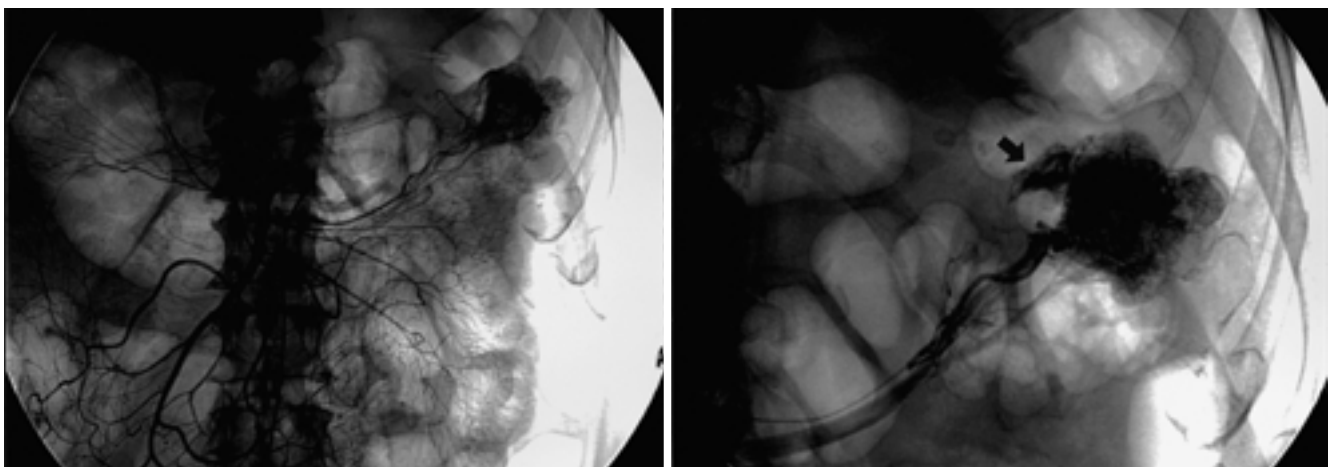
Clinical history : The patient was admitted with 2-day history of melena, abdominal discomfort and dizziness. Physical examination revealed conjunctival and mucosal pallor. Laboratory data documented iron deficiency anemia with the serum hemoglobin level of 7.7 g/dL, and hematocrit 22.4%. Ten months and 3 months earlier, he had a history of melena. Esophagogastroduodenal endoscopy revealed reflux of fresh blood in third and fourth portion of the duodenum from jejunum below the Treiz ligament. After emergency coil embolization of lower GI

bleeding of jejunum, segmental resection of proximal jejunum was performed.

Diagnosis : Lower GI bleeding from gastroint-estinal autonomic nerve (GAN) tumor in proximal jejunum

Imaging Findings and Interventional Procedures

Emergency mesenteric angiography was performed using 5-F Cobra shaped catheter (Cook, Bloomington, U.S.A.) with right femoral arterial approach, which showed hypervascular staining in proximal jejunum, and enlargement of arterial branch supplying the lesion (Fig. 1A). Superselective arteriogram was performed to precisely define the more peripheral arterial anatomy. It showed active bleeding focus, intraluminal leak of contrast media into the proximal jejunum and early visualization of draining veins (Fig. 1B). Superselective catheterization was attempted to



A
Fig. 1. A. Superior mesenteric angiogram showed hypervascular staining in proximal jejunum, and enlargement of arterial branch supplying the lesion.
B. Superselective arteriogram showed active bleeding focus in the proximal jejunum and intraluminal leak of contrast material (arrow).

embolize the arterial feeder using a microcatheter (Progreat; Terumo, Tokyo, Japan) and a 0.014-inch guide wire. After successful superselective catheterization of the jejunal arterial recta supplying the site of hemorrhage, we performed transcatheter embolization using two Vortex diamond shaped, 3 mm × 23 mm sized microcoils (Target Therapeutics, Fremont, CA) (Fig. 2A). Post-procedure angiogram showed total occlusion of the feeding vessel without evidence of contrast media extravasations (Fig. 2B). After the procedure, the patient stopped melena. His hemoglobin and hematocrit had increased to 10.5g/dL, 30.7%, respectively.

Contrast enhanced computed tomography (CT) scan of the abdomen performed one day after the coil embolization showed lobulating contoured soft tissue mass in the region of proximal jejunum with foreign body artifact induced by microcoils adjacent to small bowel mesentery (Fig. 3A, B). The mass was well marginated, homogeneously low attenuated and not enhanced. Small bowel follow-through study revealed smooth marginated intraluminal filling defect in proximal jejunum (Fig. 3C). Overlying mucosal surface was intact and small ulcer niche was noted in central portion of the filling defect. The radiologic diagnosis was a submucosal tumor of proximal jejunum such as GIST.

Segmental resection of proximal jejunum was performed. On gross examination, the tumor mass was measured 3.5 × 3.5 × 3.5 cm in size and was exposed to the serosal surface of the proximal

jejunum. The epithelial lining was intact, but there was an umbilicated deep ulcer in the mid-portion of exophytic mass. The histopathologic diagnosis was gastrointestinal autonomic nerve (GAN) tumor of jejunum with high probability of malignancy.

Discussion

Lower GI bleeding is hemorrhage distal to the ligament of Treitz and includes small bowel and colonic hemorrhage. The common etiologies include diverticulosis, angiodysplasia, neoplasm, and inflammatory bowel disease. The therapeutic options are medical management, endoscopic coagulation, transcatheter therapy, and surgery. Endoscopy is often the first method that is used to investigate and treat lower GI bleeding. Whereas endoscopy is feasible in cases of bleeding within the upper GI and colon, hemorrhage originating in the small bowel, when inaccessible by interventional techniques, can only be treated surgically. And also, failure of endoscopic diagnosis and therapy may occur as a result of massive bleeding, which limits precise localization of the site of hemorrhage. Surgery is still considered the mainstay of treatment; however, it is associated with significant morbidity and mortality. The reported mortality rates after emergency colonic resection for bleeding range from 10 - 36%.

There are two transcatheter options available to the interventional radiologist for the control of lower GI bleeding: (I) pharmacologic control with use of vasopressin and (ii) embolization. Although

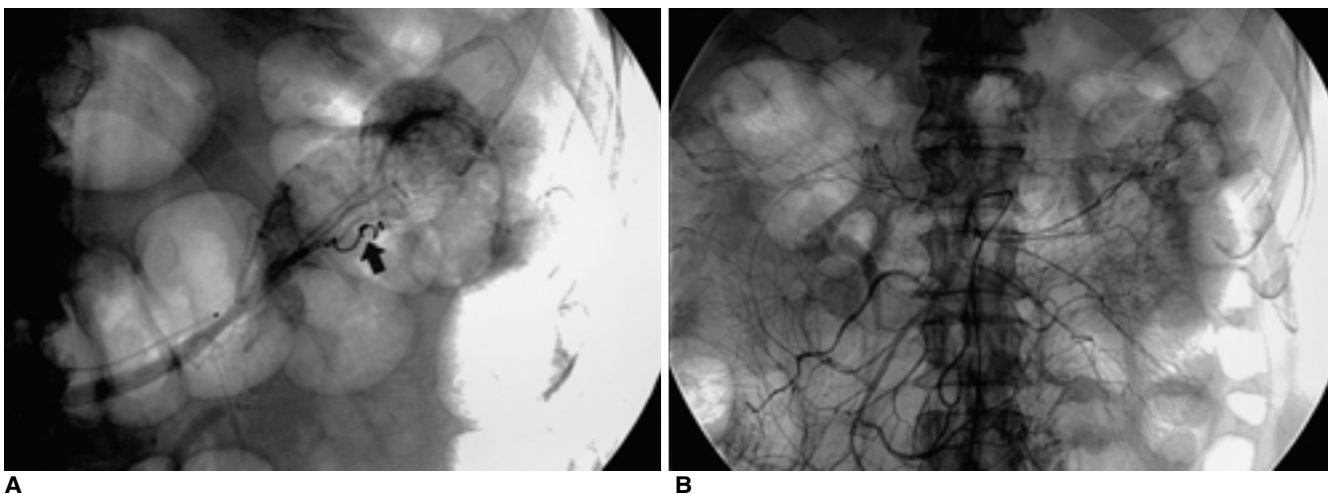


Fig. 2. A. Transcatheter embolization was performed with two microcoils (3 mm × 23 mm in size) (arrow).
B. Post-embolization angiogram showed total occlusion of the feeding vessel without evidence of contrast material extravasations.

vasopressin infusion is associated with a high initial control rate, the rebleeding rates after termination of infusion are high (20 - 50%) and it is associated with a high rate of cardiovascular complications (40% or so). Transcatheter embolization avoids the potential problems of catheter dislodgement and systemic complications. However, the small bowel, and especially the large bowel, do not have the rich collateral supply characteristic of stomach and duodenum. The potential risk of gut infarction after percutaneous embolization is therefore greater.

Recently the development of finer coaxial microcatheters, guidewires, and digital angiographic equipment have enabled more peripheral superselective catheterization of distal vessels, permitting more selective vascular intervention. We can reduce the arterial pressure to the bleeding site, while preserving the potential for collateral arterial supply to prevent ischemic damage to the intestinal wall. Studies in the

1980s showed a 10 - 20% incidence of postembolization infarction, whereas later studies in the 1990s demonstrated no or fewer cases of postembolization infarction. In this respect, microcoils would be the agents of choice, which are easy to use and theoretically pose a lesser threat of ischemia than PVA particles, which may disseminate to the smaller vessels.

Embolization may not be possible in cases of vessel spasm, spontaneous cessation of bleeding, and vascular tortuosity. Embolization can be the definitive and only treatment used in about half the cases of embolization. In these cases, patients can avoid the morbidity and mortality associated with emergency surgery. However, when bleeding is controlled, all patients should undergo colonoscopy to determine the underlying pathology. Angiodysplasia had a high rate of repeated bleeding despite initial angiographic control and may warrant elective surgical resection.



Fig. 3. A, B. A contrast enhanced computed tomography (CT) of the abdomen showed lobulating contoured soft tissue mass in the region of proximal jejunum with foreign body artifact induced by microcoils adjacent to small bowel mesentery. The mass was well marginated, homogeneously low attenuated and not enhanced. **C.** Small bowel follow-through study revealed smooth marginated intraluminal filling defect.

Also resectable neoplasms require curative surgery. Embolization in these instances will allow safer and more elective surgery.

In our case, emergency embolization was attempted to stop bleeding and a jejunal mass was found on the following CT. And then surgical resection was performed and the histopathologic report revealed GAN tumors. This is a case that we successfully treated bleeding of jejunal GAN tumors with transcatheter coil embolization technique.

GAN tumors are extremely rare neoplasms that compose a distinct subcategory of GIST, arising from autonomic nervous system plexuses of GI tract such as those of Meissner or Auerbach, also termed plexosarcoma. A symptomatology of GAN tumor is variable and often nonspecific. Generalized symptoms of low-grade fever, malaise, fatigue, and pallor can be seen. A minority of cases may present with GI bleeding. It is not possible to distinguish GAN tumors from other GIST based on radiologic techniques.

In summary, although very rare, lower GI bleeding can be caused by GAN tumors. We successfully performed emergency transcatheter coil embolization for a jejunal GAN tumor. So, in cases of lower GI bleeding, this disease entity should be born in mind, and transcatheter coil embolization can be the treatment of choice for emergency bleeding control in such a case.

References

1. Herrera GA, de Morales HP, Grizzle WE, Han SG. Malignant small bowel neoplasm of enteric plexus derivation (plexosarcoma): light and electron microscopic study confirming the origin of the neoplasm. *Dig Dis Sci* 1984;29:275-284
2. Rueda O, Escribano J, Vicente JM, Garcia F, Villeta R. Gastrointestinal autonomic nerve tumors (plexosarcomas). Is a radiological diagnosis possible? *Eur Radiol* 1998;8:458-460
3. Bandi R, Shetty PC, Sharma RP, Burke TH, Burke MW, Kastan D. Superselective arterial embolization for the treatment of lower gastrointestinal hemorrhage. *J Vasc Interv Radiol* 2001; 12:1399-1405

Case 8

가

Transcatheter Microcoil Embolization of Multiple Pseudoaneurysm of Splenic Artery

: Splenic arteries, pseudoaneurysm
Splenic arteries, interventional procedures
:46 /
:
hemoper -
itoneum
가 12.7 g/dl 8.8
g/dl CT
: Delayed bleeding from multiple pseudoaneurysm of splenic artery

CT scan splenic hilum central portion
splenic substance
(Fig. 1),
가

(Fig. 2).

5 Fr cobra - shaped catheter splenic hilum
distal portion , 3Fr Renegade
microcatheter(Boston Scientific, Watertown, MA, U.S.A.)
가

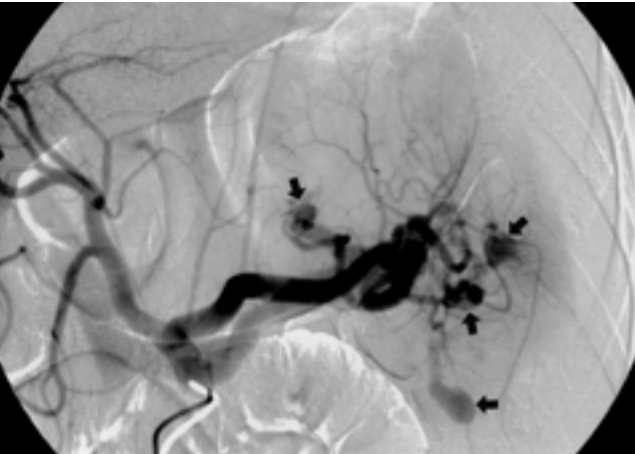


Fig. 2. Celiac arteriography shows multiple pseudoaneurysms (arrows) with AV fistulae, early draining veins in splenic substance.

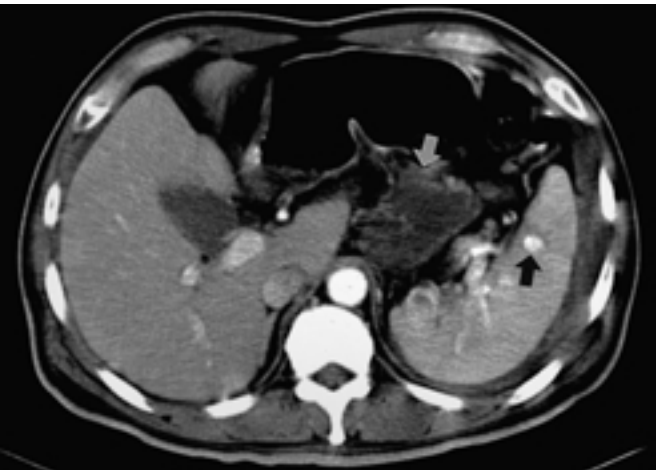


Fig. 1. A, B. CT images from a 45-year-old man after motor vehicle collision. Axial CT image shows splenic laceration (white arrow head) with multiple pseudoaneurysms (arrow). Pseudocyst in suprapancreatic area (white arrow) is also seen.



(4) 3 - 6 mm microcoil 15 (Fig. 3). 6 mm coil 0.018 inch guidewire , microcoil guidewire (Fig. 4) upper polar branch 가 가 , staining (Fig. 5). Short gastric artery Lt

gastroepiploic artery, pancreatic artery collateral artery intact . 9.9 g/dl . 5 CT , gas bubble (Fig. 6). observation acute blunt trauma CT

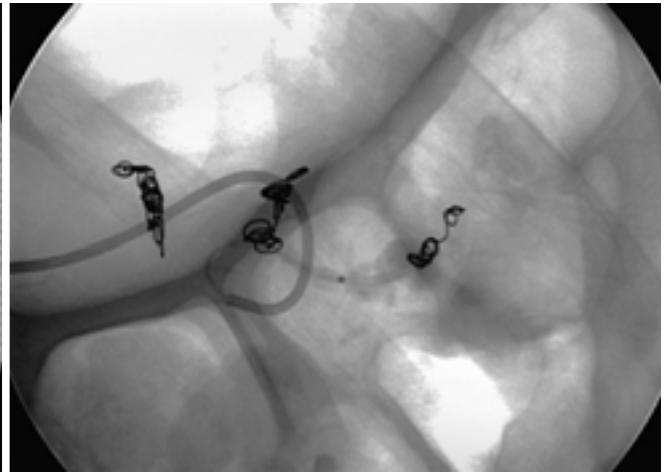
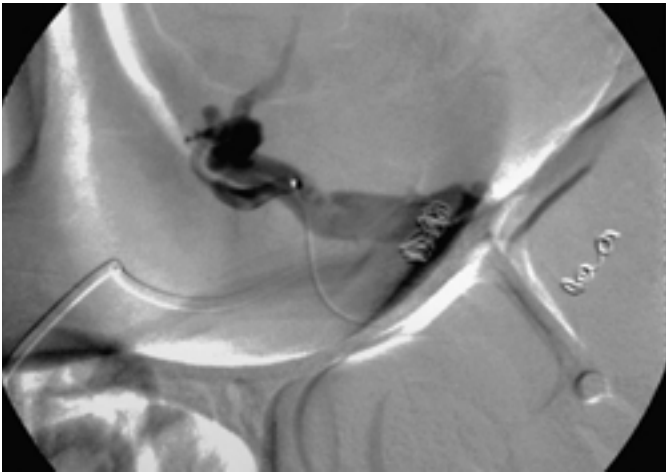


Fig. 3. A, B. Superselective arteriography shows feeding artery, pseudoaneurysmal sac, AV fistula and early draining veins. Superselective embolization of feeding arteries was done with 3-6 mm diameter Vortex and diamond shaped microcoils, 15 pieces in number.

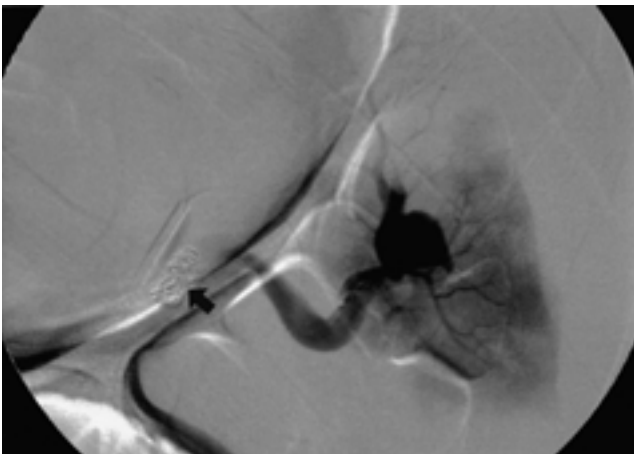


Fig. 4. 6 mm diameter microcoils are misplaced and proximally migrated, so occluded a large branch of splenic artery.

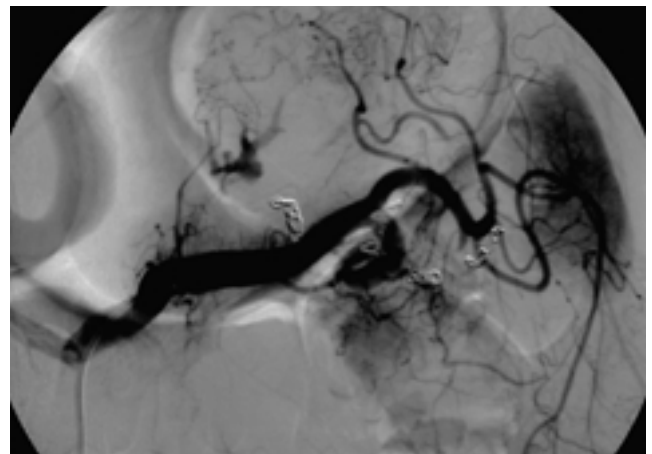


Fig. 5. Post-embolization arteriogram shows successful occlusion of multiple pseudoaneurysms (no more seen pseudoaneurysm, AV fistula, early draining veins and preservation of short gastric artery, gastroepiploic artery, pancreatic artery) but large infarcts are developed and only some portion of spleen is normally stained.

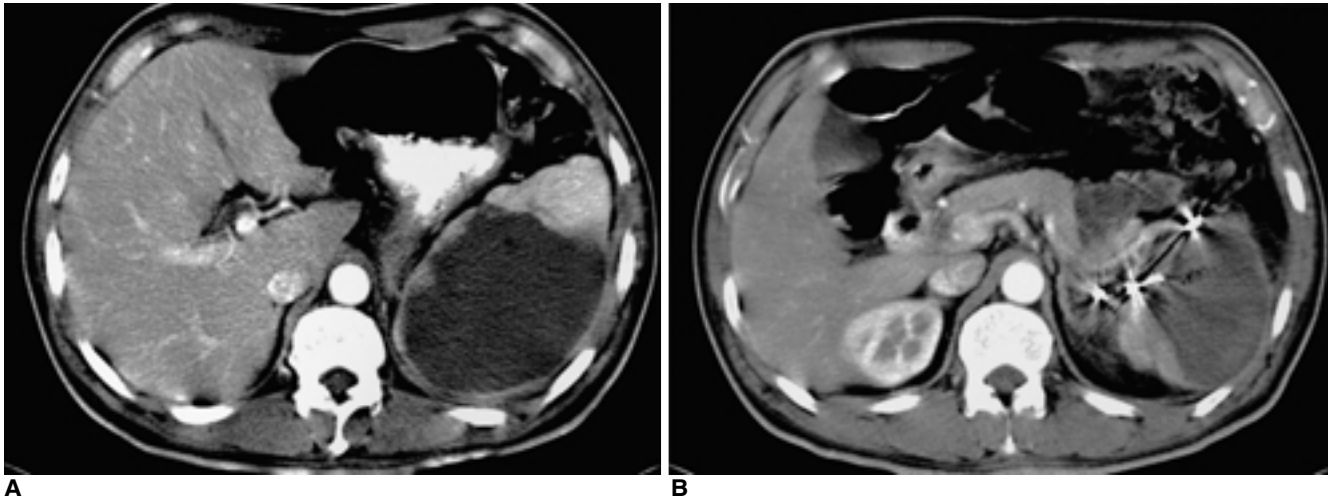


Fig. 6. A, B. Post-embolization CT scan shows successful embolization of pseudoaneurysm but as a result, large infarcts are developed and only small portion in the spleen is normally preserved.

, CT
CT
acute bleeding
surgical
hemostasis
blunt splenic injury
CT
가
vascular blush
가
splenic salvage
splenectomy
splenorrhaphy
transcatheter coil embolization
Blunt splenic injury 74% 가
CT scan 가 가
가
CT
nonsurgical hemostasis
transcatheter coil embolization (가
) 가
CT 가
omental, pancreatic vessels)
가
(100%

vs 63%).
perisplenic collaterals가 splenic parenchyma
parenchyma 25% , peripheral
가
가
가
Gelfoam , splenic parenchyma gas
가 가
(subcapsular) 가 air -
fluid level 가
free air가 가
blunt splenic trauma 가
splenic salvage
transcatheter microcoil embolization 가
가
blunt splenic injury
가
(gastric, 가
, CT
resolution
가

1. Killeen KL, Shanmuganathan K, Boyd-Kranis R, Scalea TM, Mirvis SE. CT findings after embolization for blunt splenic trauma. *J Vasc Interv Radiol* 2001;12:209-214
2. Davis KA, Fabian TC, Croce MA, et al. Improved success in nonoperative management of blunt splenic injuries: embolization of splenic artery pseudoaneurysms. *J Trauma* 1998;44:1008-1013
3. Salis A, Pais SO, Vennos A, Scalea T. Superselective embolization of a traumatic intrasplenic arteriovenous fistula. *J Trauma* 1999;46:186-188

Case 9

가

Coil Embolization of a Traumatic Pseudoaneurysm of the Uterine Artery

: Embolism, therapeutic
Hemorrhage

Bloomington, IN, U.S.A.)

:29 /

: pumping

가
3 tornado microcoil

: 가

. Loop technique

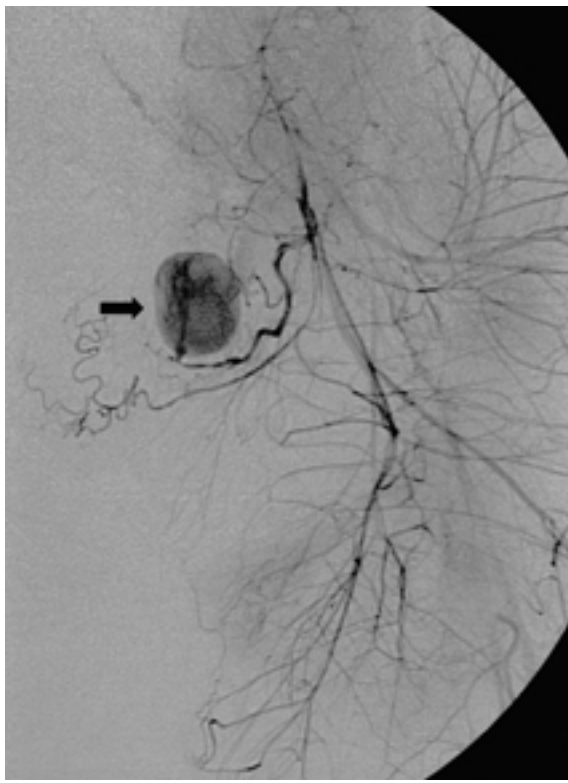
Left internal iliac angiogram left uterine artery
jet flow 가 가 , draining vein
contrast leakage가 .

(postpartum bleeding)

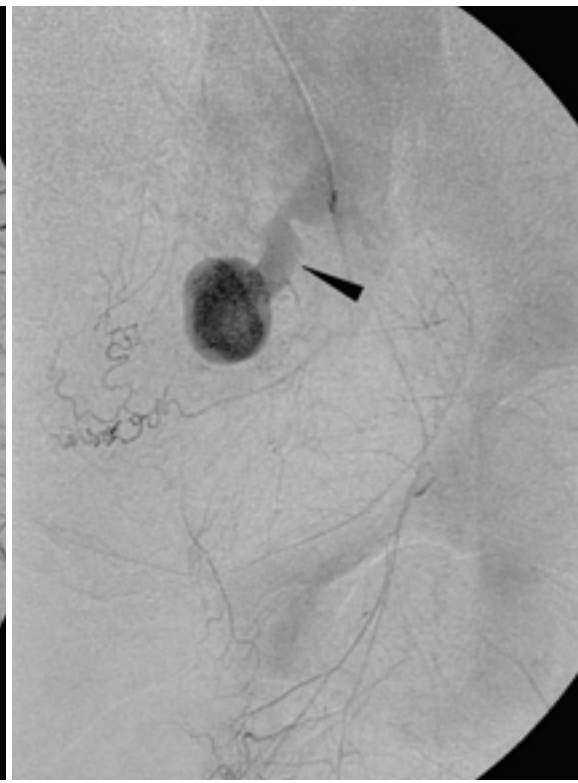
5 - F cobra catheter(Cook,

, 24

(uterine atony) 가



1



2

Fig. 1, 2. Left internal iliac arteriograms show an aneurysm (arrow) from the left uterine artery. A pseudo-vein or draining vein (arrow-head) representing contrast extravasation is noted at delayed phase.

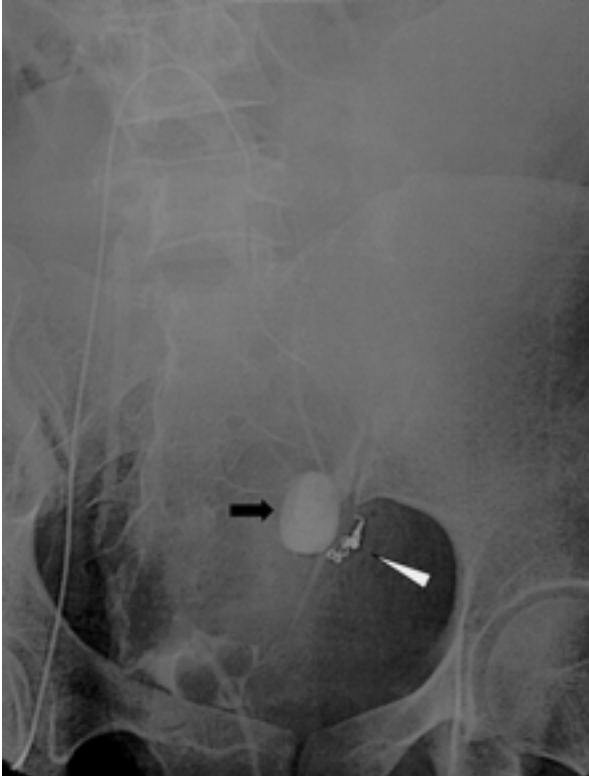


Fig. 3. Embolization of the left uterine artery was performed using three microcoils (arrowhead). Remained contrast media in the pseudoaneurysm is identified (arrow).

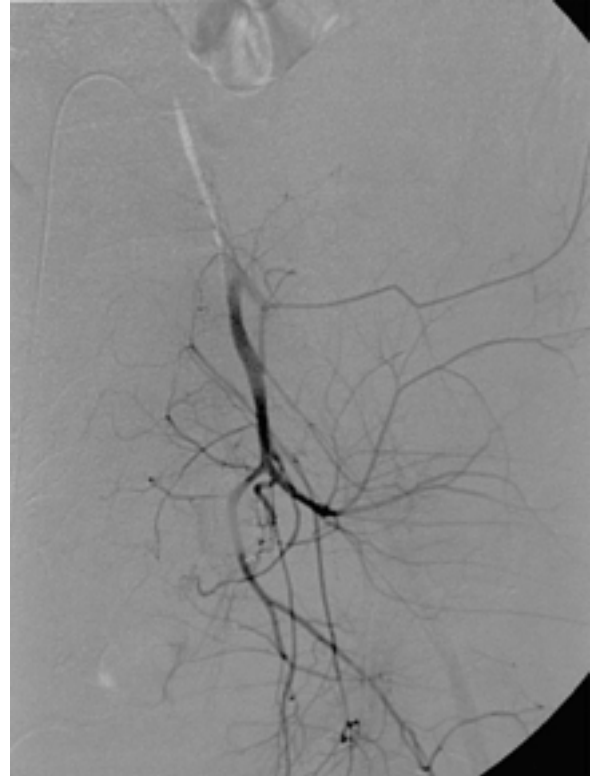


Fig. 4. Left internal iliac arteriogram following embolization shows complete occlusion of the uterine artery.

24 6
500 ml
, 1 - 3%
8 14
가
가
가
suction evacuation
curretage
가

가
가 가
90 - 95%
가
1. Pelage JP, et al. Secondary postpartum hemorrhage: treatment with selective arterial embolization. Radiology 1999;212:385-389
2. Yamashita Y, Harada M, Yamamoto H, et al. Transcatheter arterial embolization of obstetric and gynaecological bleeding: efficacy and clinical outcome. Br J Radiol 1994;67:530-534

Case 10

Ovarian Artery Embolization for Postpartum Uterine Bleeding

: Transcatheter embolization
Postpartum, uterus
Ovarian artery
:28 /
:
Hb 8.2, Hct 24.3, (Fig. 2A).
aPTT 49.3, PT 54%
: Postpartum hemorrhage due to Uterine Atony (Fig. 2B).

(Fig. 1). 가 가

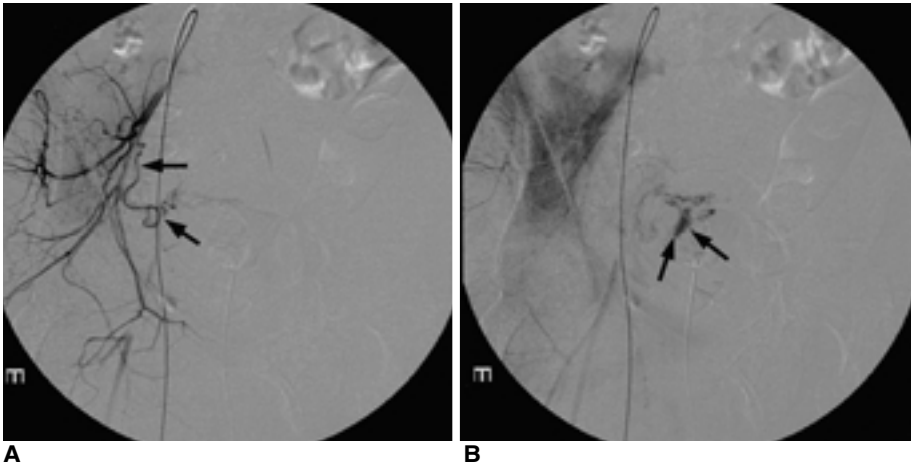


Fig. 1. A 28 year-old woman presented with vaginal bleeding immediately after normal delivery.
A. Right iliac arteriogram showed diffusely enlarged uterine artery (arrows).
B. On delayed phase, extravasation of contrast material in pelvic cavity was noted (arrows).

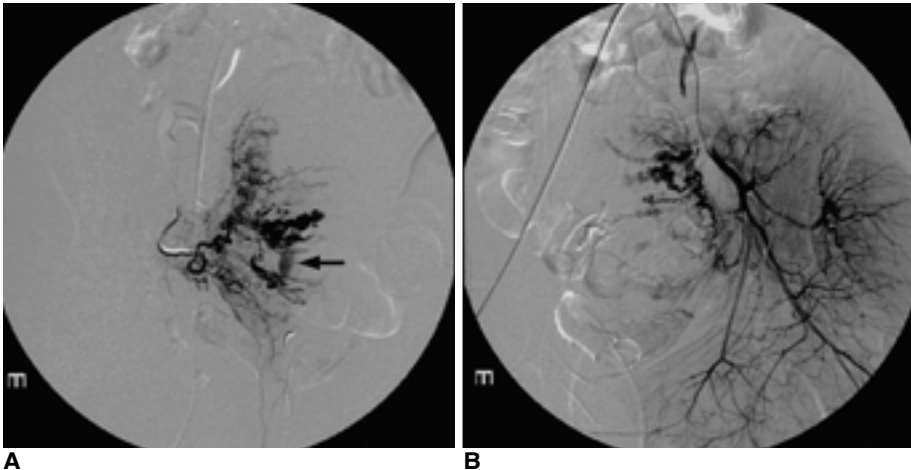


Fig. 2. A. Selective angiogram of right uterine artery showed innumerable tortuously dilated branches with extravasation of contrast material (arrow).
B. Left iliac angiogram showed prominent uterine artery and hypervascular staining of uterus without definite extravasation.

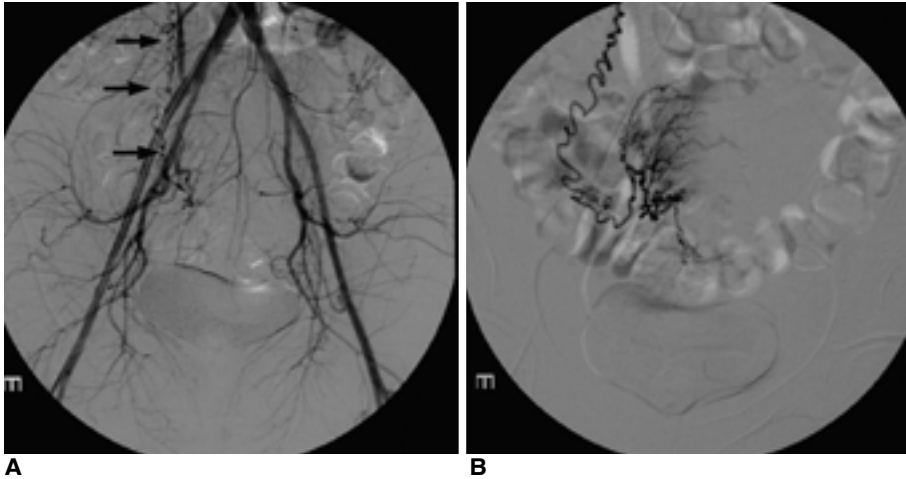


Fig. 3. A. abdominal aortogram obtained with tip of catheter located at the level of renal artery showed complete embolization of both uterine arteries. However, prominent right ovarian artery was noted (arrows).
B. Selective angiogram of right ovarian artery showed collateral flow into the uterus.

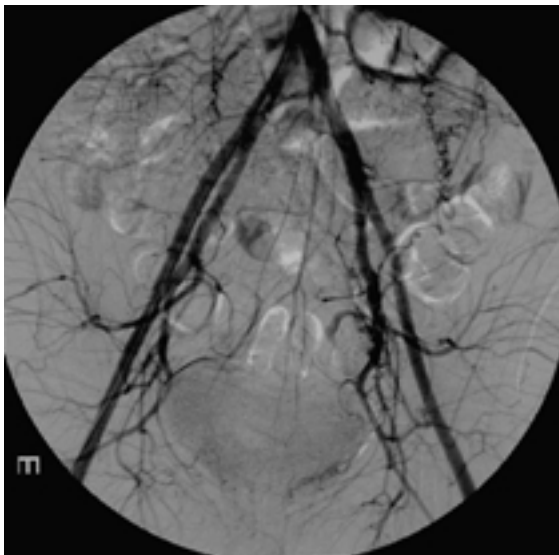


Fig. 4. Final angiogram obtained after embolization of right ovarian artery showed complete disappearance of hypervascular staining of the uterus. No more extravasation of contrast material was noted.

tract laceration

morbidity, mortality

gelatin sponge

slurry and pledgets, PVA particles, calibrated microsphere

. Gelatin sponge 가

가

가

가

PVA particle

가

. Calibrated

microsphere

가

가

()

,

25%

가

(Fig. 3A).

가

(Fig.3B).

(Fig. 4)

.

24

500 mL

uterine atony, lower genital tract

laceration, retained placental tissue, rupture of uterine body

.

가

가

uterine atony, lower genital

1. Pelage J-P, Le Dref O, Mateo J, et al. Life-threatening primary postpartum hemorrhage: treatment with emergency selective arterial embolization. *Radiology* 1998;208:359-362
2. Binkert CA, Andrews RT, Kaufman JA. Utility of nonselective abdominal aortography in demonstrating ovarian artery collaterals in patients undergoing uterine artery embolization for fibroids. *JVIR* 2001;12:841-845

Case 11

Primary Stent Insertion of Both Renal Arterial Stenoses in Takayasu Arteritis

: Takayasu arteritis
Hypertension, renovascular
Renal arteries, stents and prostheses
:23 /
:
180/110 mmHg
, Oral captopril
test renin activity가 가 aldosterone
renovascular hypertension
:Takayasu arteritis

(Fig. 1).
가
(Fig. 2). ,
(Fig. 3), (ostial lesion)
(eccentric stenosis)

6Fr arterial sheath
heparin 5000 unit sheath . 5 Fr

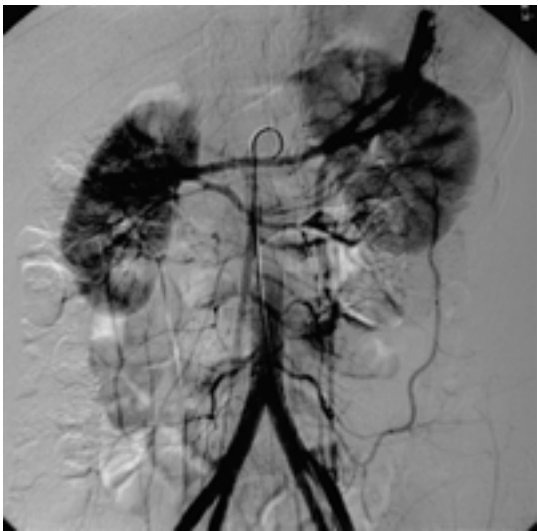


Fig. 2. Abdominal aortogram shows complete occlusion of origin of SMA and visualization of SMA through IMA.

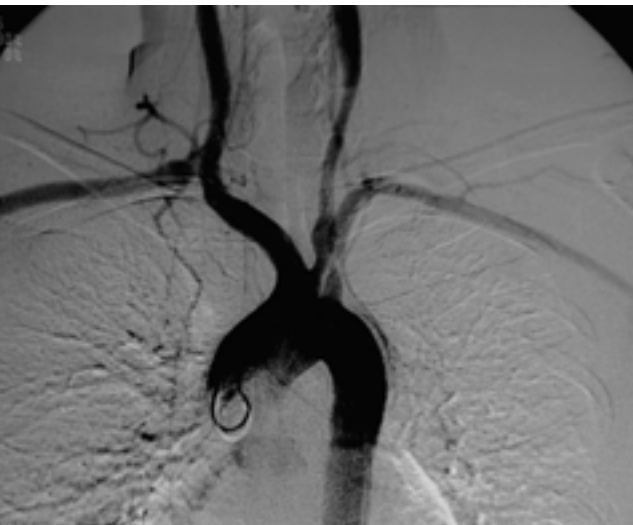


Fig. 1. Ascending aortogram shows stenoses of proximal left common carotid and subclavian arteries.

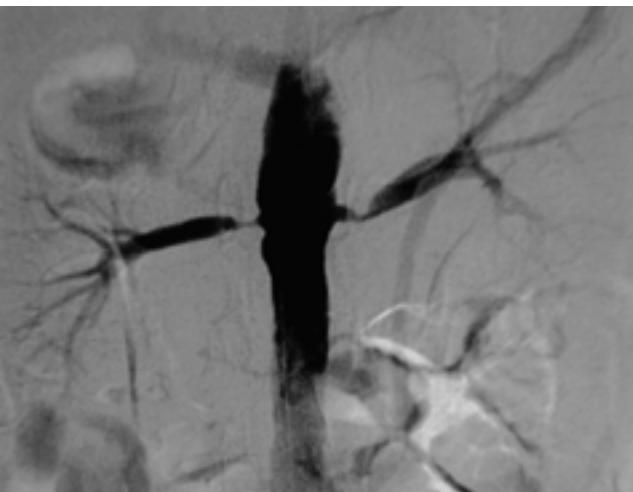
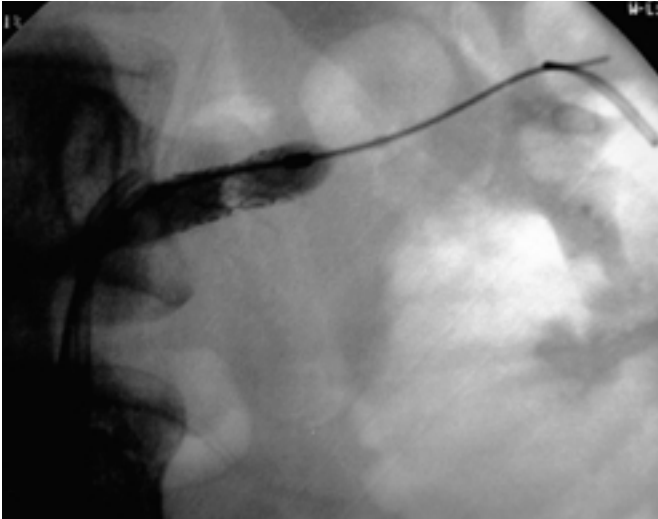


Fig. 3. Abdominal aortogram shows renal arterial stenoses on both sides. Ostial stenosis of right renal artery and eccentric stenosis of left renal artery are noted.



4



5

Fig. 4, 5. Balloon expandable stents are inserted in both renal arteries.

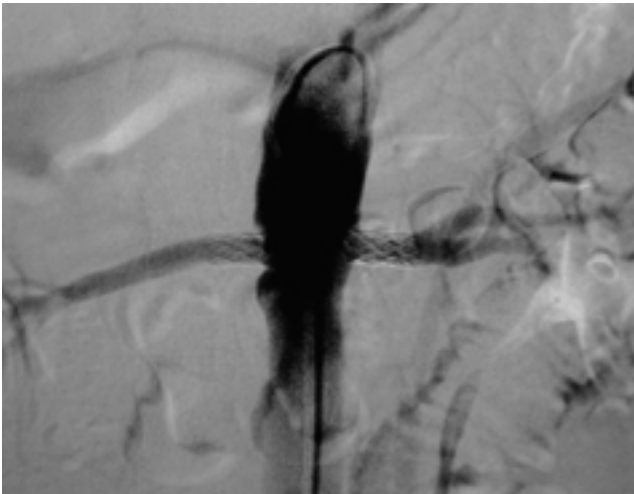


Fig. 6. Final abdominal aortogram shows improvement of both renal arterial stenoses after stents insertion.

RDC Pigtail

ostial lesion eccentric stenosis

0.035 inch guide wire
6 mm * 2 cm balloon expandable stent (Corinthian: Cordis Inc., Warren, NJ) (Fig. 4).

(Fig. 5).

(Fig. 6).

patch closure

Takayasu

가

가

revascularization graft

가

Takayasu

Sharma

가

, Takayasu

()

flow compromising dissection, 20mmHg

elastic recoil, 가

30%

eccentric stenosis

ostial lesion

elastic recoil

96 - 100% , 1 - 2 80%, Takayasu
 5 70% 80% ostial lesion
 , 50% eccentric stenosis
 , 5 50%
 , 80%

Takayasu

. Sharma

5

가

71%

Takayasu

가

가

가

ostial lesion

eccentric

stenosis

1. C.G.Isles, S. Robertson and D. Hill. Management of renovascular disease: a review of renal artery stenting in ten studies. *Q J Med* 1999;92:159-167
2. Rees CR. Stents for atherosclerotic renovascular disease. *JVIR* 1999;10:689-705
3. Park JH, Han MC, Kim SH, et al. Takayasu's arteritis: angiographic findings and results of angioplasty. *AJR* 1989;153: 1069-1074
4. Yutan E, Glickerman DJ, Caps MT, et al. Percutaneous transluminal revascularization for renal artery stenosis: Veterans Affairs Puget Sound Health Care System experience. *J Vasc Surg* 2001;34:685-693
5. Sharma S, Thatai D, Saxena A, et al. Renovascular hypertension resulting from nonspecific aortoarteritis in children: midterm results of percutaneous transluminal renal angioplasty and predictors of restenosis. *AJR* 1996;166:157-162
6. Park HS. Renal artery stenosis. In Han MC, Park JH. *Interventional Radiology*. 1st ed. Seoul; Ilchokak 1999;242-256

Case 12

Chronic Mesenteric Ischemia : Balloon Angioplasty and Stent Placement

: Arteries, stenosis or obstruction

Arteries, transluminal angioplasty

Arteries, stent and prostheses

:58 /

:

9

, 4

Coumadin

:

90%

(jejunal branch)

(Fig. 1).

5Fr multipurpose

1

Urokinase

20 unit

heparinization

8Fr renal guiding

catheter(Cordis, Roden, Netherland)

6 × 20 mm balloon

70%

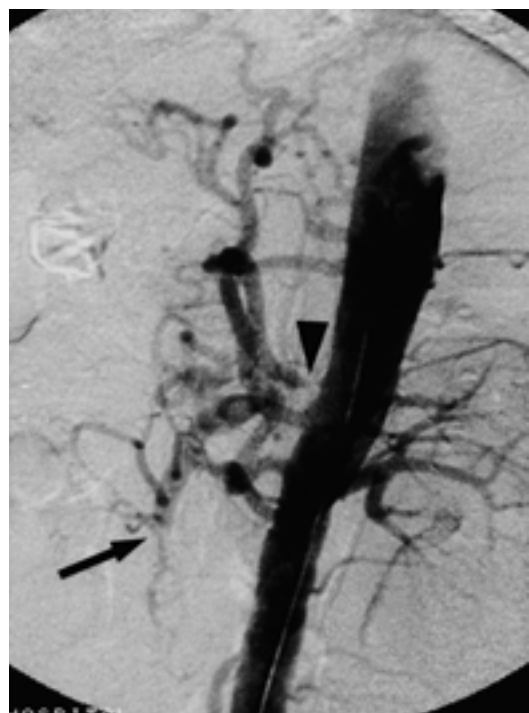
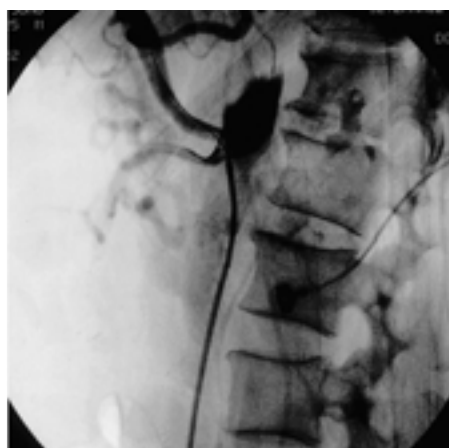


Fig. 1. Aortogram shows significant stenosis of celiac artery (arrowhead) and complete obstruction of superior mesenteric artery with emboli (arrow).



A



B

Fig. 2. A. Following balloon angioplasty, a Corinthian stent was inserted within the celiac artery.

B. Post-stenting angiogram shows that celiac artery restores normal caliber and blood flow.

6 mm, 16 mm Corinthian

IQ stent(Cordis, Roden, Netherland)

(Fig. 2).

8 Fr Oasis catheter

(Boston scientific, Watertown, MA, U.S.A.)

4 mm×20 mm balloon

(Fig. 3).

Heparin

14 stent

8 Fr renal guiding catheter

0.035 inch superstiff J - tip guide

wire(Cook, Bloomington, U.S.A.)

, 6 mm×20 mm balloon

70%

6 mm×16 mm Corinthian IQ stent

(Fig. 4).

scular dysplasia),

가

(fibromu -

1980

(elastic recoil)

가

Nyman

5

stent

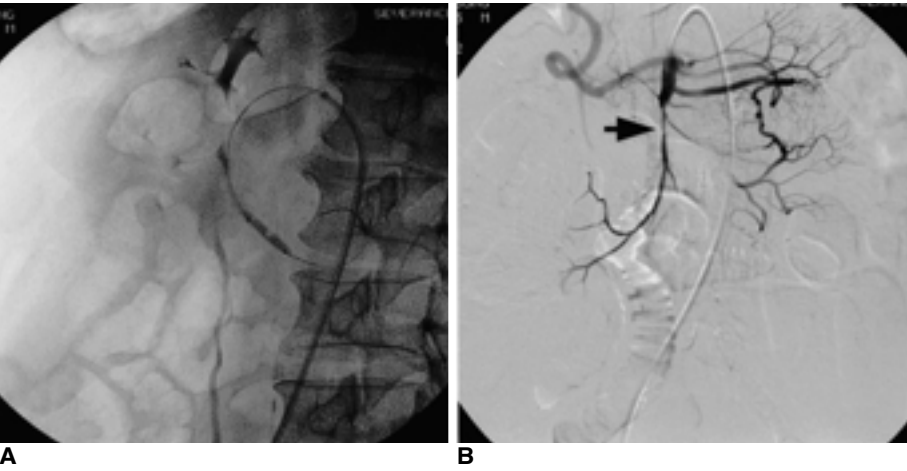


Fig. 3. A. Aspiration thrombectomy and balloon angioplasty were performed for the superior mesenteric artery. **B.** Post-angioplasty angiogram shows substantial residual stenosis (arrow).

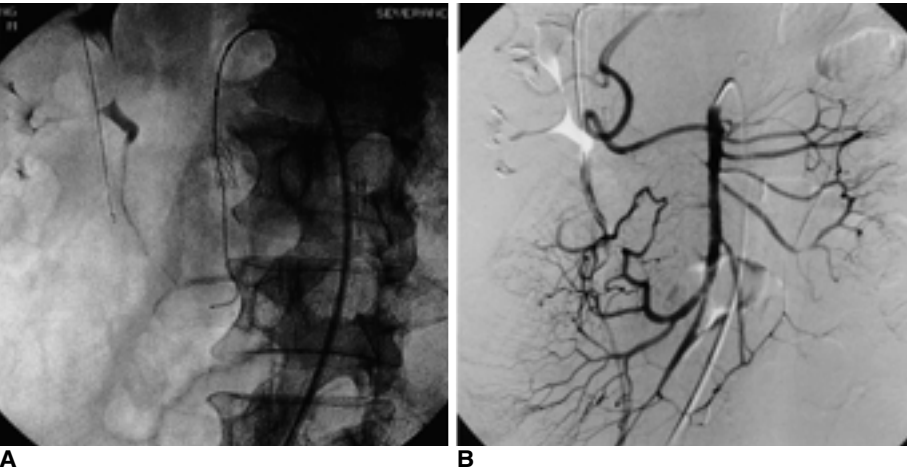


Fig. 4. A. A Corinthian stent was inserted within the stenotic portion of superior mesenteric artery. **B.** Post-stenting angiogram shows restored normal diameter of SMA and distal blood flow.

가 guiding catheter
stent

(ischemic infarct)
가 ,
(reperfusion syndrome)

가

1. Nyman U, Ivancev K, Lindh M, Uher P. Endovascular treatment of chronic mesenteric ischemia: Report of five cases. Cardiovasc Intervent Radiol 1998;21:305-313
2. Gotsman I, Verstandig A. Intravascular stent implantation of the celiac artery in the treatment of chronic mesenteric ischemia. J Clin Gastroenterol 2001;32:164-166
3. Loomer DC, Johnson SP, Diffin DC, DeMaoribus CA. Superior mesenteric artery stent placement in a patient with acute mesenteric ischemia. J Vasc Interv Radiol 1999;10:29-32

Case 13

Stent Placement for the Treatment of Stenotic Portal Vein After Liver Transplantation

: Liver, transplantation
Portal vein, interventional procedure
Liver, interventional procedure

:4 /

: Biliary atresia

1 (42)

: Portal vein stenosis after liver transplantation

CT

(Fig. 1).

needle S3 21 G chiba
5 F cobra catheter(Cook, Bloomington,
IN, U.S.A.) 0.035 inch

(Fig. 2).

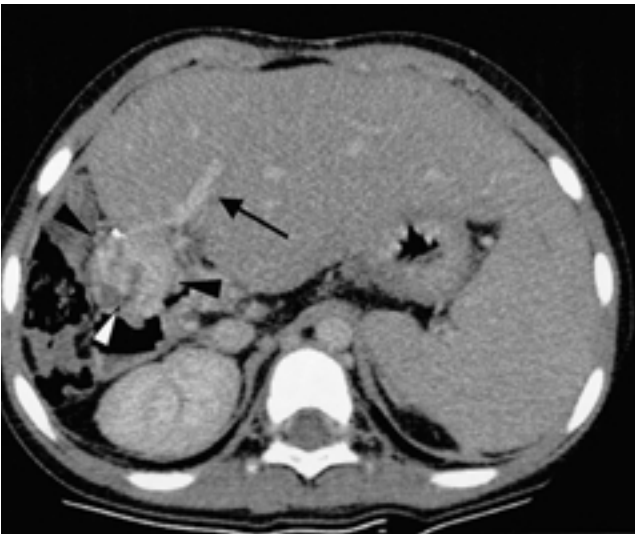


Fig. 1. Enhanced CT shows multiple collateral vessels adjacent to the portal vein anastomosis. Intrahepatic portal vein is patent.

7 F sheath
8 mm (Synergy, Medi - Tech,
Watertown, MA, U.S.A.)

11 mmHg

10 mm,
5 cm Wallstent(Medi - Tech, Watertown, MA, U.S.A.)
(Fig. 3).

mmHg

(Fig. 4).

4 hilal coil(Cook, Bloomington, IN, U.S.A.)
1

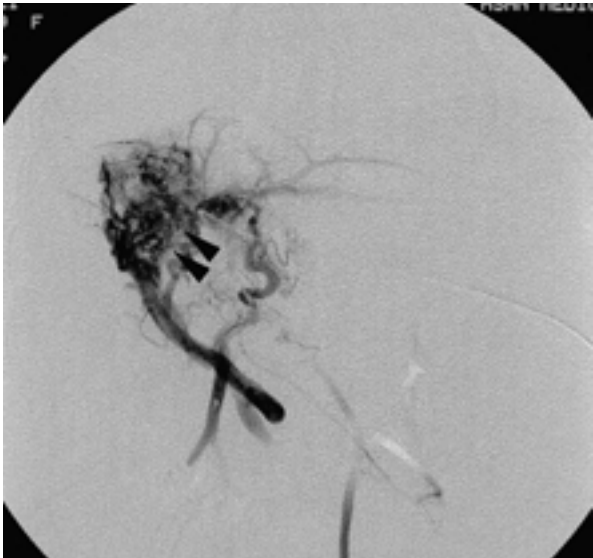


Fig. 2. Direct portogram through a S3 portal branch shows complete occlusion of portal vein at anastomotic site with multiple peri-portal collaterals.



Fig. 3, 4. Portogram obtained following stent placement shows normalized portal flow. Pressure gradient across the occlusion was zero.

tight suture

Cherukuri

4

가 가
가 가

. Funaki

74%

26% elastic recoil

Funaki

가

가

가

가

가

가

1. Cherukuri R, Haskal ZJ, Naji A, Shaked A. Percutaneous thrombolysis and stent placement for the treatment of portal vein thrombosis after liver transplantation: long-term follow-up. *Transplantation* 1998;65:1124-1126
2. Funaki B, Rosenblum JD, Leef JA, et al. Portal vein stenosis in children with segmental liver transplants: treatment with percutaneous transhepatic venoplasty. *AJR* 1995;165:161-165

Case 14

가

-

Stent-graft Placement of Proximal Anastomotic Pseudoaneurysm after Abdominal Aortic Prosthetic Reconstruction in a Patient with Behcet Disease

: Aorta, grafts and prostheses

Aneurysm, aortic

Aneurysm, therapy

Behcet disease

:38 /

: 8

7

graft

CT

가 가 .

: pseudoaneurysm after abdominal aortic prosthetic reconstruction in a patient with Behcet disease

CT

가 (Fig. 1).

1.5 cm

graft

가 가 (Fig. 2).

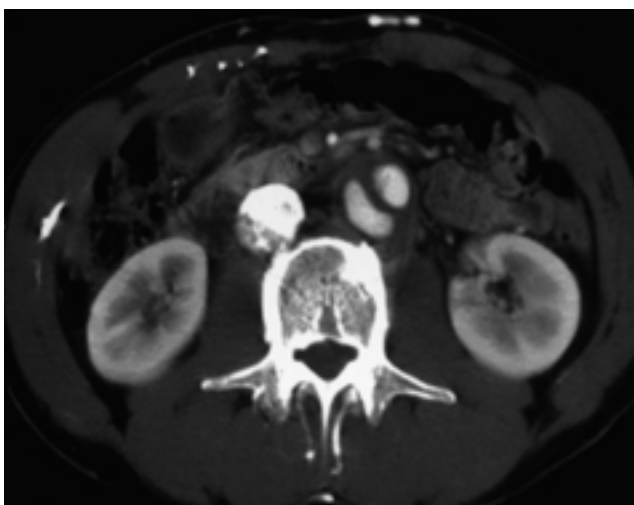


Fig. 1. Abdominal CT shows a pseudoaneurysm at infrarenal aorta.

(Fig. 2).

가

12F sheath

가 , 20×18(bare stent) - 18×50(graft) - 20×18(bare stent)mm stent-graft (S & G Biotech, Seoul, Korea)

가 가

stent-graft graft cover

distal stent

. Stent-graft graft site 20×56mm bare stent (Fig. 3).

가 가

(Fig. 4). 5

CT

가 가

stent

(Fig. 5).

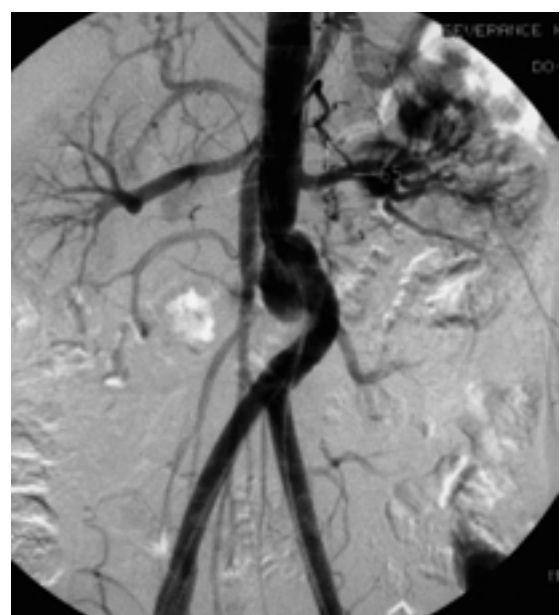


Fig. 2. Aortogram shows a pseudoaneurysm at proximal anastomotic site.

, 가
가

aneurysms in Behcet disease: management with stent-grafts-
initial experience. Radiology 2001;220:745-750

2. , , , .

2002;35:36-42

3. Tiesenhausen K, Hausegger KA, Tauss J, Amann W, Koch G.
Endovascular treatment of proximal anastomotic aneurysms
after aortic prosthetic reconstruction. Cardiovasc Intervent
Radiol 2001;24:49-52

1. Park JH, Chung JW, Joh JH, et al. Aortic and arterial

Case 15 Stent-Grafting for Inflammatory Abdominal Aortic Aneurysm

: Retroperitoneal fibrosis
 Inflammatory abdominal aortic aneurysm
 Contained aortic rupture
 : 59 /
 : 3
 . ESR 60
 mm/Hr(< 10)
 : Inflammatory abdominal aortic aneurysm

가 . CT

가 , (Fig. 1A).

1 AneuRx
 (Stent - graft (Medtronic, MN, U.S.A.)
 (Fig. 1B).

BUN/Cr 가 ,
 double - J stent (Cook, Bloomington, IN, U.S.A.)

CT



A **B**
Fig. 1. (A) CT and **(B)** Abdominal aortogram reveal infrarenal abdominal aortic aneurysm extending to right common iliac artery. Extensive soft tissue mass encases abdominal aorta from the level of renal artery to iliac bifurcation level. Mild degree of hydronephrosis is also noted bilaterally.

stent
exclusion , 가 (Fig. 2A). ,
Retroperitoneal fibrosis fibroblastic proliferation
가 (Fig. 2B). perivascular chronic inflammatory infiltration ,
Mitchinson chronic periaortitis

(secondary retroperitoneal fibrosis)
가 , 가 ,
Walker 가
(inflammatory abdominal aortic aneurysm) 80% 5
3 - 10% 1
, ESR 가
가 ,
obstructive uropathy가 , 가
가 shear stress가 ,
Rose 가

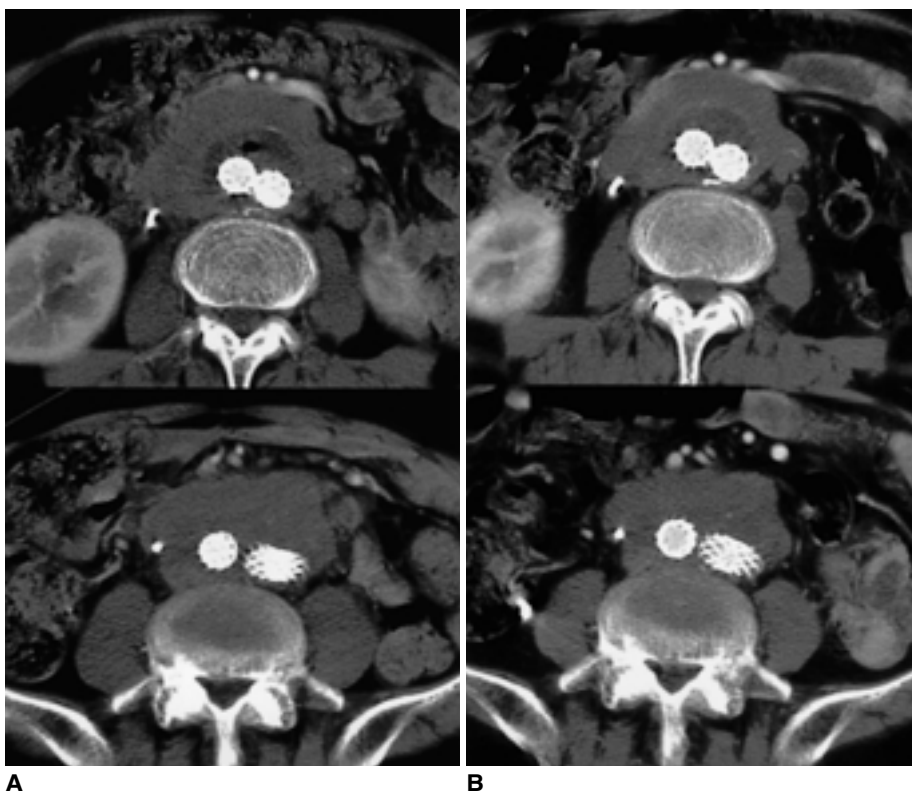


Fig. 2. A. One-month follow-up CT scan shows that the abdominal aortic aneurysm is completely excluded by stent-graft. Note that the size of the surrounding soft tissue mass has not changed. **B.** Six-month follow-up CT scan shows that the size of the surrounding soft tissue mass encasing aorta has slightly decreased, probably due to steroid administration.

1. Rasmussen, Todd E. Inflammatory aortic aneurysms: a clinical review with new perspectives in pathogenesis. *Ann Surg* 1997;225:155-164
2. von Fritschen U, Malzfeld E, Clasen A, Kortmann H. Inflammatory abdominal aortic aneurysm: a postoperative course of retroperitoneal fibrosis. *J Vasc Surg* 1999;30:1090-1098
3. Kottra JJ, Dunnick NR. Retroperitoneal fibrosis. *Radiol Clin North Am* 1996;34:1259-1275
3. Walker DI, Bloor K, Williams G, Gillie I. Inflammatory aneurysms of the abdominal aorta. *Br J Surg* 1972;59:609-614
4. Rose AG, Dent DM. Inflammatory variant of abdominal aortic atherosclerotic aneurysm. *Arch Pathol Lab Med* 1981;105:409-413
5. Nitecki SS, Hallett JW Jr, Stanson AW, et al. Inflammatory abdominal aortic aneurysms: new clinical implications from a case control study. *J Vasc Surg* 1996;23:860-869
6. Vallabhaneni SR, McWilliams RG, Anbarasu A, et al. Perianeurysmal fibrosis: a relative contra-indication to endovascular repair. *Eur J Vasc Endovasc Surg* 2001;22:535-541

Case 16

Endoluminal Treatment of Common Iliac Arteriovenous Fistula with Implantation of Stent-Graft

: Arteries, iliac

Fistula, arteriovenous

Interventional procedures, Stents and
prostheses

: 21 /

: 6 Grade II

abdominal bruit 가

. CT

. 2

: Iatrogenic left common iliac AV fistula
complicated with heart failure

0.035 inch

Super - stiff J - tip guide wire(Medi - tech/Boston Scientific,
Watertown, MA, U.S.A.)

13mm, 6cm - (,
,) 12 × 40 mm Ultrathin Diamond

Balloon Catheter(Medi - tech/ Boston Scientific, Watertown,
MA, U.S.A.) (Fig. 3).

(Fig. 4) 가

fabric tear

12 mm, 25 mm - (JOMED,
Helsingborg, Sweden) 가 .

(Fig. 5).

가 .

CT scan

(Fig. 1).

Pelvic arteriogram

(Fig. 2).

. 2

CT

(Fig. 6).



A



B

Fig. 1. (A)Axial and **(B)**coronal reformat-
ted CT scan shows fistulous com-
munication between left common iliac
artery and vein with severe dilatation of
IVC.

graft material stent 6 mm

, 16 - 22%

10 - 25%

가

Stent - graft

가

1991 Becker

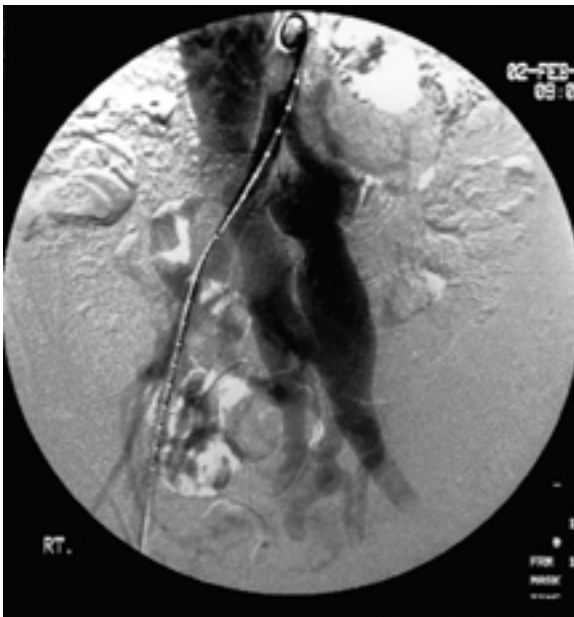


Fig. 2. Pelvic arteriogram shows early opacification of left iliac vein and IVC through iliac AV fistula.



Fig. 4. Pelvic arteriogram after insertion of a stent-graft shows leakage of contrast media at mid-portion of the stent-graft (arrow).



Fig. 3. Balloon dilatation was done after insertion of a 13 mm x 60 mm stent-graft in left iliac artery.



Fig. 5. Final pelvic arteriogram after insertion of another 12 mm x 25 mm stent-graft shows complete exclusion of iliac AV fistula without leakage of contrast media.

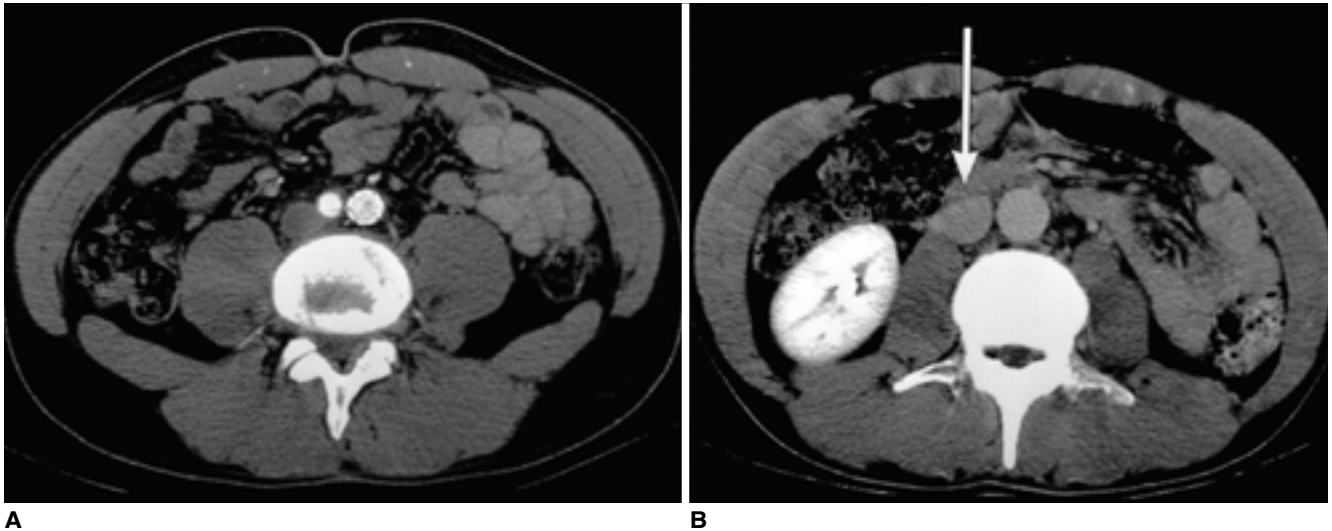


Fig. 6. Follow-up CT scan after 2 months shows (A) patent stent-graft and (B) restoration of IVC diameter to normal level(arrow).

1. Brunkwall J, Lindblad B, Ivancev K, et al. Iatrogenic AV-fistula treated by a graft-covered self-expandable stent. *Eur J Enovasc Surg* 1996;12:243-245
2. Becker GJ, Benenati JF, Zemel G, et al. Percutaneous placement of a balloon-expandable intraluminal graft for life-threatening subclavian arterial hemorrhage. *J Vasc Interv Radiol* 1991;2:225-229
3. Thalhammer C, Kirchherr AS, Uhlich F, et al. Postcatheterization pseudoaneurysms and arteriovenous fistulas: repair with percutaneous implantation of endovascular covered stents. *Radiology* 2000;214:127-131
4. Lau L, O'Reilly M, Johnston L, et al. Endovascular stent-graft repair of primary aortocaval fistula with an abdominal aortoiliac aneurysm. *J Vasc Surg* 2001;33:425-428

Case 17

Coil Embolization and Stent-Graft Placement for Treatment of Iliac Artery Aneurysm

가

: Aneurysm, iliac

Stents and prostheses

: 67 /

:

:

가

(0.003 - 0.03%).

(mass effect)

CT

6 cm

3.9 × 3.4 cm,

1.7 × 2.1

cm

가 ,

(Fig. 1).

가

가

가

가

가

가

3 cm

3 cm

가

(Fig. 2).

5 F cobra catheter(Cook,

patent lumen

가

Bloomington, IN, U.S.A.)

microcatheter(ProgreT, Terumo, Tokyo, Japan)

6

microcoil

cobra catheter

6

0.035 inch

stainless steel coil(Cook, Bloomington, IN, U.S.A.)

Embolization

arteriogram

가

(Fig. 3)

12 F sheath

12 mm,

6

cm

stent - graft(S & G Biotech,

,)

aortogram

(Fig. 4). 10

CT

가

가

(Fig. 5).

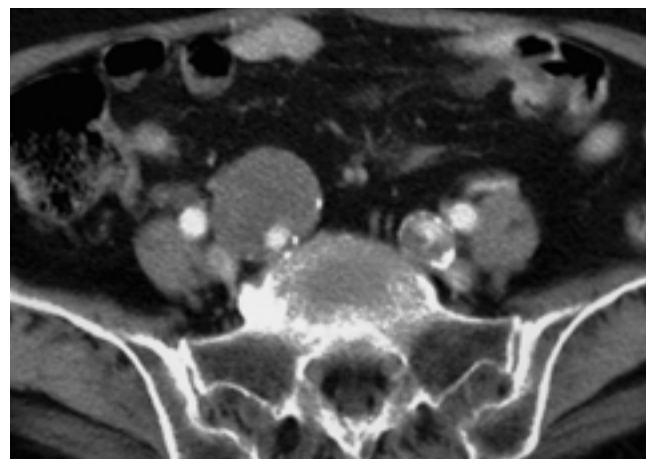


Fig. 1. Abdominal CT scan shows aneurysms of both internal iliac arteries.

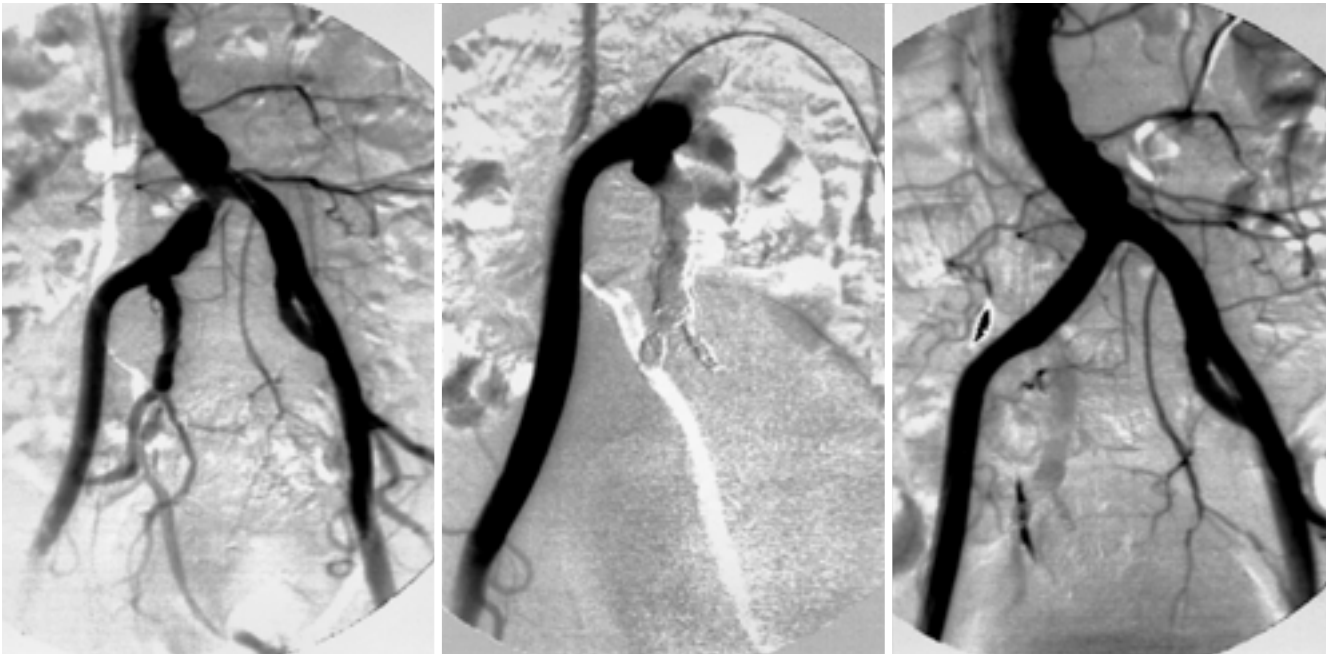


Fig. 2. Angiogram shows decreased diameter of right internal iliac artery due to thrombus in aneurysm and irregular dilatation of right common iliac artery.
Fig. 3. After coil embolization of right internal iliac artery and its branches, right common iliac arteriogram shows occlusion of the embolized arteries.
Fig. 4. Immediately after the deployment of the stent-graft in right common and external iliac arteries, the aneurysms of right common and internal iliac arteries were completely excluded.



Fig. 5. Follow-up CT scan after 10 days shows complete thrombus formation in the aneurysm of right internal iliac artery.

가
coil
stent - graft
graft
가
coil
coil
thrombin
가
coil -

50%
7% - 11%

1. Mori M, Sakamoto I, Morikawa M, et al. Transcatheter embolization of internal iliac artery aneurysms. J Vasc Interv Radiol 1999;10:591-597
2. Razavi MK, Dake MD, Semba CP, Nyman UR, Liddell RP. Percutaneous endoluminal placement of stent-grafts for the treatment of isolated iliac artery aneurysms. Radiology 1995;197:801-804

3. Parsons RE, Marin ML, Veith FJ, Parsons RB, Hollier LH. Midterm results of endovascular stented grafts for the treatment of isolated iliac artery aneurysms. *J Vasc Surg* 1999;30:915-921
4. Brunkwall J, Hauksson H, Bengtsson H, et al. Solitary aneurysms of the iliac artery system: an estimate of their frequency of occurrence. *J Vasc Surg* 1989;10:381-384
5. Cope C, Zeit R. Coagulation of aneurysms by direct percutaneous thrombin injection. *AJR* 1986;147:383-387

Case 18

Balloon Angioplasty of Arterial Stenosis in a Patient with Hemodialysis Fistula

: Dialysis, shunts

Arteries, transluminal angioplasty

: 72 /

: 2

1

thrill

:

(Immaturation)

micropuncture set

6F sheath

. Sheath

4F endhole catheter (Glide Cobra;

Terumo, Tokyo, Japan)

가

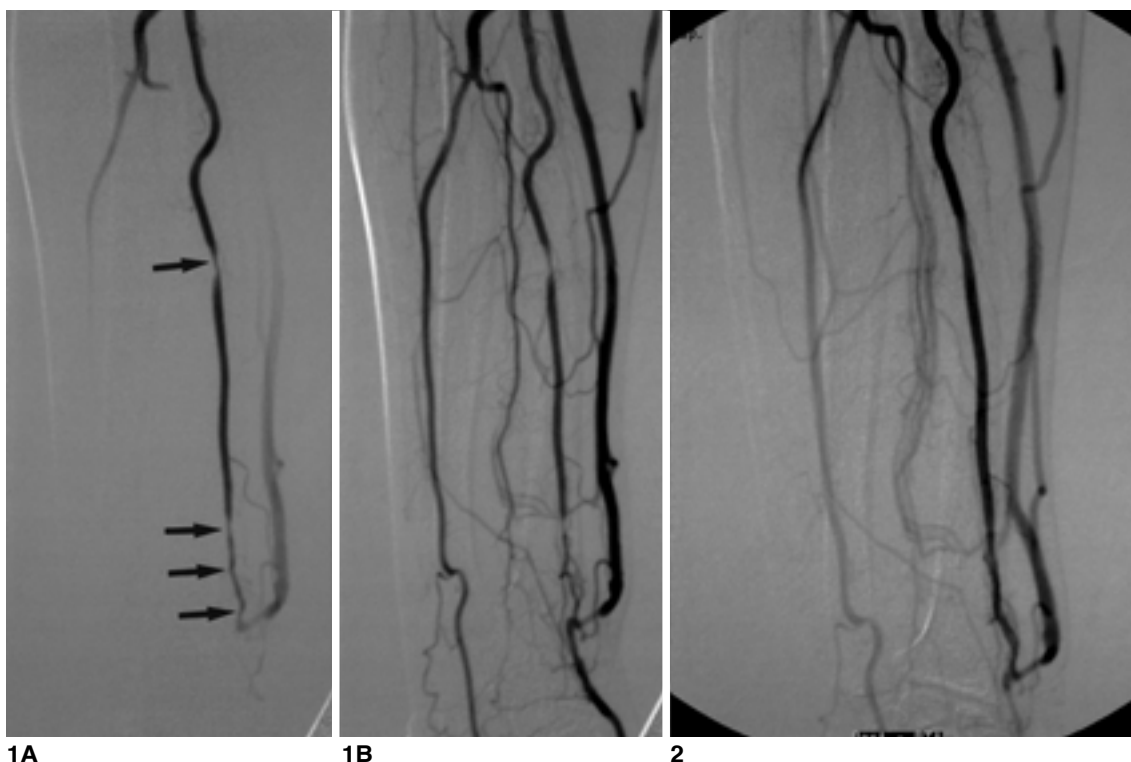
(Fig. 1A, B).

(cephalic vein)

4 Fr angiographic catheter 0.032 inch Terumo
guidewire(Terumo, Tokyo, Japan)

, 3 mm, 2 cm Savvy balloon
catheter (Cordis corporation, Miami, U.S.A.)

5 4



1A

1B

2

Fig. 1. Fistulograms show (A) multiple stenoses at mid-portion and around anastomotic site of left radial artery (arrows) and (B) collateral flow from ulnar artery through fistula.

Fig. 2. After balloon angioplasty, fistulogram shows the restoration of inner caliber of radial artery and good blood flow from radial artery into cephalic vein.

가 (Fig. 2).

가

5%

가 . National Kidney Foundation DOQI (Dialysis Outcomes Quality Initiative) guideline

가

thrill

thrill

가

Cimino fistula

92%) 4%

1 44% 85%

가

가 가

가

Trerotola intimal hyperplasia

가

, Manninen

가

가

가

가

1. Trerotola SO. Interventional radiology in the management of dialysis access sites. In: Ferris EJ, eds. RSNA categorical course in vascular imaging. 1998;323-332
2. NKF-DOQI clinical practice guidelines for vascular access (2000)
3. Manninen HI, Kaukanen ET, Ikaheimo R, et al. Brachial arterial access: Endovascular treatment of failing Brescia-Cimino Hemodialysis fistulas-initial success and long-term results. Radiology 2001;218:711-718
4. Trerotola SO, Turmel-Rodrigues LA. Off the beaten path: transbrachial approach for native fistula interventions. Radiology 2001;218:617-619

Case 19

A Hemorrhagic Complication During Thrombolytic Therapy of Lower Limb Ischemia

: Thrombolysis

Hemorrhage

: 65 /

:

4,000 u/min

가

가 1

가

2,100,000 unit

Ankle/brachial index

rt - PA

: 1) Acute thrombotic occlusion, Left iliac artery.

2) Intracranial hemorrhage

3) Lower abdominal aortic aneurysm

. Ouriel

가 ,

(Fig. 1).

(Fig. 2).

(deep femoral artery)

(Fig. 3).

(Fig. 4).

5 - F pigtail catheter (Cook, Bloomington, IN, U.S.A.)

. Pigtail catheter Cobra catheter (Cook, Bloomington, IN, U.S.A.)

multi - sidehole catheter (Cook, Bloomington, IN, U.S.A.)

500 u/hr

(,) 4,000 u/min

5 가

1,000 u/min

12



Fig. 1. Lower abdominal aortogram shows a large fusiform aneurysm (arrows) at the lower abdominal aorta and complete occlusion of the left iliac artery.

1

82%



Fig. 2. Selective arteriogram of the left iliac artery shows filling defects (arrows) with occlusion of the femoral artery.

가
가
Ouriel 4 4,000 u/min
2000 u/min
48
aPTT 1.5 - 2.0
12.5% , 1.6%
5.5%
aPTT 가
가 130 unit , 4.7
가 heparin sheath 가
가
2,100,000 u
aPTT 58.3 sec
(normal range, 30.5 - 45 sec) rt-PA
0 -
2.2%
Ouriel



3



4

Fig. 3. Follow up arteriogram of the left iliac artery during thrombolysis shows the recanalized deep femoral artery.

Fig. 4. Precontrast brain CT shows acute cerebellar hemorrhage (arrows).

가

가

,

가

가

.

1. Ouriel K, Shortell CK, deWeese JA, et al. A comparison of thrombolytic therapy with operative revascularization in the initial treatment of acute peripheral arterial ischemia. J Vasc Surg 1994;19:1021-1030
2. Ouriel K, Veith FJ, Sasahara AA. A comparison of recombinant urokinase with vascular surgery as initial treatment for acute arterial occlusion of the legs. N Engl J Med 1998;338:1105-1111

Case 20

(May - Thurner syndrome)

Hemorrhagic Stroke after Catheter Directed Thrombolysis and Intravenous Stent Placement in May-Thurner Syndrome

: Veins, stenosis or obstruction
Veins, grafts and prostheses
Veins, iliac
: 61 /
: left lower
extremity painful swelling
: May-Thurner syndrome with acute thrombosis
in left iliofemoral vein

800 IU/hr
check aPTT가 60 - 90
(urokinase 192 IU)
40% (Fig. 5A) 48
(urokinase 384 IU) 80%
(Fig. 5B), 69 (urokinase 552
IU) (Fig. 6A). 0.035 inch
5Fr

pig - tail catheter
roadmap
12 × 35 mm 10 × 90 mm Wallstents (Boston
(Fig. 1). CT
IVC bifurcation

(Fig. 2).
prone position
. 6Fr sheath
0.035 inch 5Fr end - hole catheter

(Fig. 3A),
가 lumbar plexus 가 plexus
branch 가
(Fig. 3B). CT
(Fig. 4A), 5Fr multi -
sidehole (proximal 20 cm segment) infusion catheter
(Fig. 4B), infusion catheter
5 IU/hr, sheath 3 IU/hr,
8 IU/hr urokinase(Abbokinase; Abbot Laboratories,
Abbot Park, IL, U.S.A.) . Heparin
procedure 4000IU i.v. bolus injection

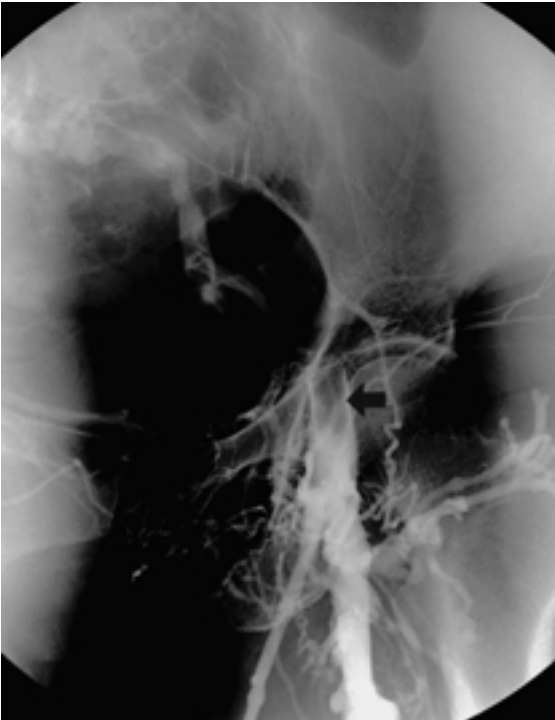


Fig. 1. Ascending venogram shows multiple collateral veins and occlusion of left common femoral vein by intraluminal filling defects (arrow) suggesting thrombus.

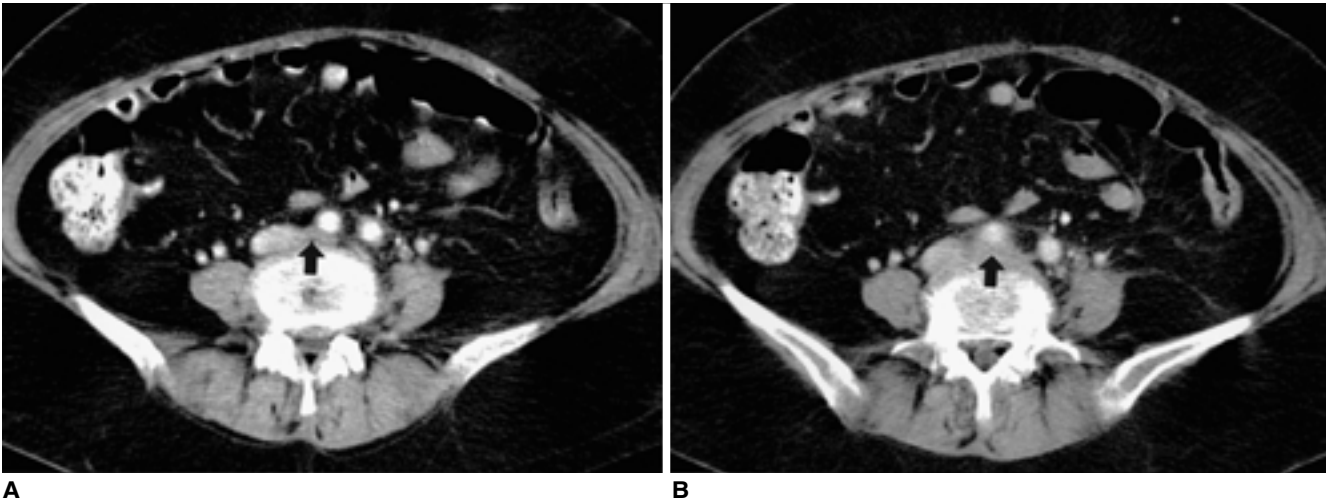


Fig. 2. A, B. Left common iliac vein (arrows) was compressed by overlying right common iliac artery on 5th lumbar vertebral body.

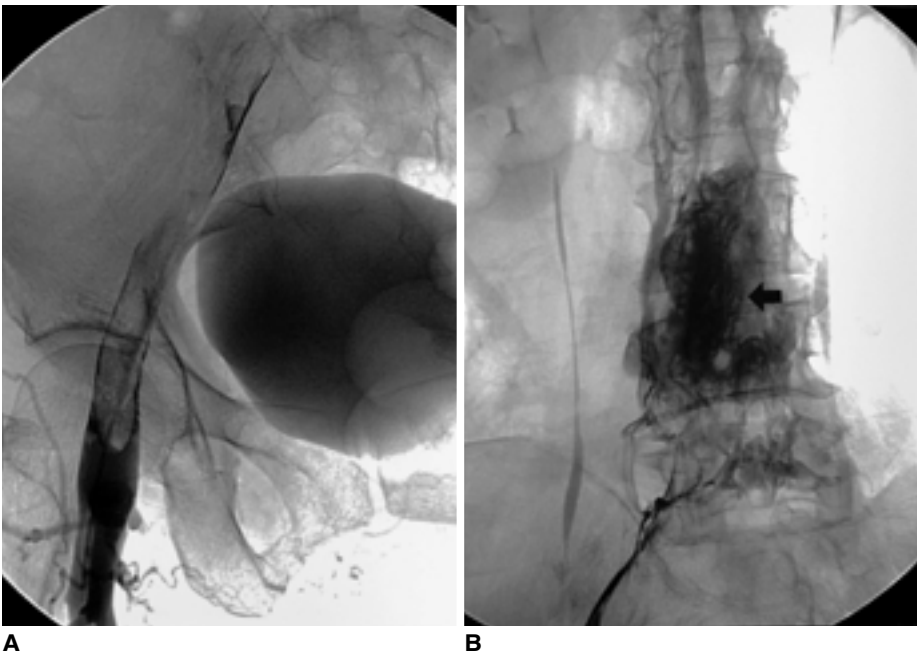


Fig. 3. A. Pre-procedure direct venogram shows thrombus as tubular filling defects in left iliofemoral vein.
B. While advancing guide wire to cross the stenotic common iliac vein, a small branch of lumbar plexus was ruptured and retroperitoneal leakage of contrast media (arrow) was developed.

Scientific/ Medi Tech, Watertown, MA, U.S.A.) IVC or May - Thurner syndrome; IVCS)
bifurcation
, 10 mm diameter bal - loon compression
(Fig. 6B). sheath ,
, bridge(spur)
, 가
(Fig. 6C).
가 Brain
CT , left temporoparietal lobe underlying disease
(Fig. 7).
IVCS (<4)
(Iliac vein compression syndrome,

MR venography가 가

가

IVCS

interventional procedure

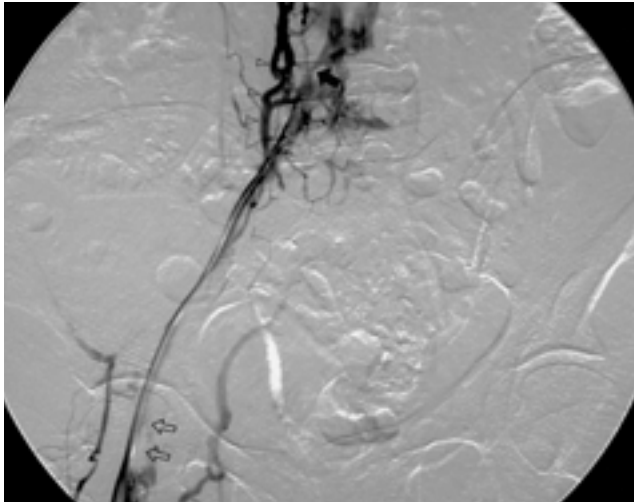
1

90%

prone position

5 - 6Fr venous sheath

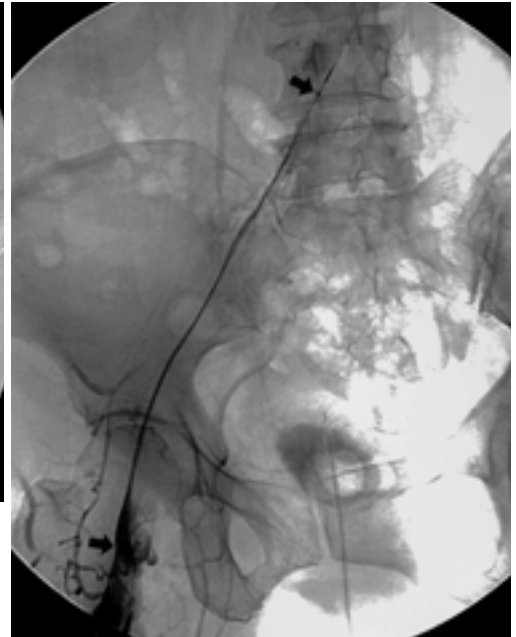
, 5Fr end - hole catheter venogram



A

Fig. 4 A. The next day delayed venogram shows that retroperitoneal leaked dye was resorbed. Note also that tight stenosis of left common iliac vein (arrow), deep vein thrombosis (open arrows) and ascending lumbar venous plexus (open arrow heads) were revealed.

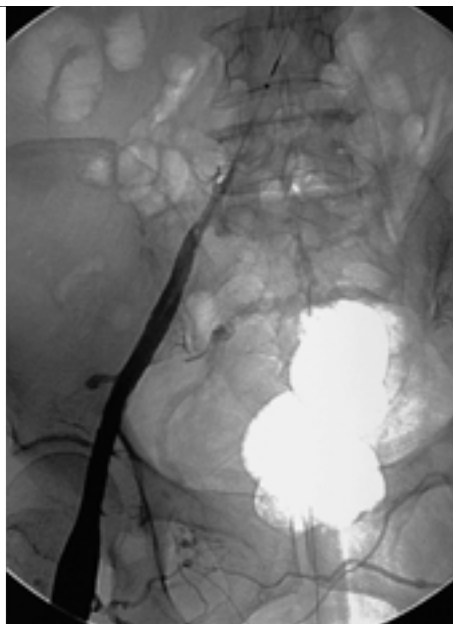
B. 5 Fr multi-sidehole (proximal 20cm segment) infusion catheter (arrows) was positioned at thrombus burden.



B



A



B

Fig. 5. A. After twenty-four hour thrombolysis, venogram shows about 40% thrombolysis.

B. On 48 hours, about 80% thrombolysis was revealed.

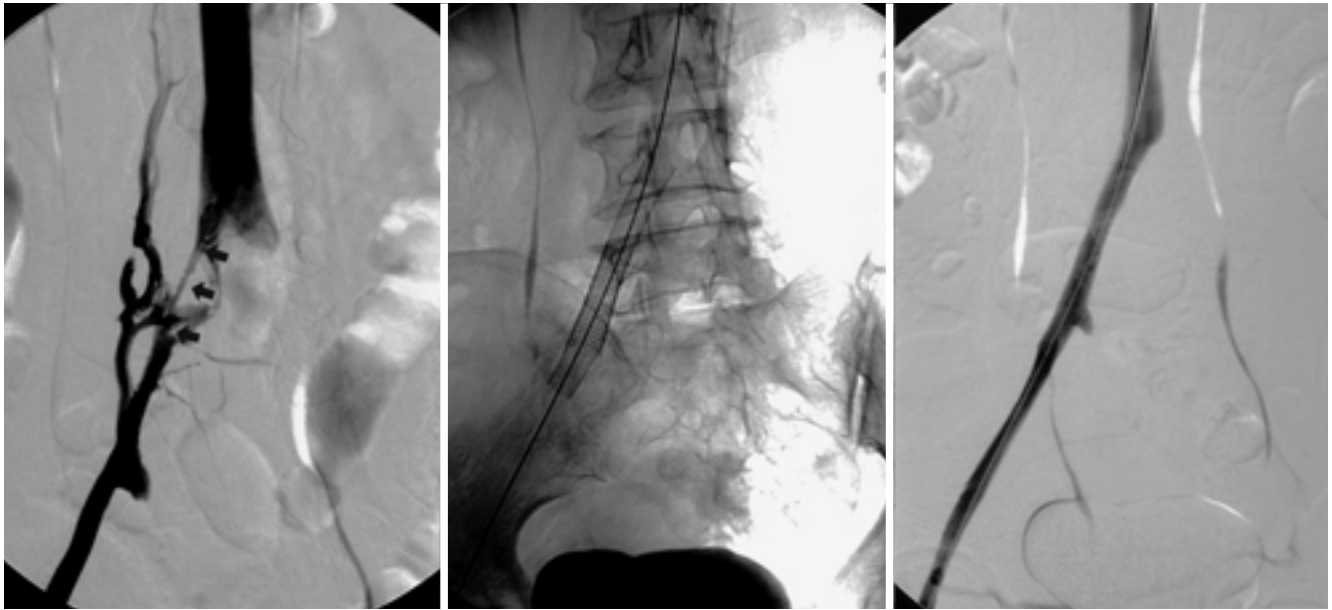


Fig. 6. A. After 69 hour (5,520,000 IU urokinase was used) iliofemoral thrombus was completely lysed. Stenotic segment of left common iliac vein (arrows) is well documented. **B.** Two Wallstents (12 x 35mm, 10x90mm) were placed across the stenotic iliac vein and balloon angioplasty was done using 10mm-diameter balloon. **C.** After Wallstents placement, venogram via popliteal vein sheath shows good luminal patency and normalized venous flow without collateral vessels.

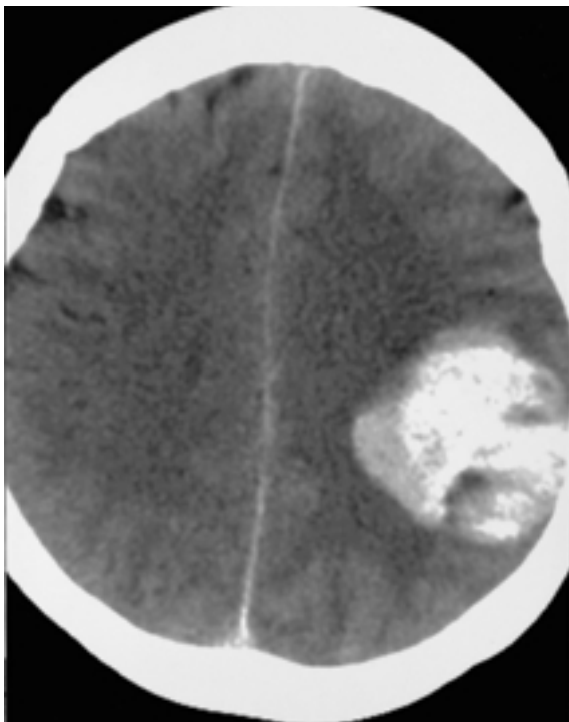


Fig. 7. After catheter-directed thrombolysis, acute stroke was developed and brain CT shows acute intracranial hemorrhage in left temporoparietal lobe.

, 50% urokinase
 , mechanical thrombectomy
 . 가
 procedure . 12 -
 14 mm . urokinase
 600 IU , 52
 . Heparin 3000 - 5000 IU bolus IV
 800 - 1200 IU/hr
 . major bleeding 4%
 . , , 가
 3% spontaneous intracranial hemorrhage가 1%
 1%
 1%
 550 IU urokinase
 spontaneous intracranial
 hemorrhage가
 ,
 1%
 , urokinase
 aPTT fibrinogen ,

extent,
 extent infusion catheter CT, MRI
 urokinase 12 - 24hr F/U
 venogram

1. O'Sullivan GJ, Semba CP, Bittner CA, et al. Endovascular management of iliac vein compression (May-Thurner) syndrome. *J Vasc Interv Radiol* 2000;11:828-836
2. Nilesch HP, Kenneth RS, Douglas BK, Andrew HC. Endovascular management of acute extensive iliofemoral deep venous thrombosis caused by May-Thurner syndrome. *J Vasc Interv Radiol* 2000;11:1297-1302
3. Berridge DC, Makin GS, Hopkinson BR. Local low dose intra-arterial thrombolytic therapy: the risk of stroke or major haemorrhage. *Br J Sur* 1989;76:1230-1233

Case 21

Repositioning of Central Venous Catheter in a Patient with Superior Vena Cava Stenosis

: Reposition, Central venous catheter

: 78 /

: 7

:

4Fr Headhunter type catheter

95%

(Fig. 1).

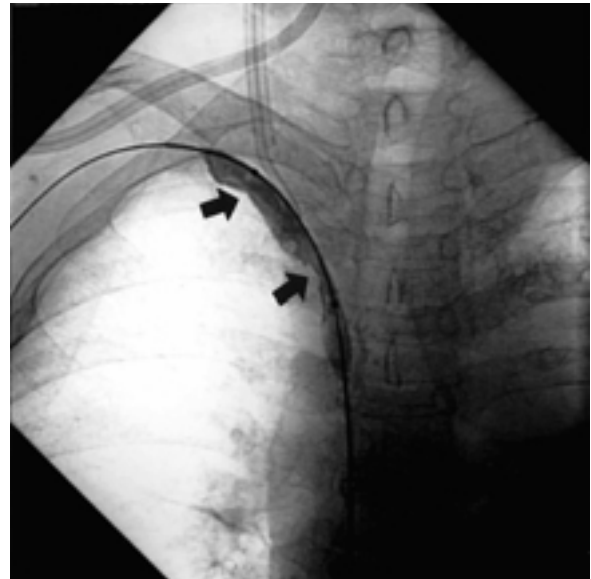


Fig. 2. Radiograph shows a formation of two waists (arrows) during the inflation of a balloon catheter with a diameter of 14 mm.



Fig. 1. Right subclavian venogram shows severe stenosis at superior vena cava (solid arrow) and the tip of the malpositioned central venous catheter (open arrow).



Fig. 3. Post-angioplasty venogram shows no improvement of severe stenosis at SVC.

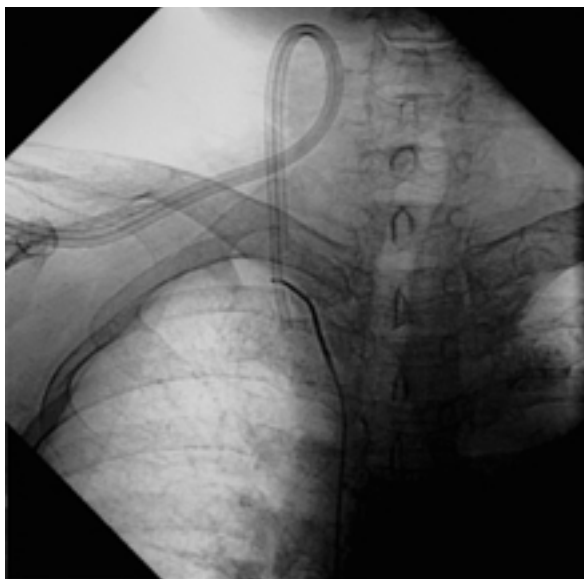


Fig. 4. Radiograph shows that the tip of the central venous catheter is caught by a snare loop inserted via right common femoral vein.

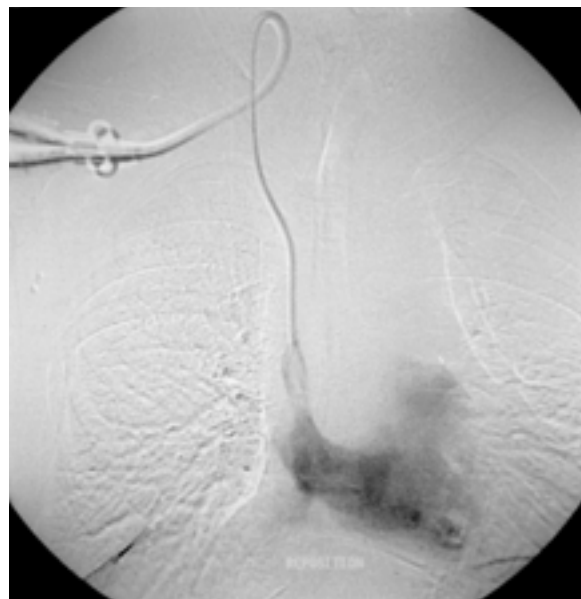


Fig. 5. Final venogram demonstrates that the tip of the central venous catheter is located near the junction of SVC and the right atrium.

14 mm

, 90%

(Fig. 2, 3), loop snare

(Fig. 4).

가

(Fig. 5).

가

가

가

,

loop snare catheter

95%

, ,

, , ,

가

,

X

가 29%

, 가

1. Hawkins IF, Paige RM. Redirection of malpositioned central venous catheters. *AJR* 1983;140:393-394
2. Louis JF, Gomes AS, Pusey E. Nonsurgical repositioning of central venous catheters. *Radiology* 1987;165:329-333
3. Hartnell GG, Hartnell GG, Wilde PH. Nonsurgical repositioning of central venous catheters. *Radiology* 1988; 168:581
4. Wilfrido R. Castaneda-zuniga, *Interventional Radiology*. 3rd ed. New Orleans, Louisiana: Williams & Wilkins, 1997;941-965

Case 22

Percutaneous Transpapillary Removal of Biliary Calculi with Use of Occlusion Balloon

: Bile ducts, calculi 20 mm mm
 Bile ducts, interventional procedure (Fig. 1). PTBD 8 Fr long
 : 85 / sheath (Cook, Bloomington, U.S.A.)
 : 0.035 inch (Radifocus M wireguide, Terumo, Tokyo, Japan) 10
 (PTBD) mm (Medi - Tech/ Boston Scientific, Watertown, Mass, U.S.A.) (Fig. 2, 3).
 basket) (stone) 11.5 mm (Medi - Tech/ Boston Scientific, Water - town, MA, U.S.A.)
 : Calculi of common bile duct 1:1
 PTBD (Fig. 4, 5). 3



Fig. 1. Cholangiogram through the PTBD catheter shows a large stone (arrows) in distal common bile duct. Another smaller stones are also noted.

Fig. 2. The PTBD catheter is changed with a 8-Fr arterial sheath (arrows). A 0.035 inch guidewire has been passed through the papilla into duodenum.



3



4

Fig. 3. Cholangiogram shows dilatation of papilla with standard angiographic balloon of 10 mm in diameter. Note that balloon is being squeezed by papilla (arrow).

Fig. 4. Cholangiogram shows an occlusion balloon (arrow) pushing calculus through the papilla.



5



6

Fig. 5. Cholangiogram shows occlusion balloon in duodenum. Calculus has been cleared.

Fig. 6. Cholangiogram obtained three days after procedure shows complete clearance of calculus.

(Fig. 6).

(sheath)

가 가 7 - 9 Fr tract
가 , tract maturation

가
PTBD T - 가 ,

Gil 38

T -

가 가

36 94.7%

1. Gil S, Iglesia P, Verdu, JF, Espana F, Arenas J, Irurun J. Effectiveness and safety of balloon dilation of the papilla and the use of an occlusion balloon for clearance of bile duct calculi. AJR 2000;174:1445-1460
2. Ueno N, Ozawa Y. Endoscopic sphincter dilation in patients with bile duct stones: immediate and medium-term results. J Gastroenterol Hepatol 1999;14:822-826
3. Meranze SG, Stein EJ, Burke DR, Hartz WH, McLean GK. Removal of retained common bile duct stones with angiographic occlusion balloons. AJR 1986;146:383-385

Gil

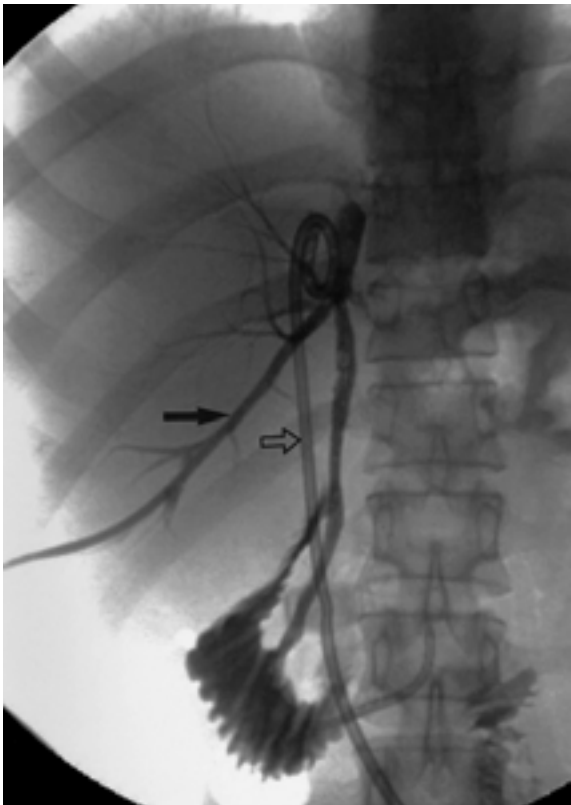
(stiff

guidewire)

Case 23

Osteomyelitis in the Rib: An Unusual Complication of PTBD in Liver Transplant Patient

: Bile ducts, percutaneous drainage
Catheters and catheterization, complica - tions
Ribs
Osteomyelitis
tube (Fig. 1A). 가 , PTBD
: 30 /
: 5
biliary fistula 가 (PTBD) . 5
가 PTBD
: PTBD tube
(Fig. 1B).
가가
, technetium - 99m methylene diphosphate
10 가 (hot uptake)
(Fig. 1C).
PTBD

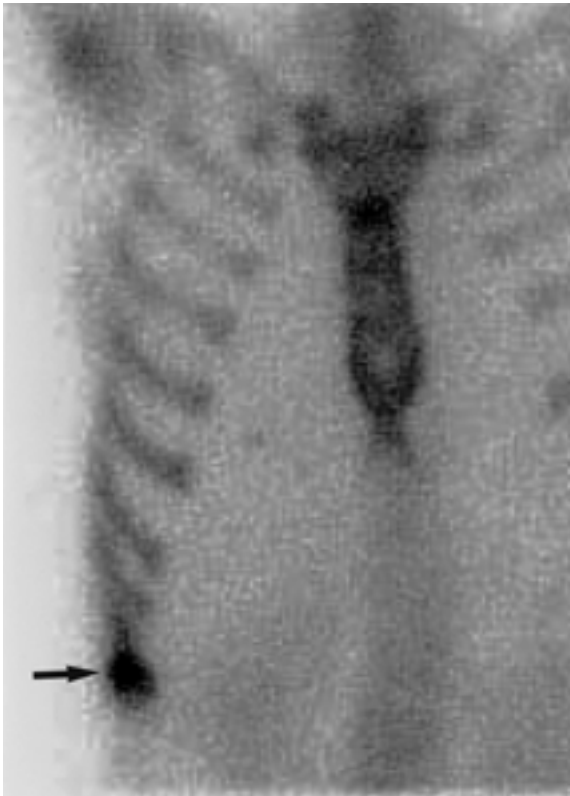


A



B

Fig. 1. A 30-year-old man presented with tenderness and pain at the wound of percutaneous transhepatic biliary drainage (PTBD). He had undergone PTBD five months ago for the management of the biliary fistula at the anastomotic site after living related donor right liver transplantation.
A. Cholangiogram using the biliary drainage tube (arrow) shows good position and patency of the drainage tube. Note another pig-tail tube (blank arrow) inserted into the abscess formed by the biliary fistula.
B. Ultrasonography of the painful area shows irregular cortical margin of the rib (arrows). Edema of the surrounding soft tissue was also observed compared to contralateral side.



C
Fig. 1. C. Technetium-99m methylene diphosphate bone scan revealed a focal increased uptake at the right tenth rib (arrow).

	PTBD	
	, PTBD	
	,	
	(1).	
	PTBD	,
PTBD		15
rib notching	2	(2, 3).
	,	
	가	
	가	

1. Lorenz JM, Funaki B, Leef JA, Rosenblum JD, Van HT. Percutaneous transhepatic cholangiography and biliary drainage in pediatric liver transplant patients. *Am J Roentgenol* 2001;176:761-765
2. Severini A, Bellomi M, Cozzi G, Bellegotti L, Lattuada A. Rib erosion: late complication of long-standing biliary drainage catheters. *Radiology* 1984;150:666
3. Gunther RW, Schild H, Thelen M. Percutaneous transhepatic biliary drainage: experience with 311 procedures. *Cardiovasc Intervent Radiol* 1988;11:65-71

Case 24

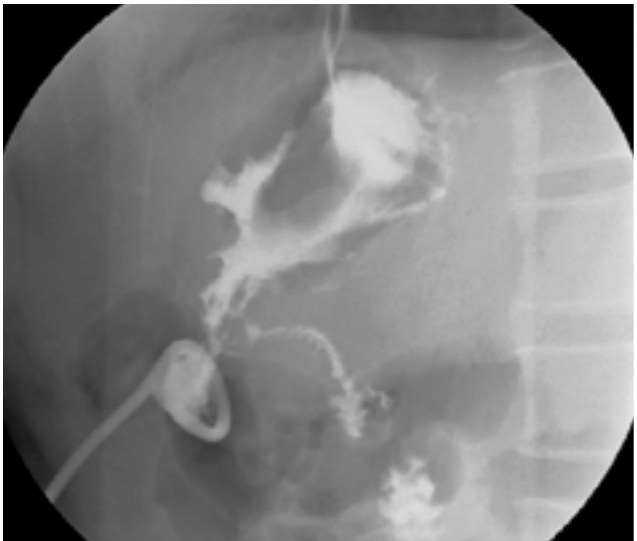
Treatment of Complicated Gastroduodenal Anastomosis with Covered Metallic Stent Placement

: Gastrointestinal tract, interventional procedure
Stents and prosthesis
Stomach, stenosis or obstruction

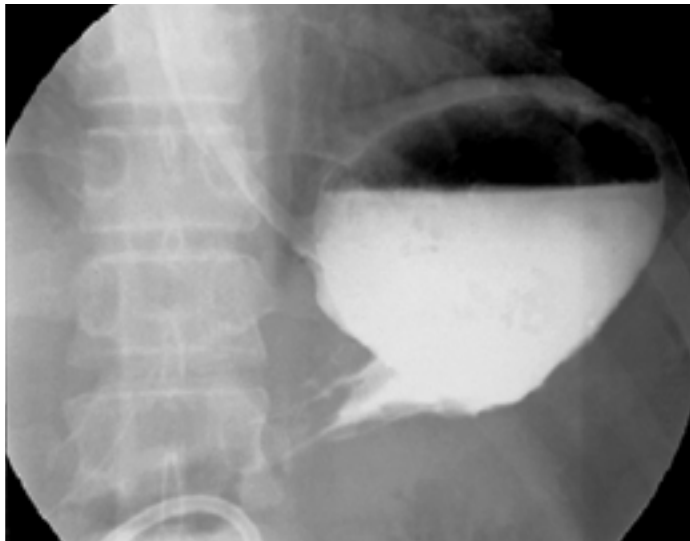
Gastrointestinal fistulas
: 55 /
: Billroth I operation 5



Fig. 1. Abdominal CT scan on postoperative 5th days shows abnormal loculated fluid collection with scanty air-bubble adjacent to anastomosis site, suggesting leakage from anastomosis site.



A



B

Fig. 2. A. Tubogram shows contrast reflux from abdominal abscess pocket to stomach and duodenum.
B. Preprocedure UGI radiograph shows severe stenosis of gastroduodenostomy site and no contrast passage to duodenum.

nitinol stent (Niti-S Pyloric covered stent; Taewoong, Seoul, Korea)

0.035 - inch (Terumo, Tokyo, Japan)

5Fr Cobra (Cook, Bloomington, U.S.A.)

0.038 - inch Superstiff J - tip guide wire (Meditech/Boston Scientific, Watertown, Mass), 8 cm, 18 mm covered

patency가 (Fig. 3A, B), 12

patency가

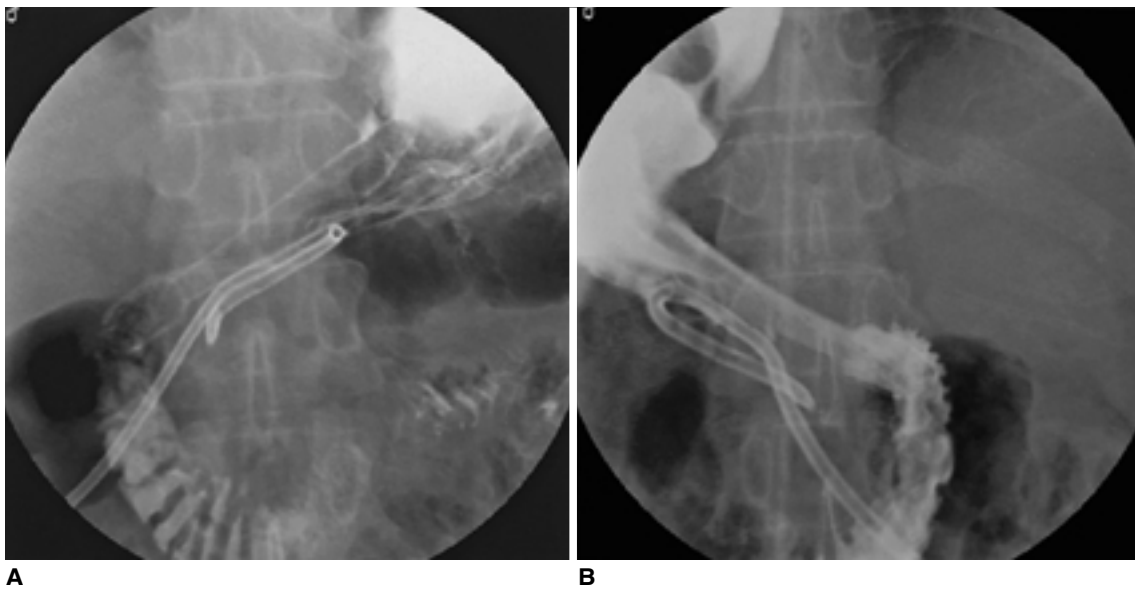


Fig. 3. UGI radiographs after covered metallic stent placement show (A) fully expanded stent, and (B) good passage of contrast media.

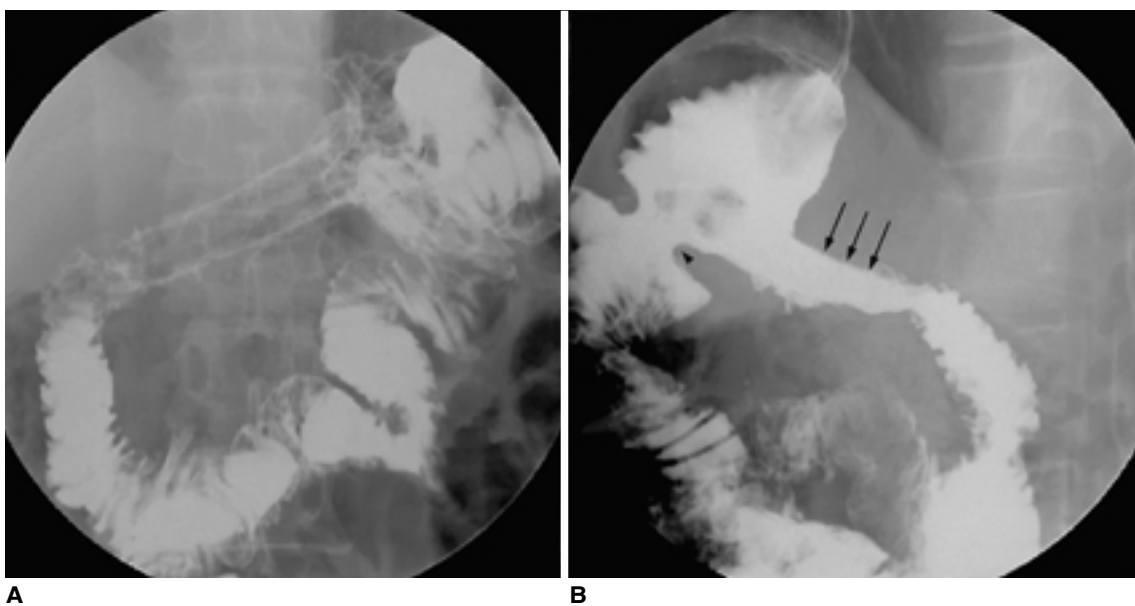


Fig. 4. UGI radiographs after 2.5 months following stent placement show (A) the stent without complication such as migration, reocclusion or contrast leakage, and (B) good patency at gastroduodenostomy (arrows) and gastrojejunostomy (arrowhead).

(Fig. 4A, B).

가 가

가

가

가

self

sealing

가 가

1. Park KB, Do YS, Kang WK, et al. Malignant obstruction of gastric outlet and duodenum: palliation with flexible covered metallic stents. *Radiology* 2001;219:679-683
2. Kyoto Y, Iwasaki Y, Kaji T, et al. Gastrointestinal fistulas: treatment with covered stents. *Abdom Imaging* 2001;26:570-573
3. Dormann AJ, Deppe H, Wiggighaus B. Self-expanding metallic stents for continuous dilatation of benign stenoses in gastrointestinal tract-first results of long-term follow-up in interim stent application in pyloric and colonic obstructions. *Z Gastroenterol* 2001;39:957-960

Case 25 NBKA

Ablation of a Renal Cyst with NBKA

: Kidney, Cyst, Ablation

: 43 /

:

: Autosomal Dominant Polycystic Kidney Disease

histoacryl - blue
(Fig. 1B). 5

CT

(Fig. 1C).

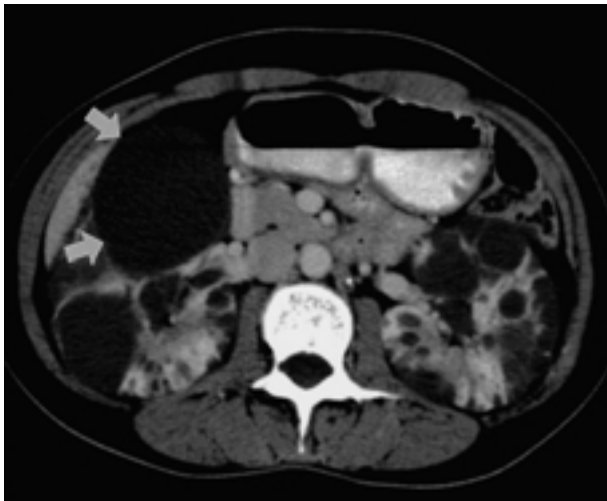
CT mid - pole
(Fig. 1A).

13 cm

22 G

22 G

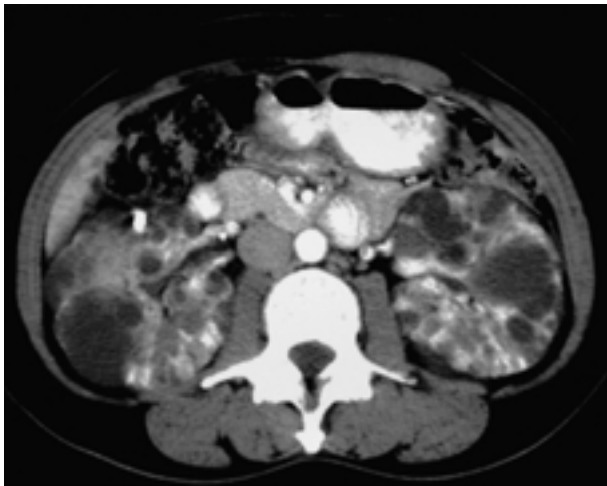
가
1 cc NBKA (N - butyl 2 -



A



B



C

Fig. 1. A 43-year-old woman presented with right upper quadrant pain. She was previously diagnosed as autosomal dominant polycystic kidney disease.

A. A large cyst with maximum diameter 13 cm is seen in the anterior aspect of mid-pole of right kidney (arrows), projecting anterior on the contrast-enhanced CT image.

B. Her KUB obtained after ablation of previous right renal cyst with mixture of Lipiodol and NBKA shows an irregular lipiodol material in the collapsed cyst (arrow).

C. Follow-up CT imaging 5 months after ablation shows a pin-point lipiodol material in the completely collapsed cyst of right kidney.

cyanoacrylate, Histoacryl - Blue, Braun, Melsungen, Germany) 0.5 cc

NBCA

5 %

81%

NBCA 1.5 cc

86%

NBCA

가

가

absolute ethanol, ethanolamine oleate, povidone iodine, acetic acid, dextrose solution, quinacrine, tetracycline, minocycline, glucose, phenol, atabrine, bismuth phosphate, fibrin glue
absolute ethanol 가

1. Kim SH: Renal cyst sclerotherapy. In Han MC, Park JH (eds): Interventional radiology, Ilchokak, Seoul, 1999;620-625
2. Kim SH, Moon MH, Lee HJ et al. Renal cyst ablation using enbucrilate. Radiology (in press)